NCHRP Project 9-50

PERFORMANCE-RELATED SPECIFICATIONS FOR ASPHALTIC BINDERS USED IN PRESERVATION SURFACE TREATMENTS

FINAL REPORT
APPENDICES

Prepared for
National Cooperative Highway Research Program (NCHRP)
Transportation Research Board
Of
The National Academies

Y. Richard Kim, Ph.D., P.E., Javon Adams, Ph.D.,
Cassie Castorena, Ph.D., Mohammad Ilias Ph.D., Jeong Hyuk Im, Ph.D.
North Carolina State University, Raleigh, NC

Hussain Bahia, Ph.D., Preeda Chaturabong, Andrew Hanz, Ph.D., Petrina T. Johannes, Ph.D.,
University of Wisconsin-Madison, Madison, WI

Appendix A. Long-Term Validation Plan for EPG Specifications

CONTENTS

LIST OF FIGURES

CHAPTER A-1. LONG-TERM EPG SPECIFICATION VALIDATION PLAN

The overall concept of the long-term validation plan is to test emulsions used in surface treatments in accordance with the EPG specification and grade the emulsions accordingly. Once each emulsion is graded, field sections will be constructed using these same asphalt emulsions in locations nationwide that are appropriate for the specified temperature and traffic grade of each emulsion. Long-term field performance monitoring is critical to the proper validation and implementation of the developed EPG specifications. The constructed field validation sections will be monitored at regular intervals over the design life of the surface treatments to determine if the field performance is consistent with the results of the EPG specification tests for these asphalt emulsions. If necessary, adjustments will be made to the specifications to account for the findings in the long-term validation plan. The subsequent sections outline further details regarding the long-term field validation plan.

Field Validation Section Construction Overview

This section provides a brief overview of the general plan for constructing each of the long-term field validation sections. Specific construction timelines and section geometries may vary slightly from those presented herein depending on the circumstances for each construction team and location.

Figure A-1 details the typical construction timeline that was used previously for the construction of the field validation sections. Similar timelines will be utilized for the chip seal, microsurfacing, and spray seal validations sections with some variation in timing to account for the differences in sample extraction time required for the different surface treatment types. For example, spray seals do not require the extraction of specimens or repairs to the sampling area.

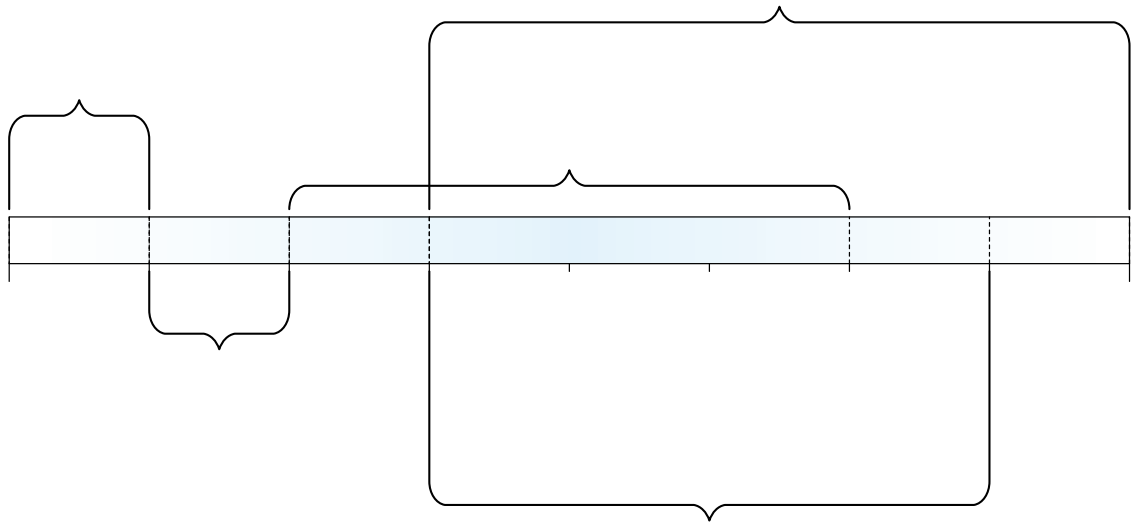

Figure A-1. Field construction timeline for typical field validation sections.

Field Section Layout and Sampling Overview

The typical field validation section layout is displayed in Figure A-2. Each section has a 250-foot transition area at the beginning and end in order to avoid any problems at the beginning of the section when the emulsion sprayer may be approaching its application speed, or at the end of the section as the emulsion sprayer slows to a stop. As this can cause the potential for variability in applied emulsion application rates at the start and end of each section. Following the transition area at the start of each section is a 250-foot sampling area from which samples are extracted for laboratory testing. Following the sampling area is a 500-foot section designated as the field testing and performance monitoring area which is to be permanently marked for field performance monitoring.

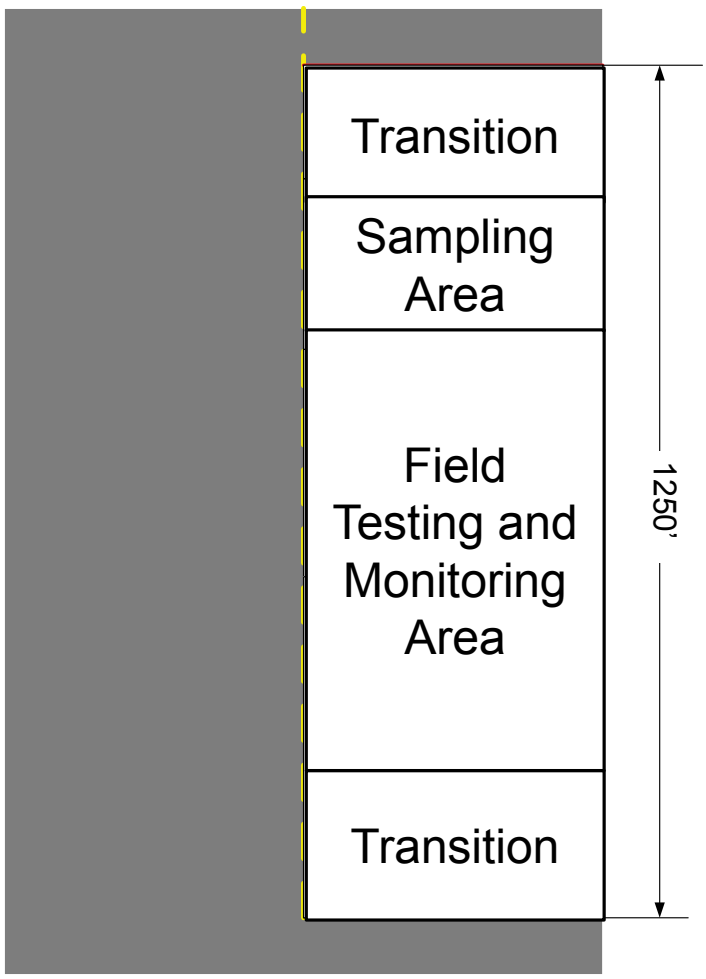

Figure A-2. Field validation section layout (not to scale).

The procedure for sampling includes preparation of the 175 mm x 300 mm felt disks upon which chip seal surface treatments are constructed. Also, steel Vialit plates are placed directly onto the roadway in line with the felt samples. The research team carefully places high quality ground paper onto the road surface and tapes down the felt disks and Vialit plates onto the ground paper, as illustrated in the schematic presented in Figure A-3. Figure A-4 shows the sample extraction area prior to the start of the surface treatment construction for both felt and

Vialit samples. It should be noted that no section performance monitoring is conducted in the sampling area. After extraction, samples are placed onto wooden boards for sample stability during transport from the field back to the laboratory after construction.

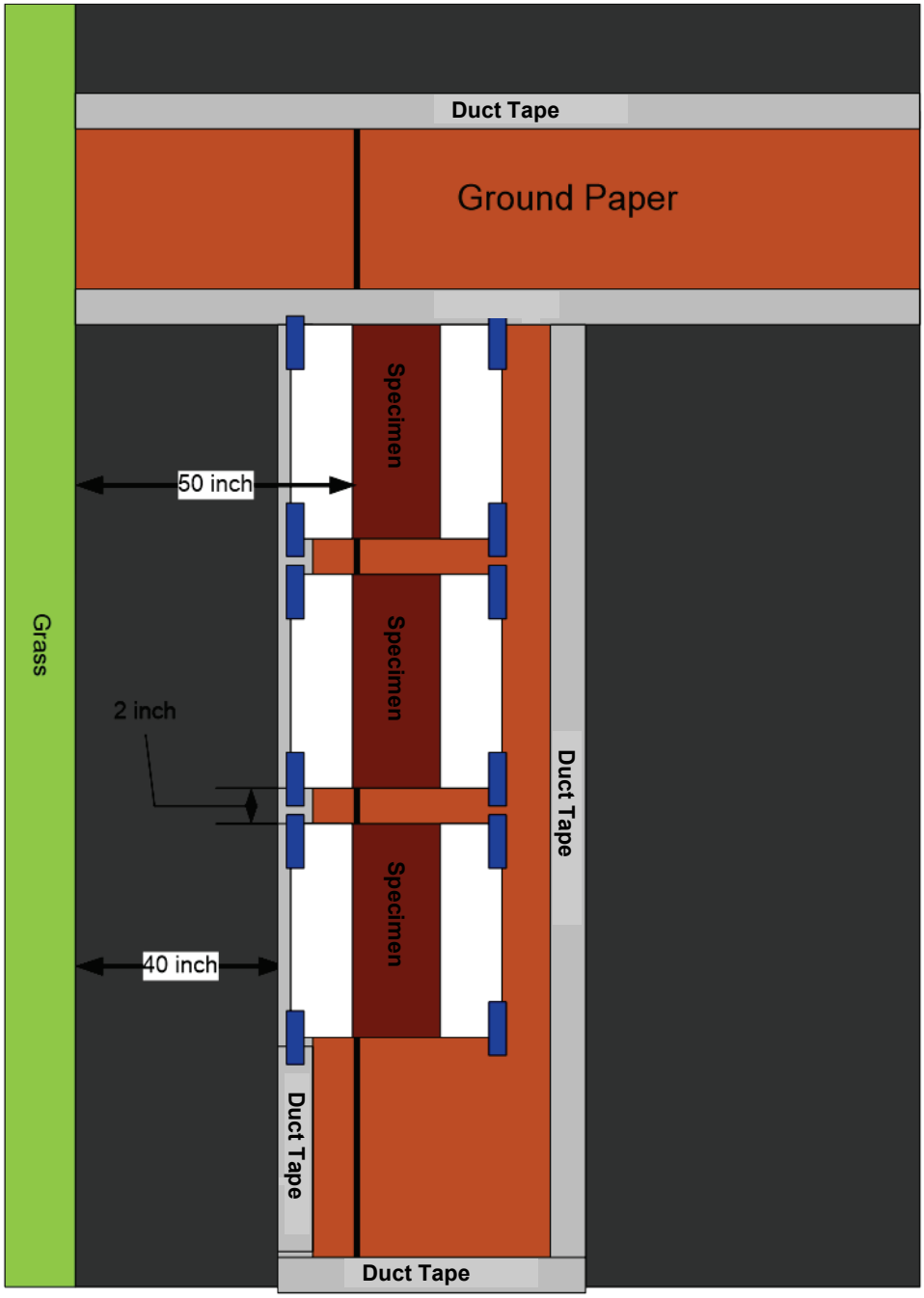

Figure A-3. Sample template mounting procedure within sampling area.

Figure A-4. Photograph of layout of Vialit and MMLS3 field test samples.

Figure A-5 shows the process of extracting a sample from a chip seal section after surface treatment construction is complete.

Figure A-5. Field sample extraction process.

Requirements for Participation in Long-term Validation Plan Field Construction

At the onset of the long-term field validation process, a request will be made to state departments of transportation (DOTs) who typically construct chip seals, microsurfacing, and spray seals to request participation in the long-term validation plan. For inclusion in the long-term validation plan, each pavement practitioner will be asked to agree to the following tasks:

- Provide information about and access to typical emulsion and aggregate materials used for surface treatment construction at the respective locations where field validation sections are to be built. Emulsion samples will need to be obtained prior to construction in order to undergo EPG specification testing for grading purposes. Five gallons of each emulsion to be tested should be obtained in plastic containers. Emulsion samples should be obtained directly from emulsion suppliers during the spring/summer seasons when freezing during transport is unlikely.
- Participate in preconstruction meetings to introduce research-based field construction methodology to the surface treatment construction team. These meetings will be used to familiarize the construction team with the research objectives of the field construction as well as with field test methods to be conducted to ensure that all research objectives can be met.
- Participate in a construction planning meeting to discuss prospective sites for construction (to be determined based on a particular site's need for a surface treatment type addressed by the EPG specifications, existing surface conditions, vertical and horizontal road alignment, traffic level, etc.) and to discuss the specific responsibilities of the research team and construction team on the day of construction.
- Visit viable construction locations for field construction with the research team to select the final construction sites.
- Conduct preconstruction staking and pavement marking to define the field section geometry (e.g., section start and end points) for each field validation section to be constructed.
- Provide samples of the field construction materials (i.e., aggregate and emulsion) for testing under the EPG specifications.
- Construct sections using a performance-based mix design to eliminate design variability.
- Construct chip seal sections and provide the appropriate traffic control for execution of the research plan. This traffic control should remain in place until all research objectives are met on the day of construction.
- Accommodate for extracting samples from the field validation sections after construction for laboratory performance testing using the one-third scale model mobile loading simulator (MMLS3).
- Provide additional traffic control for field monitoring the constructed sections in accordance with the performance monitoring schedule.
- Collect and provide traffic data about the roadways where long-term field validation sections are constructed to ensure that the effect of traffic loading is properly assessed. If possible, provide information regarding the percentage of heavy vehicles that access the validation sections to determine if adjustments to the EPG specifications are needed to account for significant truck traffic.

Once the participating surface treatment construction teams have been determined and each team formally agrees to the above list of requirements, the research team will finalize the construction plan for the EPG specifications based on certain factors to ensure the representation and inclusion of various climates and traffic levels in the long-term validation plan for the EPG specifications. In finalizing the field construction plan, the research team will develop a detailed schedule for preconstruction meetings and construction dates. This timeline will start with preconstruction meetings followed by field construction and testing. The proposed construction dates would be determined in collaboration with the respective construction teams.

It should be noted that prior to construction, the grade of the emulsion will be determined so that prospective construction locations can be identified that meet both the climate and traffic requirements for each grade of emulsion material.

Location Selection Criteria for Long-Term Validation Plan

Factors that will be used in the selection of prospective locations for long-term field validation sections include:

- Current high temperature performance grade based on climate
- Current low temperature performance grade based on climate
- Traffic levels of prospective construction locations
- Long-Term Pavement Performance (LTPP) climatic zones
- Aggregate type typically used (cationic or anionic)

In addition to testing different grades of emulsions at different traffic levels, the long-term validation plan will require that EPG specification validation sections for each surface treatment type are constructed in each of the four climatic zones. These zones include:

- Wet-freeze
- Wet-no freeze
- Dry-freeze
- Dry-no freeze

A wet region is defined as a region where the average annual rainfall is over 508 mm, whereas a dry region experiences average annual rainfall below 508 mm. A freeze region is defined as a region with an average freezing index of more than 83.3 degree-Celsius days. For example, 10 degree-Celsius days could mean there are 10 days with a mean air temperature of 1°C below freezing or five days with a mean air temperature of 2°C below freezing (Wang, 2005).

By fabricating field validation sections in freeze and no freeze zones, the appropriateness of the specification limits developed to address low temperature distresses in the surface treatments can be validated.

Once each field location is identified, the specific section of each roadway that will be used for field data collection must be determined. Based on its extensive field research experience, the research team will determine suitable 1,000-foot field validations sections along the roadway. Within each 1000-foot field section, appropriate 500 feet of sampling areas and 500 feet of monitoring areas will be defined. The following considerations will be used to determine if an area is suitable for field validation sections:

- No pre-existing pavement conditions
- No sampling or monitoring areas located on steep downhill grades or near intersections
- No driveways or intersections near the monitoring area
- No sampling or monitoring sections located along super-elevated horizontal roadway curvatures

These requirements, in conjunction with effective construction practices will help ensure that the observed performance for each field validation section is based on the performance of the asphalt material and not due to the effect of unexpected construction-related variables.

Development of a Material Acquisition Plan

It is important for the long-term validation of the EPG specifications to acquire a wide variety of emulsion grades that typically are used for each surface treatment type. Therefore, a significant part of the selection process for determining which DOTs to include in the study is to ensure that the collective materials tested amongst the participating DOTs represents the range of emulsion types used for each surface treatment (e.g., cationic vs. anionic, modified vs. unmodified, high float emulsions, etc.). Once the participating DOTs have been identified, the emulsion material used by each state DOT (or contractor) to fabricate the surface treatments must be acquired for laboratory testing under the EPG specifications. For this purpose, the research team will need to execute a plan to have the materials delivered to the laboratory for testing. As the expected range of locations included in the long-term validation plan may not be practical for driving to collect these materials, many emulsion samples will need to be shipped to the research team for testing. Ideally, this shipping process will begin in the spring prior to construction because emulsion production resumes during this season, and temperatures are warm enough to mitigate the risk of freezing during shipping. All possible precautions should be taken to avoid freezing emulsions during transport, especially for emulsions shipped from northern locations where, even during the spring season, night temperatures can still approach freezing in some places. Materials from any northern test locations could be shipped later in the spring season to minimize this risk. Once these materials arrive, they will be stored in a forced-draft oven until they are tested.

A sample of every emulsion material included in the long-term validation plan will need to be acquired at two different time periods. The first emulsion sample will be acquired from the emulsion supplier in order to test and grade the emulsion prior to construction. This first sample will be used to identify the appropriate climatic and traffic conditions under which the test section should be constructed. Ideally, this sample will be collected and tested as close to the day of construction as practically possible to minimize the likelihood of significant changes in the emulsion material. The second sample will be acquired directly from the emulsion spray tanker on the day of construction. This second sample will be used to ensure that the emulsion grade did not change from the first sample to the actual construction-day sample as a means of quality assurance. If significantly different results between the first and second samples are obtained, the second sample will be used for analysis purposes, as it would represent the emulsion that was used in the construction of the field validation section. All emulsion acquisition should be scheduled in such a manner to ensure that all EPG specification testing for each emulsion is completed within two weeks of arrival at the laboratory.

Field Validation Section Construction and Design

Each field validation section will use emulsion and aggregate materials that typically are used locally to construct each respective surface treatment. Also, surface treatment construction procedures (e.g., chip seal rolling/compacting protocol, sweeping, etc.) will not be changed from practices typically used by the construction team to avoid operator error due to changes in the construction process/equipment.

Because this research does not seek to investigate the mix design procedures used nationwide for surface treatment construction, the mixture design typically used by the construction DOT will be utilized in this research as well. The reason for this decision is that no widely accepted performance-based mix design exists for chip seal, microsurfacing, and spray seal design. Therefore, the research team will rely on the local experience of the DOTs for guidance regarding the appropriate mix designs that have been used successfully for surface treatment construction on similar roadways to those used for constructing the long-term validation sections. The alternative design approach would be to standardize the design procedure for all field sections; however, this approach could lead to inferior performance when compared against locally calibrated designs for surface treatments. Also, each local DOT will determine the layer thickness for the chip seal or microsurfacing treatment to be constructed in their respective region.

Quality Control and Quality Assurance

Various measures should be taken in order to control and assure the quality of the surface treatments constructed under the long-term EPG specification validation plan. First, surface treatment construction teams should be utilized who have extensive experience successfully constructing surface treatments in their respective locations. Prior to construction, equipment cleaning and all necessary calibrations should be completed in order to minimize construction-related performance problems. Sections should be swept to remove dust and debris from the existing surface, and any minor distresses observed on the existing pavement surface should be noted and corrected (e.g., crack sealing) prior to construction. Existing pavement surfaces that exhibit major distresses should not be candidates for constructing field validation sections.

During construction, the asphalt sprayer nozzles should be monitored closely for clogging, and the chip seal surface should be visually evaluated for signs of streaking. Likewise, the aggregate spreader, and the resulting surface after aggregate application, should be monitored for inconsistency in aggregate application rates, which could result in problems such as bare spots in the seal. Detailed notes should be made of any irregularities that occur during field construction that might lead to performance issues in the constructed sections.

After construction is complete, the research team will extract specimens from a predefined sampling area within each field section to obtain chip seal and microsurfacing specimens for the following purposes:

- To measure the emulsion application rate (EAR) and aggregate application rate (AAR) for each section using ignition oven testing (as specified by ASTM D 6307) for rate validation.
- To extract and weight Vialit specimens to determine the EAR for spray seals.
- To conduct laboratory aggregate loss and bleeding tests using the MMLS3 to measure the performance of each chip seal treatment.

Experimental Design Factor Summary

The experimental design for the long-term validation plan will include testing for and capturing the effects of the following factors for each surface treatment type:

- Chip seal, microsurfacing, and spray seal treatment types
- Four LTPP climatic zones
    - Wet and dry conditions
    - Freeze and no-freeze conditions
- Multiple performance grades within each zone
- Multiple traffic levels (i.e., low, medium, and high) within each climatic zone
- Multiple aggregate types (for chip seals and microsurfacing)

Performance Monitoring Schedule

After the construction of each field validation section is complete, the research team will monitor the performance of the section at the following time intervals:

- Immediately after summer construction
- Before the first winter
- After the first winter
- After the second summer (with the first summer being the summer of construction)
- After each winter and summer of each subsequent year of the design life of the seal.

Most aggregate loss from a chip seal occurs under the initial loading after the roadway is reopened to traffic. Likewise, tackiness and tracking problems related to spray seals occur immediately after traffic reopening. Therefore, early monitoring of the roadway is critical. Likewise, monitoring before and after the first winter is important, because a comparison of the two observations can help determine if low temperature raveling in chip seals and thermal cracking in microsurfacing has occurred in the sections due to the asphalt binder becoming brittle and susceptible to fracture at low temperatures. Monitoring after the second summer will capture the pavement's susceptibility to high temperature distresses such as bleeding/rutting and also late raveling resistance of chip seal and microsurfacing binders. Lastly, by monitoring after every subsequent winter and summer, the long-term performance of the surface treatments can be validated for the EPG specifications.

Monitoring of each field validation section will include:

- Laser scanning to assess surface texture and embedment depth (for chip seals only)
- Photographs of each section to capture visual changes in the treatments
- A qualitative pavement condition survey
- Traffic monitoring (conducted by the respective DOTs)

Photographs of the sections will be taken during field monitoring. These photographs should include longitudinal photos of both wheel paths, as these are the areas where critical distresses for chip seal treatments are most prevalent. Both close-up and distance photos in the longitudinal direction of the validation section should be taken. Any distresses observed should be photographed and noted.

In order to conduct the qualitative pavement condition survey in different locations across the nation, a consistent condition rating method needs to be developed. This qualitative rating method should clearly define how distresses and performance will be measured and/or categorized qualitatively for each surface treatment type. Also, the conditions under which the survey should be conducted should be specified (e.g., conducting the survey when the surface is dry and absent of significant shade, etc.). Existing pavement condition protocol used nationwide will be reviewed and a pavement condition survey will be developed for each surface treatment type in order to assess surface treatment conditions consistently for a wide variety of locations. Additionally, each field section should be monitored to obtain traffic count data, ideally sorted by FHWA vehicle class with measured weight. The collection of traffic data is critical for evaluating the appropriateness of limits based on the traffic levels in the developed EPG specifications.

REFERENCES

Wang, Y. *Improving Pavements with Long-Term Pavement Performance (LTPP): Products for Today and Tomorrow*. Publication FHWA-RD-03-049. FHWA, U.S. Department of Transportation, 2005.

Appendix B. Literature Review – Critical Surface Treatment Distresses and Rankings

CONTENTS

LIST OF FIGURES

LIST OF TABLES

CHAPTER B-1. DISTRESSES IN SURFACE TREATMENTS

In order to carry out the objectives for the EPG specification research, it was first necessary to identify the types of distresses that occur in each PST type and then, from this list of possible distresses, identify those that are most critical and most appropriate for developing the EPG specifications. The critical distresses have been identified for each surface treatment type through a literature review and via feedback from industry experts.

Spray Seal Distresses

Through the literature review, the research team found that the primary distress associated with spray seals is the adhesion between the spray seal and the underlying layer. This distress is sometimes referred to as *wear*, and when it occurs, the spray seal peels up and away from the underlying layer. However, the literature review of spray seals reveals a lack of critical performance measures by which to evaluate spray seal surface treatments. Although surface wear is a performance characteristic associated with spray seals, it is not believed to be a critical issue for spray seal surface treatments. Additionally, bleeding performance in spray seals is not believed to be a significant problem because the spray seal emulsion material is developed at a low viscosity, which allows it to flow more easily into the voids and cracks in the existing surface (Wood et al. 2006). In order to achieve a low viscosity, the emulsion is diluted prior to application and therefore contains a lower amount of asphalt residue than emulsions used in other seal types (i.e., chip seal surface treatments). Moreover, any bleeding issues that occur in the seal are likely to be caused by excess application of the emulsion, which is related to the mix design of the spray seal and not the spray seal emulsion or residual binder performance.

Tracking of asphalt from a freshly applied spray seal surface onto tires of passing vehicles was identified as an issue for spray seal treatments. This tracking is an issue as it affects the rate of emulsion in the wheel path after trafficking. The curing time required or spray seals is a critical aspect of the construction process. Spray seal treatments require the emulsion to cure to a certain level before the surface can be trafficked; the tackiness of the spray seal is indicative of the curing rate. If the road is reopened to traffic before sufficient curing has taken place, tracking of asphalt on tires can occur.

Chip Seal Distresses

The distresses that have been identified as occurring in chip seals are listed below. The following paragraphs describe each distress.

- Raveling
- Stripping (wet raveling)
- Bleeding
- Flushing
- Cracking
- Rutting (multiple seals)

Raveling

Raveling, sometimes referred to as aggregate loss, is an important performance characteristic in chip seal surface treatments. Raveling is defined as the loss of aggregate materials from the surface of the chip seal treatment (Walubita et al. 2005). One of the main problems associated with raveling is the potential for windshield damage from aggregate particles that have been ejected from the chip seal surface and may become projectiles. In addition, raveling reduces the frictional characteristics of the pavement surface, which can result in the loss of skid resistance and cause other associated problems, such as bleeding (Jackson et al. 1990). Although raveling can occur within the wheel path, it is most common in the areas outside of the wheel path where aggregate embedment is not as deep due to less traffic loading (Senadheera and Khan 2001).

Early raveling is a phenomenon that occurs under early traffic loading on a newly constructed chip seal surface. Different binders have varying resistance to early raveling when loaded. Though construction and mixture design factors have a large effect on early raveling, this performance characteristic is also shown to be affected significantly by the emulsion type that is used (Lee 2007).

Low temperature raveling can occur when the pavement temperature drops and the asphalt binder becomes brittle. In this brittle state, the binder can become less able to withstand the force of traffic loading, which can lead to the loss of aggregate particles from the chip seal. This phenomenon occurs both at night when the temperature tends to drop, and during the cold winter season. Researchers have identified that low temperature raveling is a primary distress in chip seal surface treatments (Walubita et al. 2005). This phenomenon is related directly to the residue characteristics of the binder used in constructing the chip seal.

Stripping

Stripping is defined as the loss of the adhesive bond between the asphalt binder and the aggregate in surface treatments. When stripping occurs, the binder generally migrates to the surface and leads to a loss of texture depth and a decrease in the frictional characteristics of the treatment surface. Essentially, trapped moisture is generally responsible for stripping in surface treatments. Moisture trapped within the surface treatment air voids, and within the porous aggregate, separates the bond between the asphalt binder and the aggregate particles (Colas Solutions 2010). This phenomenon leads to a loss of cover aggregate and can lead to other distress types. In short, stripping is raveling that is induced through the combined effects of moisture and traffic, and is therefore referred to as *wet raveling*. Some documents that discuss surface treatments utilize the term *stripping* to describe dry raveling. For this project, the research team considers the aggregate loss that can be attributed to moisture damage under loading as stripping.

Bleeding

Bleeding is characterized by the appearance of a reflective black surface on the chip seal (Roque 1991). This phenomenon can occur due to the over-application of emulsion during the construction phase, the deep embedment of aggregate into the chip seal or existing pavement

surface (Gransberg and James 2005), and/or because of high temperature raveling. In the latter scenario, aggregate particles dislodge from the chip seal and expose the underlying surface that is coated by the asphalt residue and produces the characteristic shiny surface. Bleeding most often occurs in the wheel path of the roadway where the treatment undergoes the most frequent and consistent loading (SHRP 1993). Figure B-1 illustrates bleeding in a chip seal surface treatment.

Figure B-1. Wheel-path bleeding after one year in-service.

The main problem associated with bleeding is the reduction in surface texture and subsequent loss of skid resistance which presents a safety hazard for drivers (Walubita et al. 2005).

Flushing

Flushing is the migration of the asphalt binder to the pavement surface at high temperatures, causing a reduction in the surface texture depth of the treatment. Throughout the literature, the terms *bleeding* and *flushing* are often used interchangeably. Therefore, it is important to define the ways these terms are interpreted and used for the purposes of this research. Both bleeding and flushing involve the same basic performance mechanism, which is the reason the terms are often loosely substituted for each other. Both distresses involve excess binder filling the voids and permeating through to the surface. The difference between the two distresses is the underlying cause for the excess binder at the surface (Lawson et al. 2007). Bleeding is caused due to permanent deformation within the binder under stress loading at high temperatures. Bleeding is directly related to the performance of the asphalt binder. Conversely, flushing is caused by the application of excessive amounts of emulsion such that the road surface is flushed with asphalt binder. Flushing is a design-related issue in surface treatments and is not related to the performance of the binder. Like bleeding, the primary problem associated with flushing is the loss of skid resistance.

Cracking

Cracks that develop in surface treatments allow water to infiltrate the underlying pavement layers can compromise the structural integrity of the pavement system. This

infiltration of water into the pavement system can lead to shear failure and permanent deformation in the asphalt surface treatment over time. Ultimately, if the asphalt base layer is exposed to moisture, pavement failure can occur at accelerated rates (Transit New Zealand 2005). Cracking in surface treatments often occur during the winter season, but these cracks can, in some instances, self-heal in the summer.

Cracking is a broad term that includes multiple types of mechanisms, such as fatigue, thermal/shrinkage, and reflective cracking. Although long-term aged binder performance under repeated loading can be considered a form of fatigue, fatigue cracking is not a performance characteristic assessed in surface treatments due to the thin-layered nature of surface treatments (Epps et al. 2001).

Thermal/shrinkage cracking, also called *transverse cracking*, is thought to be significant in micro-surfaces, for example, because such cracking is related to environmental effects caused by contraction of the asphalt pavement under cold weather conditions. Thermal/shrinkage cracking is associated most closely with the properties of the asphalt binder residue in the surface treatment. Some binders have material properties that are more resistant to thermal cracking than others. As observed for both hot mix asphalt (HMA) binders and residual binders from asphalt surface treatment emulsions.

Researchers consider transverse cracking to be related more to the underlying pavement structure than to the surface treatment itself which provides no structural strength (Walubita et al. 2005). Another form of cracking that occurs in chip seal surface treatments is reflective cracking, whereby cracks from the underlying surface migrate up through the surface treatment. One of the features of surface treatments is their ability to help mitigate reflective cracking on the pavement surface. However, the ability to retard reflective cracking was not determined to be a critical distress to address in the EPG specification.

Rutting

In multilayer chip seal surface treatments, such as triple seals, permanent deformation can occur under repeated loading in the wheel path. This permanent deformation is referred to as *rutting*. The main problem associated with rutting is that during rainy conditions the rut fills with water, which can lead to dangerous hydroplaning issues for vehicles. Structural deficiencies in the underlying pavement layers can also lead to rutting on the asphalt pavement surface, but the research team has focused on rutting performance as it relates to the material properties of the binder used in surface treatment construction (Senadheera and Khan 2001). Any structural deficiencies of the existing pavement surface should be corrected prior to fabricating a surface treatment at a given location.

Determination of Critical Chip Seal Distresses

The following performance characteristics (or distresses) are prioritized and ranked based on the literature review conducted for chip seal surface treatments as well as survey information collected from government highway agencies and asphalt surface treatment practitioners. The performance of chip seal mixtures will be evaluated based on the following distress types ranked from most important to least important:

1) Raveling
2) Bleeding and Flushing

3) Cracking
4) Stripping
5) Rutting

For this prioritization, raveling is considered as one distress across multiple conditions (i.e., intermediate and low temperatures as well as long and short term), even though the mechanisms governing the distress are different at different temperatures. Also, bleeding and flushing are combined here because the survey and literature do not always make a clear distinction between the two. Further justification for these rankings of chip seal distresses is given in the subsequent section of this report.

Survey Results Considered in Performance Characteristic Rankings

In 2005, Gransberg surveyed various pavement maintenance agencies regarding chip seal performance. These agencies were asked to rank the most common distresses that were observed during construction of chip seal surface treatments. Table B-1 provides the results of this survey.

From these survey results, it is seen that bleeding is the most common distress observed in all of the countries included in the survey. This distress is followed by streaking (which is a construction-related and not a material-related distress), and corrugation. Corrugation is a distress that occurs due to shoving in the pavement surface in areas of traffic starts and stops (i.e., intersections). Corrugation is associated with the strength and design of the underlying pavement layers but not necessarily the characteristics of the chip seal directly. Among the material-related distresses, significant cracking and raveling are reported by the survey respondents. One item of note is that the number of cracks reported includes all forms of cracking, and no distinction is made between the specific types of cracking referred to by the respondents.

Table B-1. Survey Results of Most Common Distresses in Chip Seal Surface Treatments (Gransberg and James 2005)

	U.S.	Canada	Australia	New Zealand	South Africa	United Kingdom	Total
Bleeding	54	9	4	2	1	1	71
Streaking	43	5	0	1	0	1	50
Corrugation	41	2	1	0	0	0	44
Cracking	30	5	3	2	0	0	40
Raveling	24	8	1	2	1	1	37
Transverse Joints	29	4	0	0	0	0	33
Longitudinal Joints	17	3	1	0	1	0	22
Potholes	4	6	2	0	0	0	12

Table B-2. In-house Chip Seal Construction Issues Survey Results (Gransberg and James 2005)

Issue	U.S.	Canada	Australia	New Zealand	South Africa	United Kingdom	Total
Early Raveling	18	3	0	1	0	0	22
Early Flushing	15	1	1	1	0	0	18
Flushed Intersections	14	2	0	1	0	0	17
Flushed Patches	9	2	1	1	0	1	14
Raveling Patches	5	1	0	1	0	1	8
Raveling – Evenings	4	2	0	0	0	0	6

Table B-3. Contracted Chip Seal Construction Issues Survey Results (Gransberg and James 2005)

Issue	U.S.	Canada	Australia	New Zealand	South Africa	United Kingdom	Total
Early Raveling	25	6	0	1	0	0	32
Flushed Intersections	15	4	0	1	0	0	20
Early Flushing	13	3	2	2	0	0	20
Flushed Patches	13	3	1	1	0	1	19
Raveling – Evenings	6	3	0	0	0	0	9
Raveling Patches	1	1	0	0	1	1	4

From the same surveyed group, pavement maintenance agencies were asked about the primary performance issues that occurred for those agencies that constructed chip seals in-house as well as those that subcontracted their chip seal construction operations. Table B-2 and Table B-3 present these survey results, respectively. The information presented in these tables indicates that, among the issues related to the construction of chip seal surface treatments, flushing and raveling are deemed the most important.

Additional information with regard to chip seal performance is found in NCHRP Synthesis 342. For this report, a survey was conducted to assess the key distresses identified from visual performance ratings in North America. Figure B-2 presents the results of this survey.

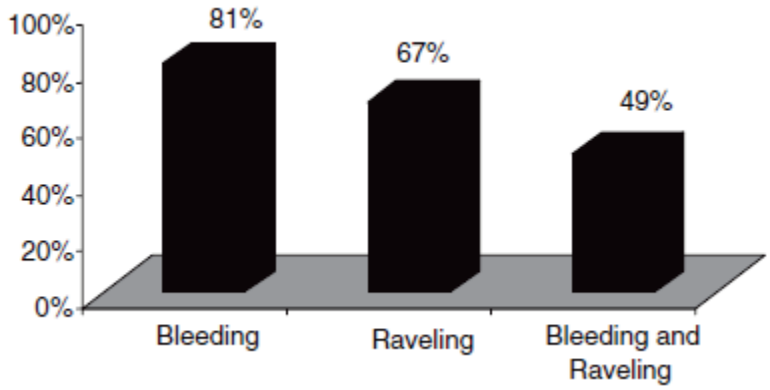

Figure B-2. Most common distress modes identified by survey respondents to NCHRP Synthesis 342 (Gransberg and James 2005).

In this survey, 81 percent of the survey respondents identified bleeding as the most common distress, 67 percent stated that raveling was the most prevalent problem, and 49 percent identified both bleeding and raveling as distresses occurring equally in chip seal surface treatments. This survey provides further support for ranking bleeding and raveling as the most critical performance characteristics in chip seal surface treatments.

Additionally, a survey conducted by the University of Wisconsin-Madison (UWM) on behalf of the Emulsion Task Force (a subcommittee of the Pavement Preservation Expert Task Force) sought to determine the distress modes related to asphalt surface treatments. In this survey, 29 respondents with expertise in this area (17 industry professionals, 4 members of academia, 7 state agency employees, and 1 federal employee) provided feedback. The surveyed group identified chip loss and bleeding as the two main modes of failure in chip seal surface treatments.

Survey results obtained from various sources, such as those presented herein, are strongly reflected in the aforementioned overall ranking of performance characteristics associated with chip seal surface treatments in this report.

Select Literature Review Findings Considered in Performance Characteristic Rankings

In addition to these survey results, the literature review conducted by the research team further solidifies the rankings of the performance characteristics. For instance, other research efforts state that chip seal deterioration occurs because of bleeding, raveling, and oxidation of the binder, which leads to cracking (Epps et al. 2001). The New Zealand chip seal guidelines support this concept as they directly identify texture loss and cracking as the main sources of chip seal failure. More specifically, texture loss as a failure source is defined as premature binder rise, flushing, bleeding, or aggregate loss (Transit New Zealand 2005). Among these critical performance characteristics identified by the literature, bleeding and raveling are still widely considered the two most problematic distresses in chip seal surface treatments for ranking purposes (Benson and Gallaway 1953, Holmgren et al. 1985).

With the surveys and a variety of examples from the literature clearly identifying bleeding and aggregate loss as the most critical performance characteristics in chip seal surface treatments, the literature review for this study sought to identify other distress characteristics that are relevant to chip seal performance. Rutting also has been identified by the research team as a

relevant performance characteristic in chip seal surface treatments, although the literature review and survey information do not support this distress being as critical as bleeding or aggregate loss for chip seals. This omission in the literature of rutting as a critical distress is likely due to the fact that rutting applies only to thick chip seal surface treatments, such as triple seals. Also, permanent deformation performance often is related to the structural strength of the underlying pavement layers, which is not always a material-related performance issue. However, rutting in triple seal surface treatments can be related to binder properties, and therefore can occur independently of the underlying pavement layers' structural strength.

Lastly, stripping has been acknowledged as a significant performance characteristic in chip seal surface treatments. Stripping can occur both in the early stages and in the later stages of a chip seal's useful life. If the asphalt in the surface treatment is displaced by water during wet conditions under traffic loading, a loss of aggregate will result. In many surveys and documents, aggregate loss due to moisture damage in the seal and aggregate loss caused by other mechanisms are combined, i.e., there is no clear delineation between wet and dry aggregate loss. However, for asphalt concrete, the effects of moisture-induced processes are defined separately from non-moisture-induced processes, and it is believed that the industry would be better served by similarly delineating dry and wet aggregate loss performance. It is for this reason that the research team considers stripping and raveling as two separate distresses, even though the net effect is the same (loss of cover aggregate). Efforts to reduce moisture susceptibility traditionally have involved adding anti-stripping agents to the asphalt binder prior to emulsification. Furthermore, laboratory evidence suggests that certain polymer-modified asphalts are effective in reducing stripping characteristics (Shuler 1998).

Summary

Thus, from the survey results and literature review conducted by the research team it is clear that bleeding and raveling are the most critical performance characteristics associated with chip seal surface treatments. Raveling is ranked by the research team as the most critical performance characteristic for chip seal surface treatments because the loss of aggregate particles also leads to bleeding (ranked as the second most critical distress) in the chip seal. Additionally, other distresses, such as stripping and low temperature aggregate loss, are associated with the aggregate retention capabilities of the chip seal surface treatment.

Microsurfacing Distresses

Hanz and Franco (2009) conducted a survey of 87 agencies regarding potential research needs in the field of emulsified asphalts. One question asked in the survey focuses on the failure modes of micro-surfaces. Respondents provided their input on this issue, and the major distresses identified include:

- Raveling
- Surface Wear
- Stripping
- Bleeding
- Flushing
- Rutting/Shoving

- Cracking
- Delamination

Raveling

Raveling, sometimes referred to as *shelling*, refers to the loss of aggregate from a microsurfacing (Wolshon 2005). When the surface of these systems ravels, the surface of the pavement loses skid resistance, and bleeding and flushing may occur with further trafficking. The reasons for raveling are: low binder content in the mix, inadequate rolling during mixing, poor chemistry or incompatibility between the aggregate and binder, infiltration of water, oxidation of the binder, opening to traffic too early, insufficient fines in the mix, debonding of poor quality aggregate, the abrasion action of tires, and poor construction practices (Gransberg 2010, Fugro 2004, Hanz and Franco 2009, and ISSA 2010a).

Surface Wear

Surface wear is in many ways similar to raveling, but differs in that only the fines are lost (Fugro 2004). Visually, this loss of fines creates a smooth surface that produces reduced skid resistance. Like raveling, surface wear can occur due to: poor chemistry or incompatibility between emulsion and aggregate, low binder content in the mix, inadequate rolling during mixing, infiltration of water, oxidation of binder, opening to traffic too early, insufficient fines in the mix, debonding of poor quality aggregate, the abrasion action of tires, and poor construction practices (Gransberg 2010, Fugro 2004, Hanz and Franco 2009, and ISSA 2010a). However, surface wear generally is considered to be a long-term distress, and so, aging of the surface seal can also be an important component in the resistance to surface wear (Fugro 2004).

Stripping

Stripping is the loss of aggregate particles in the presence of moisture. In the case of chip seals, the results of stripping and raveling are identical (loss of aggregates), but the causes differ; so, the two phenomena are separated. The same factors that lead to raveling can also cause stripping, but the presence of moisture may exacerbate the process due to further degradation of the bond between the asphalt binder and the aggregate particles.

Bleeding

According to Lawson (2007), "Bleeding is the upward movement of asphalt in a seal coat or surface treatment resulting in the formation of a film of asphalt on the roadway surface." Bleeding generally occurs during the construction period when the asphalt remains in a liquid form and bonds to the aggregate and tires like glue. Bleeding reduces skid resistance, causes aggregate loss, makes the pavement surface shiny and glossy, causes rutting in the wheel path, and increases pavement noise. The reasons for bleeding include: high emulsion or binder application rate, loss of aggregate from the surface due to a stiff binder and/or low binder content, high temperature, slow setting of emulsion due to high humidity, a seal that is too soft, or a mixing process that includes too much time between applying the asphalt and the aggregate (Lawson 2006, Hanz and Franco 2009).

Rutting

Rutting is a permanent deformation of the pavement within the wheel path. It can occur due to the structural failure of the pavement section or due to an over-accumulation of deformation in the various layers of the pavement (Parker and Brown 1990). Because micro-surfaces are thin layer treatments, rutting is considered when the surface treatment is applied in thicker layers. In some cases, for example when microsurfacing is used to fill ruts, rutting becomes a potential concern and the long-term performance of the pavement depends on rutting resistance in the thick micro-surface layer (Fugro 2004, Gransberg 2010). In these cases, the microsurfacing is placed as a thicker application (see Figure B-3), and rutting in the microsurfacing can cause a safety issue in this thicker layer because water can pool within the wheel path and cause a vehicle to hydroplane. Because micro-surfaces are often placed within already rutted areas, pre-existing structural causes not related to the surface itself may be present that can cause rutting problems. These structural deficiencies should be remedied prior to microsurfacing application.

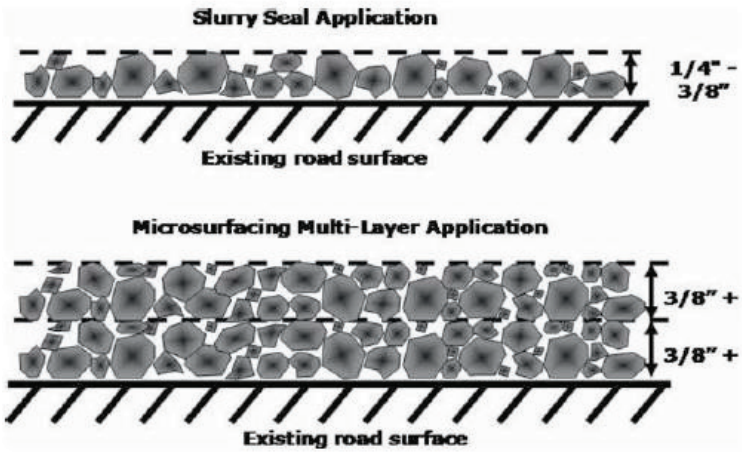

Figure B-3. Single layer and double layer microsurfacing application (Gransberg 2010).

Cracking (Thermal, Reflective, and Age-Induced Cracking)

Thermal cracking occurs due either to a single rapid drop in temperature or due to repetitive temperature cycling (Guylaine and Claude 2000). In either case, the restrained motion of the microsurfacing leads to the build-up of stresses as the temperature drops. If this built-up stress exceeds the strength of the material, or if the stress occurs with regularity (i.e., a fatigue-like process), then cracks will develop. These cracks are characterized as being relatively straight transverse cracks with regular spacing. When such cracks form in the pavement, water can infiltrate the system and accelerate further deterioration (Guylaine and Claude 2000). Another type of cracking that can occur in a microsurfacing is a reflective crack, which can occur when the system is applied to a cracked surface or a jointed pavement. In this case, the cracks on the existing surface propagate upward with time and can show up on the new surface in a relatively short period. Aging of the microsurfacing can accelerate these processes because, as the asphalt ages, it becomes stiff and brittle.

Determination of Critical Microsurfacing Critical Distresses

Based on the literature review regarding micro-surfaces, the research team has ranked the distresses in the following order (from most critical to least critical):

1) Cracking
2) Raveling/Surface Wear
3) Bleeding/Flushing
4) Rutting

Bleeding and flushing are combined into a single distress in this list because, as with chip seals, in-service assessments often are not detailed enough to differentiate the two distresses. Also, the material factors that lead to both distresses are related.

The performance of micro-surfaces is viewed from two perspectives, short-term distress and long-term distress (Fugro 2004). Short-term distresses include flushing, raveling, poor surface texture, and delamination, and long-term distresses include surface wear, stripping, rutting and cracking. This pattern of distress concerns follows from the basic premise for applying microsurfacing, which is that these treatments do not improve structural capacity or prevent reflective cracking, but rather they are used to increase the pavement life by increasing skid resistance, restoring smoothness (e.g., rut-filling), and by sealing the existing joints and cracks. Gransberg (2010) conducted a survey among state and provincial maintenance engineers to determine the key distresses in micro-surfaces. Table B-4 provides a summary of the survey results.

Table B-4. Summary of Common Post-Construction Microsurfacing Distresses

Distress	Number of Respondents		
	U.S.	Canada	Total
Cracking	15	5	20
Streaking	9	2	11
Raveling	6	4	10
Delamination	7	1	8
Transverse Joints	5	3	8
Bleeding	4	1	5
Longitudinal Joints	4	0	4
Corrugation	1	1	2

According to this survey, cracking is the most common distress reported for microsurfacing. This finding corroborates that from Fugro (2004): "[t]he most frequent long-term problems are cracking and rutting, which are most likely not related to the mix-design or construction process but rather the result of inappropriate project selection." Microsurfacing treatments are not intended to be a solution for reflective cracking. If the seal is applied to a heavily cracked section, then the proper construction technique requires that the existing cracks be pre-sealed before the surface treatment is applied (Austroads 2004). The third most reported distress is raveling, which is consistent with the Fugro (2004) survey results that also find raveling to be a primary short-term distress.

Broughton and Lee (2012) performed a survey among 138 Texas Department of Transportation (TxDOT) personnel for accumulating information about microsurfacing in Texas and received 39 responses (i.e., 28%). Based on the survey, the post-construction defects most commonly noted with microsurfacing in Texas are (from most prevalent to least prevalent):

- Cracking
- Delamination
- Raveling
- Pot-holes
- Corrugation
- Surface texture variations
- Streaking
- Transverse joints
- Bleeding
- Longitudinal joints

Like the Gransberg survey, this survey found that cracking is the primary mode of distress for microsurfacing. In addition, Table B-5 shows the defects of microsurfacing observed immediately after construction and within three to five years after construction in Texas; again, crack reflection is the primary reported distress. Table B-5 also indicates that cracking and delamination are included as both short-term and long-term defects, but raveling is considered as only a long-term defect. It is possible, based on these descriptions, that raveling in this case is the same as the surface wear distress described by Fugro (2004).

Table B-5. Common Defects of Microsurfacing in Texas

Immediately After Construction		**3 to 5 Years After Construction**	
Defects	Respondents (%)	Defects	Respondents (%)
Cracking	19	Cracking	27
Streaking	17	Delamination	23
Surface Texture Variation	14	Raveling	11
Delamination	13		

The main purpose for applying a microsurfacing is to improve skid resistance and water proofing (ISSA 2010). Skid resistance depends on the roughness of the surface, and as the surface aggregate wears away (either through surface wear or raveling), this roughness is lost and the skid resistance diminishes (Metcalf 2007). Raza (1994) found that raveling becomes a problem for microsurfacing within a few months after construction. This research also found that stripping can become a problem for microsurfacing when the existing pavement surface is porous and the micro-surface is placed on the pavement without sealing. Broughton and Lee (2012) found that the main failure mechanism of microsurfacing is surface wear, which in their analysis includes the effects of oxidation, abrasion with time, and possibly moisture damage. This conclusion is particularly important because Broughton and Lee also conducted the aforementioned survey that found that in-field personnel believe cracking to be a primary failure mechanism.

Raza (1994) found that bleeding is a distress in several states when microsurfacing is used to fill ruts of more than 40 mm in a single pass. When a rut is filled in this way, separation can occur whereby the coarse aggregate particles remain at the bottom of the seal and the fines migrate to the top, which results in surface bleeding. Bleeding caused by this phenomenon can be avoided by applying the micro-surface in multiple layers when it is used to fill ruts deeper than 25 mm. In addition, when the surface is uneven, a rut box should be used, and the minimum depth for each layer should be no more than 15 mm. Fugro (2010) and Raza (1994) also point out that rutting itself is an important performance criteria for microsurfacing.

REFERENCES

Austroads Incorporated. *Sprayed Sealing Guide.* Publication No. AP-676/104, Sydney, Australia, 2004, p. 104.

Benson, F. J. and B. M. Gallaway. *Retention of Cover Stone by Asphalt Surface Treatments*. Bulletin 133, Texas Engineering Experiment Station, Texas A&M University System, 1953, p. 58.

Broughton, B. and S. Lee. *Microsurfacing in Texas,* Texas Department of Transportation Report No. FHWA/TX-12/0-6668-1, January, 2012.

Colas Solutions, Inc. *Surface Defects*. http://www.colassolutions.com/solutions/defects.html. Accessed November 17, 2010.

Epps, A. L., C. J. Glover, and R. Barcena. *A Performance-Graded Binder Specification for Surface Treatments*. Publication FHWA/TX-02/1710-1, FHWA, U.S. Department of Transportation, Texas Transportation Institute, 2001.

Fugro-BRE/Fugro South, LP. *Phase I Report: Slurry Seal/Micro-Surface Mix Design Procedure*. California Department of Transportation, Sacramento, Contract 65A0151, March, 2004

Fugro-BRE/Fugro South. *Phase II Report: Slurry Seal/Micro-Surface Mix Design Procedure.* California Department of Transportation, Sacramento, 2010.

Gransberg, D. D. and D. M. B. James. *Chip Seal Best Practices*. NCHRP Synthesis 342. Transportation Research Board, National Research Council, Washington, D.C., 2005.

Gransberg, D. D. and D. M. B. James. *Microsurfacing: A Synthesis of Highway Practice*. NCHRP Synthesis 411. Transportation Research Board, National Research Council, Washington, D.C., 2010.

Guylaine, B. and L. Claude. *Thermal Cracking of Asphalt Pavement*. 2nd Eurasphalt and Eurobitume Congress, Proceeding 0267, Barcelona, 2000. http://www.eecongress.org/2000/pdfbook3/session2/Proc0267uk.pdf. Accessed February 15,

Fugro-BRE/Fugro South, LP. (2004). "Phase I Report: Slurry Seal/Micro-Surface Mix Design Procedure," California Department of Transportation, Sacramento, Contract 65A0151

Hanz, A. and C. Franco. *Research Needs in Application of Emulsified Asphalts*. Emulsion Task Force (ETF) Update. Presentation by Modified Asphalt Research Center, Phoenix, Arizona, 2009.

Holmgreen, R. J., J. A. Epps, C. H. Hughes, and B. M. Gallaway. *Field Evaluation of the Texas Seal Coat Design Method.* Research Report 297-1F, Texas Transportation Institute, Texas A&M University System, 1985, p. 174.

International Slurry Surfacing Association (ISSA) (2010). "Inspector's Manual for Slurry Systems," ISSA, Annapolis, MD., 2010a, pp. 106.

Jackson, D., N. Jackson, and J. Mahoney. Washington State Chip Seal Study. *Transportation Research Record*, No. 1259, Transportation Research Board, National Research Council, Washington, D.C., 1990, pp. 1-10.

Lawson, W. D., M. Leaverton, and S. Senadheera. *Maintenance Solutions for Bleeding and Flushed Pavements Surfaced with a Seal Coat or Surface Treatment*. Texas Department of Transportation Research and Technology Implementation Office, Report 0-5230-1, 2007.

Lee, J. and Y. R. Kim. Performance-Based Evaluation of Asphalt Surface Treatments Using the Third Scale Model Mobile Loading Simulator. North Carolina State University, Raleigh, NC. 2007.

Metcalf, S. *Keys to Successful Slurry Seal and/or Micro-Surfacing Project.* Pavement Preservation Task Group (PPTG) Conference, April 2007.

Parker, Jr., F. and E. R. Brown. *A Study of Rutting of Alabama Asphalt Pavements.* Final Report Project No. ST-2019-9, 1990.

Raza, H. *Surface Rehabilitation Techniques: Design, Construction, and Performance of Microsurfacing, Instructor's Guide.* Publication FHWA-SA-94-072, FHWA, U.S. Department of Transportation, 1994.

Roque, R., M. Thompson, and D. Anderson. Bituminous Seal Coats: Design, Performance Measurements and Performance Prediction. *Transportation Research Record 1300*, Transportation Research Board, National Research Council, Washington, D.C., 1991, pp. 90-97.

Senadheera, S. P. and J. R. Khan. *Standardized Seal Coat Terminology Pamphlet.* Texas Department of Transportation. Research Implementation Study Number 5-1787, Center for Multidisciplinary Research in Transportation, Texas Tech University, 2001, p. 4.

Strategic Highway Research Program (SHRP). Distress Identification Manual for the Long-Term Pavement Performance Project. SHRP-P-338. National Research Council. Washington, D.C., 1993. pp. 11-12

Shuler, S., P. S. Khandal, and M. Stroup-Gardiner. *Flexible Pavement Rehabilitation and Maintenance: Design and Construction of Chip Seals for High Traffic Volumes*. 1998, p. 98.

Transit New Zealand. *Chipsealing in New Zealand.* Transit New Zealand, Wellington, New Zealand, 2005.

Walubita, L., A. Epps-Martin, and C. J. Glover. *A Surface Performance Graded (SPG) Specification for Surface Treatment Binders: Development and Initial Validation*. Publication FHWA-TX-05/1710-2. FHWA, U.S. Department of Transportation, 2005, pp. 26-47.

Wang, Y. *Improving Pavements with Long-Term Pavement Performance (LTPP): Products for Today and Tomorrow*. Publication FHWA-RD-03-049. FHWA, U.S. Department of Transportation, 2005.

Wolshon, B., *NCHRP Synthesis 340: Convertible Roadways and Lanes.* A Synthesis of Highway Practice, Transportation Research Board, National Research Council, Washington, D.C., 2004, p. 105.

Wood, T. J., D. W. Janisch, and F. S. Gaillard. 2006. *Minnesota Seal Coat Handbook.* Minnesota Department of Transportation, Office of Minnesota Road Research, 2006.

Appendix C. Mixture Performance Tests for Development of EPG Specifications

CONTENTS

LIST OF FIGURES

LIST OF TABLES

CHAPTER C-1. SURFACE TREATMENT MIXTURE DESIGN

Chip Seal Mix Design

All chip seal specimens were fabricated using the performance-based mix design developed by the research team. This mix design determines the emulsion and aggregate application rate required to achieve a design embedment depth of 50 percent. Chip seals designed using this performance-based method were proven to resist aggregate loss and bleeding in chip seal surface treatments under both laboratory and field traffic loading. This mix design method as well as the laboratory and field validation of this design method is fully detailed in the report by Kim and Adams (2011).

Chip seal specimens for this research were fabricated using an aggregate application rate of 15 lbs/yd^2 as determined from the performance based mix design modified board test to yield a single, uniform aggregate layer for granite aggregate source used throughout this research. Likewise, the performance based mix design was used to determine the appropriate emulsion application rate at which emulsions should perform acceptably in terms of aggregate retention and bleeding resistance. By using the material application rates determined from the performance-based mix design, design-related error in comparing the performance of different emulsions in mixtures was removed from the analysis. It should be noted that the emulsion application rates used for specimen fabrication varied by emulsion type. This variance in emulsion rate was necessary because emulsions often have different residual asphalt contents (or residual asphalt binder remaining after curing is complete). Therefore, in order to remove any variability due to differences in the residual asphalt content between different emulsion types, all specimens in the development of the EPG specification were fabricated to have the same residual asphalt rate (i.e., 67% residual asphalt content) after curing of the emulsion. This design residual asphalt content of 67 percent was obtained from the emulsion used during the laboratory and field validation of the performance-based mix design (Kim and Adams 2011). During the validation of the performance-based mix design it was found that chip seals fabricated using a CRS-2L emulsion with a 67 percent residual asphalt content at a rate of 0.18 gal/yd^2 resisted both aggregate loss and bleeding under laboratory and field traffic loading for the same aggregate source, gradation, and application rate (e.g., 15 lbs/yd^2) used in this EPG specification developmental research. Therefore, the residual asphalt content of that emulsion was used as a baseline upon which to determine the appropriate design emulsion application rates for each emulsion type used in the development of this EPG specification.

In order to keep the residual asphalt content of each specimen consistent between each emulsion type tested in this research for an unbiased comparison, the emulsion application rate needed to be varied slightly such that each specimen has the same residual asphalt rate after curing. A summary of the residual asphalt contents for all emulsions included in this research, and the corresponding emulsion application rates applied is shown in Table C-1.

Table C-1. Residual Asphalt Contents for Chip Seal Emulsions

Emulsion Name	Residual Asphalt Content (%)	Equivalent Emulsion Rate (in gal/yd^2)	Equivalent Emulsion Rate (in grams)
CRS-2 (NC)	63	0.19	36
CRS-2 (F)	64	0.19	35
PP-CRS-2 (A)	60	0.20	37
CRS-2 (A)	60	0.20	37
CRS-2L (NC)	69	0.18	33
CRS-2L (F)	66	0.18	34
CRS-2L/P (C)	68	0.18	33
PP-CRS-2P (E)	63	0.19	36
CRS-2P (A)	62	0.20	36
CRS-2P (E)	67	0.18	34
HP-CRS-2P (E)	68	0.18	33
PP-HFRS-2 (C)	62	0.20	36
HFRS-2 (C)	65	0.19	35
HFRS-2P (A)	60	0.20	37
CRS-1 (B)	62	0.20	36
CRS-1h (B)	60	0.20	37
RS-2 (B)	62	0.20	36

In the table, the equivalent emulsion rates have been rounded to the nearest 0.01 gal/yd^2 and 1 gram, respectively. The residual asphalt content from the CRS-2L emulsion used in the laboratory validation of the performance based mix design was 67 percent. After curing, all specimens fabricated for all emulsion types listed in Figure C-1 are left with a residual asphalt rate of 0.12 gal/yd^2 for an unbiased comparison of binder performance. This residual asphalt content was found by multiplying the performance-validated design EAR of 0.18 gal/yd^2 by the residual asphalt content of 67 percent for that emulsion. The resultant residual asphalt rate after curing for the emulsion used in validating the performance-based mix design, yielded satisfactory performance in terms of both aggregate loss and bleeding in the laboratory validation of the performance based mix design. Although the change in EAR between emulsions is minimal, keeping the residual asphalt amount consistent eliminated a potential variable from the residual asphalt based analysis in the development of the EPG specification. If the difference in residual asphalt contents between binders was neglected, specimens fabricated with some binders would have higher residual asphalt remaining after curing than other binders, which might have biased the performance data.

Single Seal and Triple Seal Specimen Fabrication for EPG specification Development 9-50

For high temperature analysis, multilayered chip seals were used in order to capture both bleeding and rutting performance with the same specimens. Multilayered seals are often used on higher traffic arterials and areas where light cracking has occurred. For this high temperature performance study, triple seal specimens were fabricated using the mix design optimum rates for each of the three layers of chip seal and traffic loaded using MMLS3 at the test temperature consistent with the climatic condition being evaluated.

Meanwhile, for testing at the intermediate temperature and low temperature, single-seal Vialit specimens were fabricated in order to capture the aggregate loss performance of the seals. These specimens were designed in accordance with the performance-based mix design procedure as well.

Microsurfacing Mix Design

The components of the microsurfacing mixture (aggregate, emulsion, water, mineral filler, and additives) were proportioned according to the International Slurry Seal Association (ISSA) mix design. Emulsion residue and aggregate contents were kept constant for all mixtures produced. According to ISSA A143, the residue content should be within 5.5 to 10.5 percent of dry aggregate, mineral filler should be between 0 percent and 3 percent of dry aggregate, additives should be added as needed to control the breaking and curing times of emulsion (Caltrans 2009), and water should be in sufficient quantity to allow for proper consistency (workability) of the mixture. For this microsurfacing research, the mixture proportions were selected as 9 percent residue content and 1 percent mineral filler (cement). Water was added as needed to achieve sufficient mixture consistency. For the emulsions used in this study, the required water content ranged from 10 percent to 12 percent of dry aggregate weight, except for quick setting emulsions where required water content was approximately 15 percent to 16 percent of dry aggregate weight. Quick setting emulsions required more water because breaking occurs quickly and does not allow sufficient time to mix and pour the microsurfacing mixture into the test mold.
As with the chip seal mix design approach, all specimens were fabricated such that the residual asphalt content was the same for all specimens after curing.

CHAPTER C-2. SPECIMEN FABRICATION

Chip Seal

All chip seal specimens tested during this research were fabricated using a specimen fabrication method developed by the research team which closely simulates the field chip seal fabrication process. This method, referred to as ChipSS fabrication, utilizes specialized and customized equipment developed over several years of chip seal research efforts at North Carolina State University (NCSU). The first step in constructing chip seal specimens is to obtain felt paper in the desired size and shape of the chip seal specimen to be fabricated.

Typically, this felt paper is 305 mm x 356 mm, on which 178 mm x 305 mm samples are fabricated. In order to make the 178 mm x 305 mm samples on the felt paper, a template is placed on top of the sample during the emulsion spraying process to confine the emulsion within the desired area. A paint spray gun is used to apply the emulsion to the felt paper in a manner that simulates the emulsion being sprayed from the truck in the field. It is recommended that this paint gun sprays at a rate of 20.4 liters per hour or higher (27.3 gallons per hour or higher for polymer-modified emulsions because they are more viscous than unmodified emulsions). Lastly, a weight scale is used to keep track of the amount of emulsion that has been sprayed/spread onto the felt paper to ensure accurate EARs during the sample fabrication. A few hours prior to beginning the emulsion application process, all the paint sprayer parts are put into the oven at the same temperature (60°C) as the emulsion being used for fabrication. This step is important to ensure that the parts do not cool the emulsion during the fabrication process. The emulsion spraying process is shown in Figure C-1.

Figure C-1. Chip seal emulsion spraying procedure.

In the emulsion spraying process, it is important to apply the emulsion as close to the target EAR as possible and to apply the emulsion for a consistent amount of time from specimen to specimen. For example, the emulsion should be applied in less than 60 seconds using the paint sprayer and typical CRS-2 emulsion. The time it takes to remove the emulsion from the oven, stir it gently, and then load it into the paint sprayer should also be less than 60 seconds to minimize any decrease in temperature.

Following the emulsion application step, the felt paper with freshly applied emulsion is positioned beneath the chip seal aggregate spreader, named ChipSS. This aggregate spreader consists of three main parts: the box, the rotating drum, and a moving table. The box is mounted to the table, and the rotating drum is located outside the bottom of this box. An electric motor drives the table along the ChipSS device. The speed (box speed) is controlled by a speed controller attached to the motor. The drum rotates as the table moves, and its

speed is controlled at a rate that is dependent upon the drum speed setting as well as the aggregate type being used. An optional auger attachment can be mounted inside the box to reduce segregation when using fine aggregate stockpiles. As the table moves across a sample, the bottom of the box is opened manually to a constant opening size using a lever handle to allow the aggregate chips to fall onto the sample surface. The rotating drum ensures that the particles are spread uniformly. ChipSS is used to spread the aggregate after the emulsion has been applied to the felt paper. Only the section of the felt paper covered by emulsion will retain the aggregate, and the excess applied outside of the sample area is swept off using a small brush. Through this process, a single layer of aggregate is obtained that completely covers the specimen at the desired rate. Figure C-2 presents the process of ChipSS fabrication.

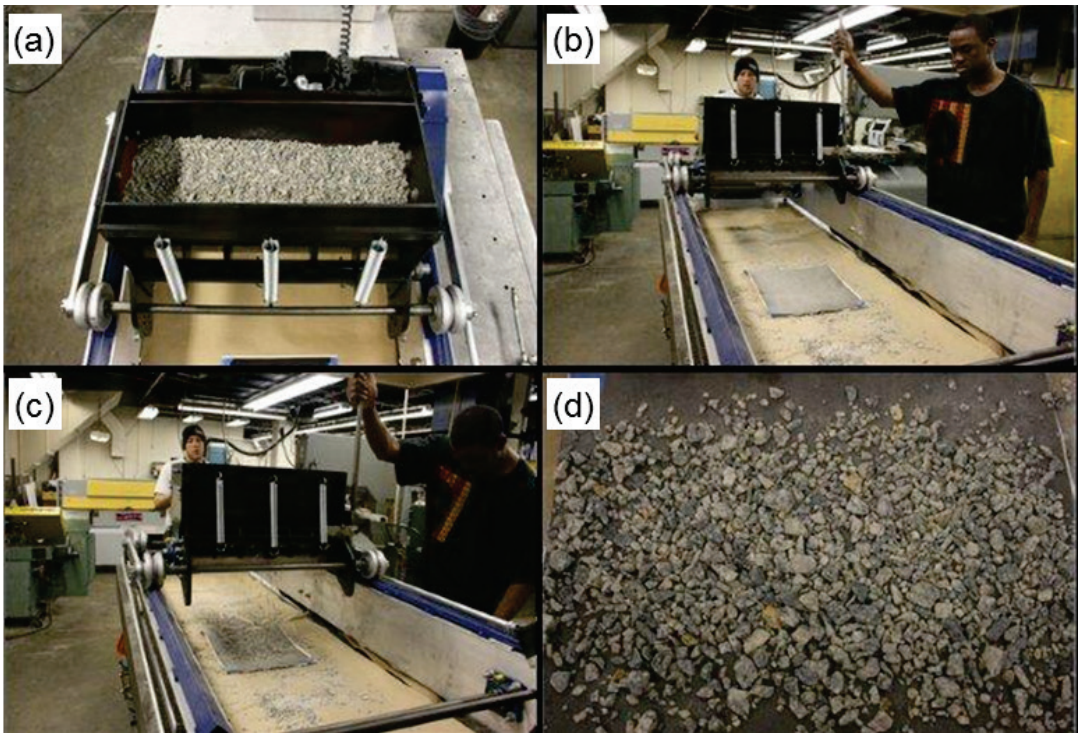

Figure C-2. ChipSS aggregate spreading machine and procedure: (a) box filled with aggregate, (b) ready to spread aggregate on the felt disk, (c) spreading aggregate on the felt disk, and (d) spread aggregate on the felt disk.

Prior to starting the sample fabrication process, ChipSS is calibrated to drop the target amount of aggregate required to achieve the desired aggregate application rate (AAR) for the sample being fabricated. The AAR is controlled by two parameters: the box speed and the drum speed. The box speed is the speed at which the box moves across the sample, and the drum speed is the speed at which the rotating drum (located inside the aggregate hopper) rotates and releases the aggregate. As the box speed is lowered, the AAR increases. This method is considered a better alternative than manually spreading the aggregate because spreading the aggregate by hand tends to pick up mostly coarse aggregate particles, which

will alter the gradation of the aggregate source being used for specimen fabrication. The ChipSS machine allows a consistent and automated method of aggregate spreading that minimizes gradation tampering and variations in manual spreading techniques.

When the spreading process is complete, the next tasks in ChipSS fabrication are compaction and determination of the final AAR. The device used to compact chip seal specimens is shown in Figure C-3. The compactor itself is rotated back and forth on top of the chip seal sample to ensure the particles are fully embedded into the hot asphalt emulsion. This device is meant to simulate the compactor that follows behind the aggregate truck in the field, and so it is used in conjunction with a rubber mat in order to replicate a combination roller (Lee and Kim 2008). Using this device, the steel applies compaction force while the thin rubber material helps minimize the breakage of aggregate particles that occurs when the steel wheel alone is used for compaction. The compaction procedure involves three compaction passes across the horizontal face of the sample, and three additional compaction passes perpendicular to the first three passes.

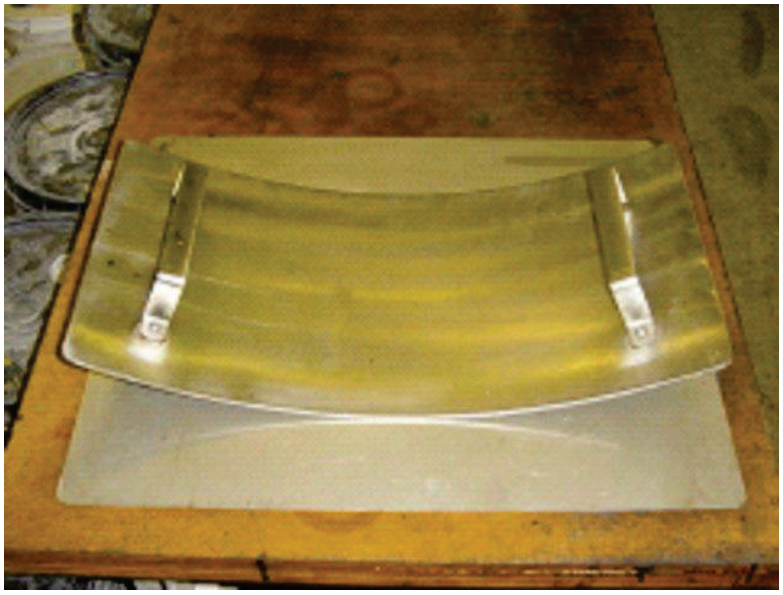

Figure C-3. Chip seal sample manual compactor.

Following compaction, the newly fabricated sample is then cured in an oven at 35°C for 24 hours to simulate the full field curing process. After the curing period is complete, the specimen is ready for testing.

The sample fabrication process outlined in this section was used for all chip seal mixture specimens tested in this research.

Microsurfacing Sample Fabrication

Since the microsurfacing fabrication process varied as a function of the mixture test method being conducted, the sample fabrication methods for each test method are provided in Chapter C-3 along with the associated test method description.

CHAPTER C-3. MIXTURE PERFORMANCE TEST METHODS

This section details the mixture performance test methods utilized in this research for testing chip seal and microsurfacing treatments.

Chip Seal Mixture Test Methods

Third-Scale Model Mobile Loading Simulator (MMLS3)

The third-scale model mobile load simulator (MMLS3) simulates the traffic loading conditions experienced by asphalt surface treatments under field traffic loading conditions. The MMLS3 applies repeated wheel loads to the asphalt surface at a constant and accelerated rate (990 wheel loads applied every 10 minutes) and causes the surface treatment to respond similarly to its response in the field. The machine itself consists of a rotating drum that drives a train of buggies across a test sample mounted beneath the machine. The train includes a total of eight buggies, four of which have third-scale wheels (relative to standard dual tire wheels). A maximum of three samples (356 mm length per sample) can be secured underneath the MMLS3 for testing at one time. The cumulative sample length of 1,066.8 mm is the effective loading length for the MMLS3. With a wandering width of 177.8 mm, the effective MMLS3 loading area is 7,467.6 mm. The MMLS3 test procedure and equipment are shown in Figure C-4. The one departure from the picture shown in Figure C-4 (d) is that the top of the MMLS3 temperature chamber is covered during testing to maintain the test temperature.

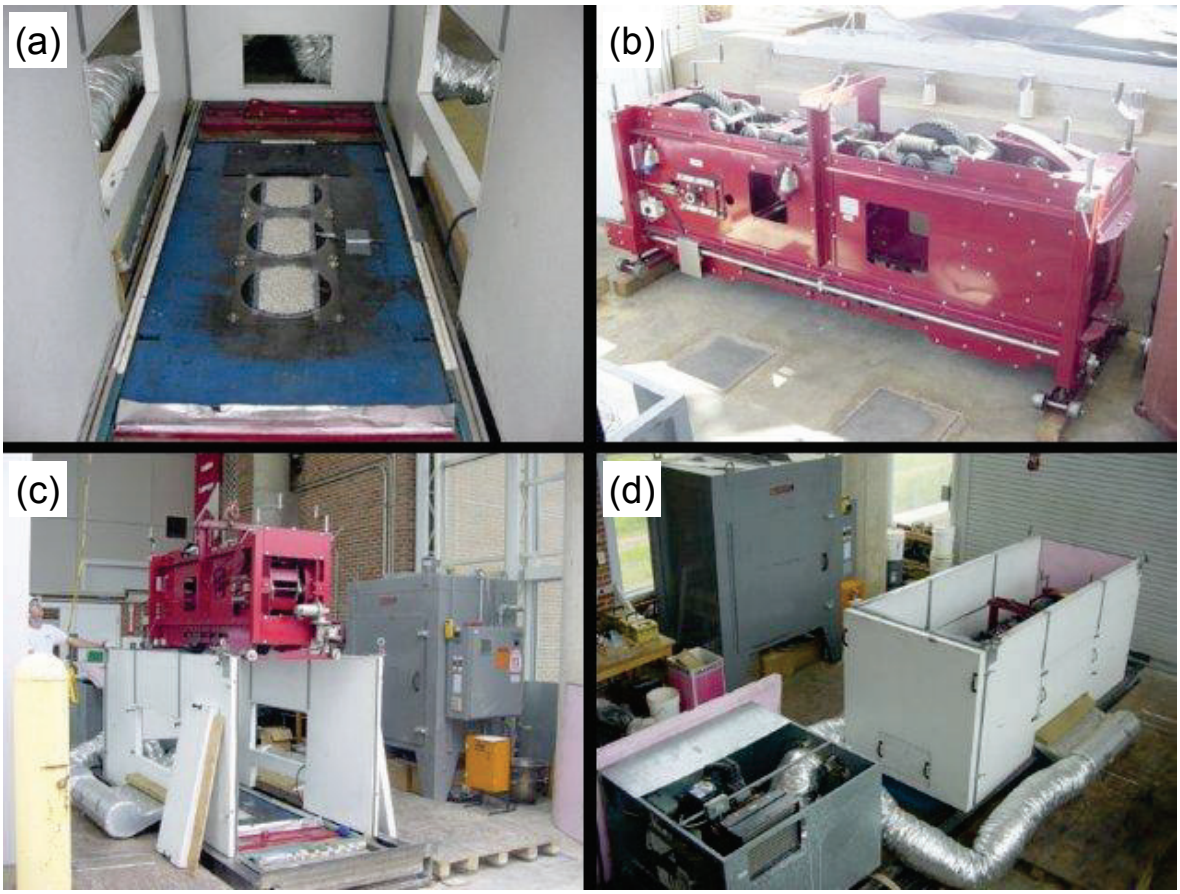

Figure C-4. MMLS3 test preparation: (a) installation of specimens on steel base, (b) side view of MMLS3, (c) positioning the MMLS3 in the temperature chamber, and (d) complete MMLS3 test setup.

For MMLS3 testing, specimens were fabricated through a procedure that closely simulates the surface treatment fabrication in the field for chip seals; and that follows the current design requirements for microsurfacing. The test method allows for complete temperature control between approximately 10°C and 60°C using an environmental chamber and cooling/heating unit. The MMLS3 test has been found in previous research to show a strong correlation with field traffic loading and resulting texture depth changes in the field.

Through previous research efforts, a straightforward methodology that requires little experience has been developed for running the MMLS3 test. Specimens are first secured underneath the MMLS3 machine to a steel base using screws or clamps to fix the specimens to the base, and then the test temperature is set on the heating unit control box. After allowing adequate time for the temperature to reach its target, green and red buttons on the control box are pressed to start and stop the machine, respectively. The machine itself requires two different control/power sources both emanating from the single control box. One plug provides power to the motor that rotates the wheels on the machine to traffic load the specimens, and a second plug powers the motor that controls the wandering of the

machine. Wandering is utilized for raveling testing, but not for bleeding and rutting evaluation.

The ability of the MMLS3 to replicate field processes has been shown in several research efforts (Lee and Kim 2008, Adams and Kim 2013). One such effort correlates the mean profile depth (MPD) of chip seal surface treatments that were trafficked under MMLS3 traffic loading with the MPD of specimens loaded under actual field traffic. The MPD is a parameter that is representative of the exposed texture depth of a chip seal surface treatment and is inversely related to the embedment depth. Transit New Zealand (2005) defines the MPD as:

$$MPD = \frac{Peak\,level\,(1st) + Peak\,level\,(2nd)}{2} - Average\,level \tag{1}$$

Figure C-5 shows the various chip seal parameters that make up Equation (1). In the diagram, the MPD clearly indicates the roughness (i.e., macro-surface texture) and aggregate exposure depth of the chip seal. Roughness is important, because it provides the skid resistance and friction needed for vehicles to brake adequately. The aggregate exposure depth is important because it is a function of the aggregate embedment depth, which is the most important factor that controls the aggregate loss and bleeding performance of chip seals. A small MPD value indicates the likelihood of bleeding and skid resistance problems. A large MPD value after construction indicates the possibility of excessive aggregate loss and, therefore, bleeding due to aggregate loss.

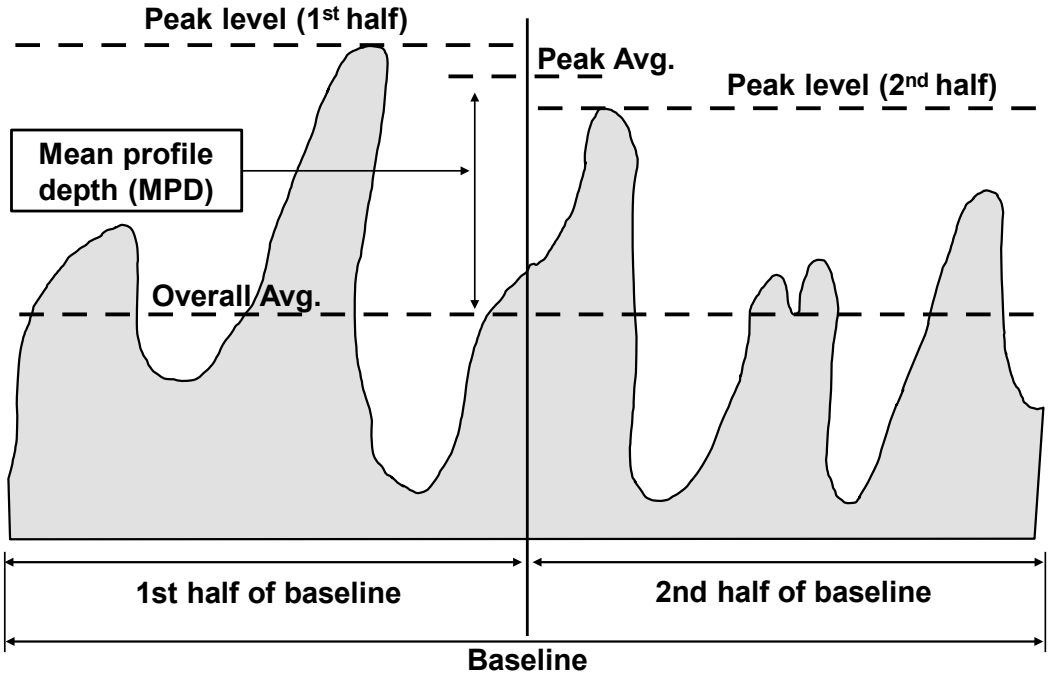

Figure C-5. Schematic diagram of the mean profile depth determination.

To obtain the data used to calculate the MPD, the research team developed a three-dimensional (3-D) laser profiler to obtain surface texture information. The laser itself measures the distance between the sensor and the pavement surface in both the longitudinal and transverse directions of the pavement and produces a 3-D map of the pavement surface texture for analysis. Specifically, the laser is setup to scan a 100 mm line on the pavement surface in the transverse direction and obtains one distance measurement every half millimeter along that 100 mm line. After each 100 mm. line scan, the laser moves 0.5 mm in the longitudinal direction, parallel to the wheel traffic direction, and takes another 100 mm line scan in the transverse direction. This process if repeated until the end of the scan area is reached.

The extracted field specimens and field test sections used for this surface texture analysis by Adams and Kim (2013) were constructed using both granite and lightweight aggregate, and were fabricated by a North Carolina Department of Transportation (NCDOT) pavement maintenance unit (PMU) experienced in chip seal construction. In all cases CRS-2L emulsion was used in the construction. The test sections were fabricated on roads with volumes (in ADT) of 1,000 and 5,000 vehicles/day. For each section constructed, specimens were extracted for laboratory testing from part of the test section, and on-site field testing was conducted using the 3-D laser profiler on the other part of the section. The extracted specimens were taken back to the laboratory to be trafficked using the MMLS3 machine, whereas the on-site sections were left in place and trafficked under regular vehicular loading. In both cases, texture depth was measured as a function of time. In total, eight field-

constructed specimens from each section were used to measure the changing MPD under MMLS3 accelerated wheel traffic loading. In the field, the 3-D laser profiler was used to take MPD measurements during the first few days following construction and also in the subsequent weeks following construction to obtain data similar to those for the MMLS3 traffic-loaded specimens. For this experiment, traffic count data were acquired for one year after construction and were converted (based on the FHWA vehicle class information) to equivalent wheel passes that could be compared directly to the known wheel passes from the MMLS3 machine. Figure C-6 and Figure C-7 present partial results from the experiment.

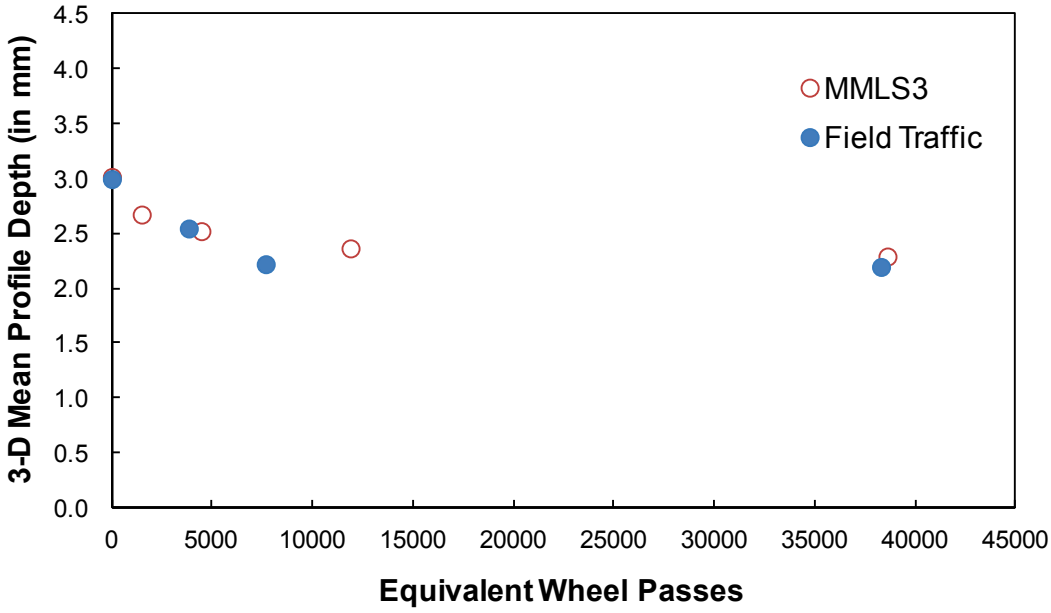

Figure C-6. Texture depth correlation between MMLS3 and field traffic-loaded granite specimens (Adams and Kim 2013).

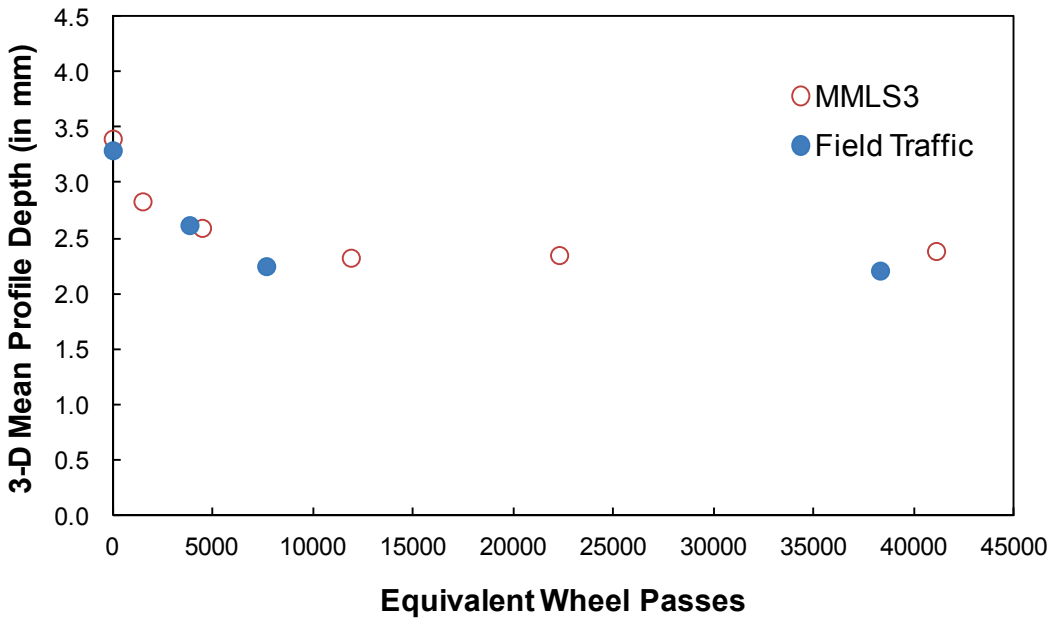

Figure C-7. Texture depth correlation between MMLS3 and field traffic-loaded lightweight specimens (Adams and Kim 2013).

The data presented in Figure C-6 and Figure C-7 indicate that the MMLS3 traffic loading correlates strongly with the field traffic loading with regard to the changes in MPD. Because the exposed texture depth of the chip seal is related to roughness and skid resistance, as well as to the bleeding and aggregate loss characteristics of the seal, the results show the MMLS3's ability to simulate field traffic in the laboratory setting.

MMLS3 for Raveling Evaluation

The aggregate retention performance of chip seal surface treatments can be assessed using the MMLS3 test method. In these tests, measurements of aggregate loss are taken at 10, 20, 40, 80, and 160 minutes in order to study both short-term and long-term raveling. Taking the measurements involves stopping the machine, removing the specimens from the base, and measuring the weight of the specimen as a function of loading time. In these tests, the MMLS3 is allowed to wander. The wandering occurs over a width of 178 mm and over a time span of 10 minutes. Thus, in 10 minutes the machine traffics all parts of the sample evenly. For this reason, no measurements are taken at a time interval less than 10 minutes because the sample would not have been evenly trafficked.

MMLS3 for Bleeding Evaluation of Chip Seals

The MMLS3 testing machine also can be used to evaluate bleeding and flushing in a chip seals. The basic process of fabrication and sample mounting used in raveling studies are followed also in the case of bleeding and flushing evaluation. Like raveling, the tests are

conducted with traffic wandering; however, the test temperature is much elevated. The MMLS3 bleeding test is carried out after first conducting a 120-minute raveling test at 25°C. At the completion of the raveling test, the samples are conditioned for one hour at the high temperature EPG being tested, and then samples are loaded by the MMLS3 with bleeding measured at different time intervals during the loading. This process simulates the bleeding potential of chip seals during the summer months in the field. Performance is quantified using digital analysis of images taken before loading, and at different time intervals throughout the loading period. It is important to note that every time the sample is removed from the MMLS3 temperature chamber to capture a digital image, it should be allowed sufficient time to allow the chamber and specimen to return to test temperature prior to resuming MMLS3 loading. Figure C-8 presents the digital image processing flowchart.

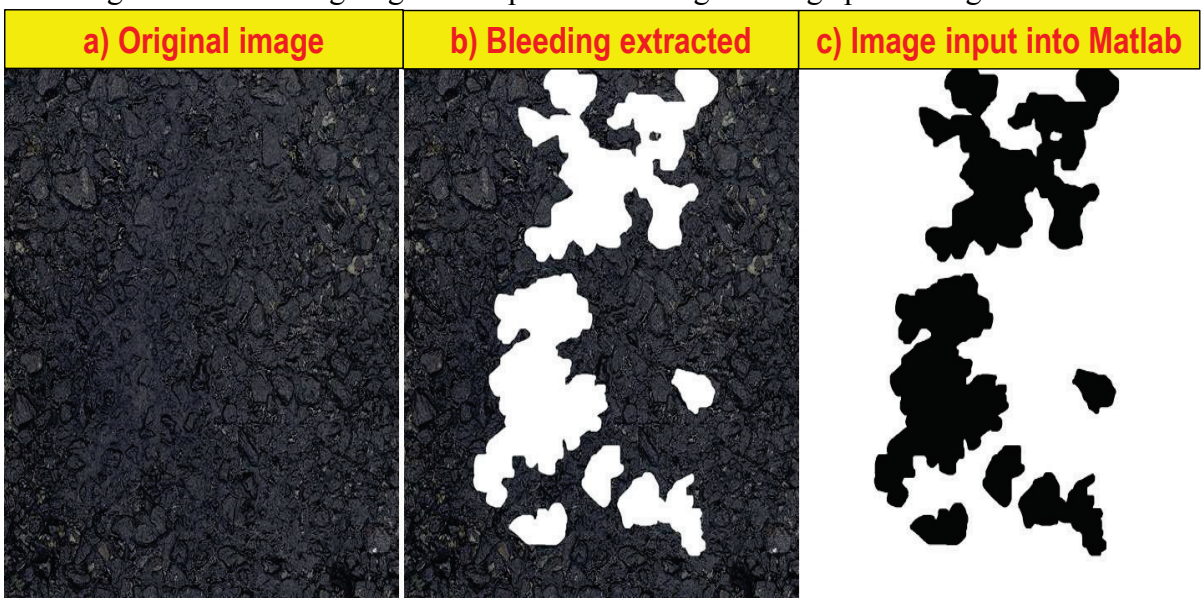

Figure C-8. Image processing procedure for chip seal specimens: (a) original scanned specimen image, (b) identification of bled area, and (c) bleeding input into Matlab software for pixel-based image processing.

As shown in Figure C-8, the chip seal sample was scanned after high temperature MMLS3 testing. To scan the specimen surface without disturbing the chip seal surface, the scanner is turned upside down and mounted over the specimen at a fixed height. The areas of the image where bleeding had occurred were identified and extracted from the original image into a new image layer. The extracted bleeding layer is then processed via MATLAB code designed to determine the percentage of the image area that is black (or bled). The percentage of bleeding for the specimen is obtained simply by dividing the area of bleeding on the chip seal specimen by the total area of the specimen. The percentage of bleeding is automatically output from the MATLAB processing as the percentage of black pixels to white pixels in the specimen area.

MMLS3 for Multi-Layered Chip Seal Rutting Evaluation

Rutting can be defined as the accrual of irrecoverable strains, or plastic deformation, within the wheel paths of a pavement. Rutting can occur in thick chip seal surface treatments (double and triple seals) and can manifest itself as either a later displacement of the asphalt-aggregate mixture, and/or as the material consolidates under traffic loading. Rutting, like bleeding, is evaluated at elevated temperature conditions. Samples are mounted beneath the MMLS3, conditioned to the proper testing temperature, and then tested for up to 250,000 cycles (approximately 42 hours of continuous loading). During these experiments the MMLS3 is not allowed to wander. The rut depth is measured periodically using a profilometer, which measures the transverse profile of the pavement surface every 10 mm (Kim et al. 2005). This method has been used to assess the rutting performance of triple seals constructed with different emulsion types. In these experiments, the average rut depth of a triple seal is measured and compared between emulsion types.

Figure C-9 shows the cross-sectional image of an MMLS3 traffic-loaded specimen. This illustration helps explain the rutting mechanism associated with chip seal surface treatments. In theory, volume densification of the chip seal material and shear flow cause rutting and permanent deformation in the chip seal under MMLS3 traffic loading, which can be seen in Figure C-9. The changed density and shear flow create a rut in the chip seal structure, even though the triple seal is a relatively thin asphalt layer.

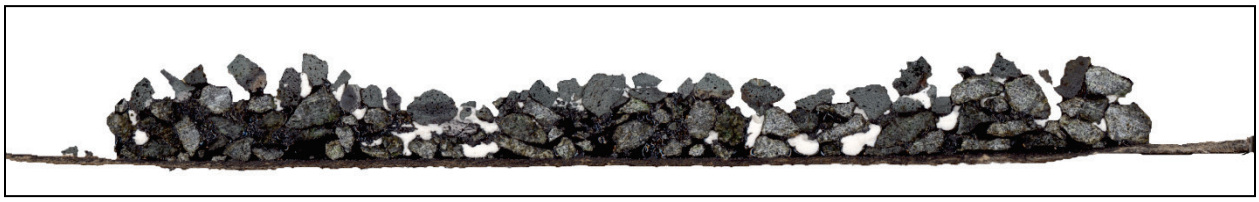

Figure C-9. Cross-section of a triple seal specimen after MMLS3 loading (Lee and Kim 2007).

Figure C-10 shows a schematic diagram of a typical cross-section of a triple seal before and after the MMLS3 rutting test is conducted. In the figure, various areas of interest in the direction transverse to traffic are defined. The area identified as the trafficked area is the wheel path of the MMLS3. The shear flow area represents the area of the specimen on either side of the rut. Figure C-10 shows the humps that are created as the material is displaced due to the shear flow of the material under MMLS3 loading. The average profile value within the trafficked area is calculated to obtain the rut depth. That is, the rut depth is determined by measuring the difference between the highest point on the side humps and the average of the profiles of the trafficked area.

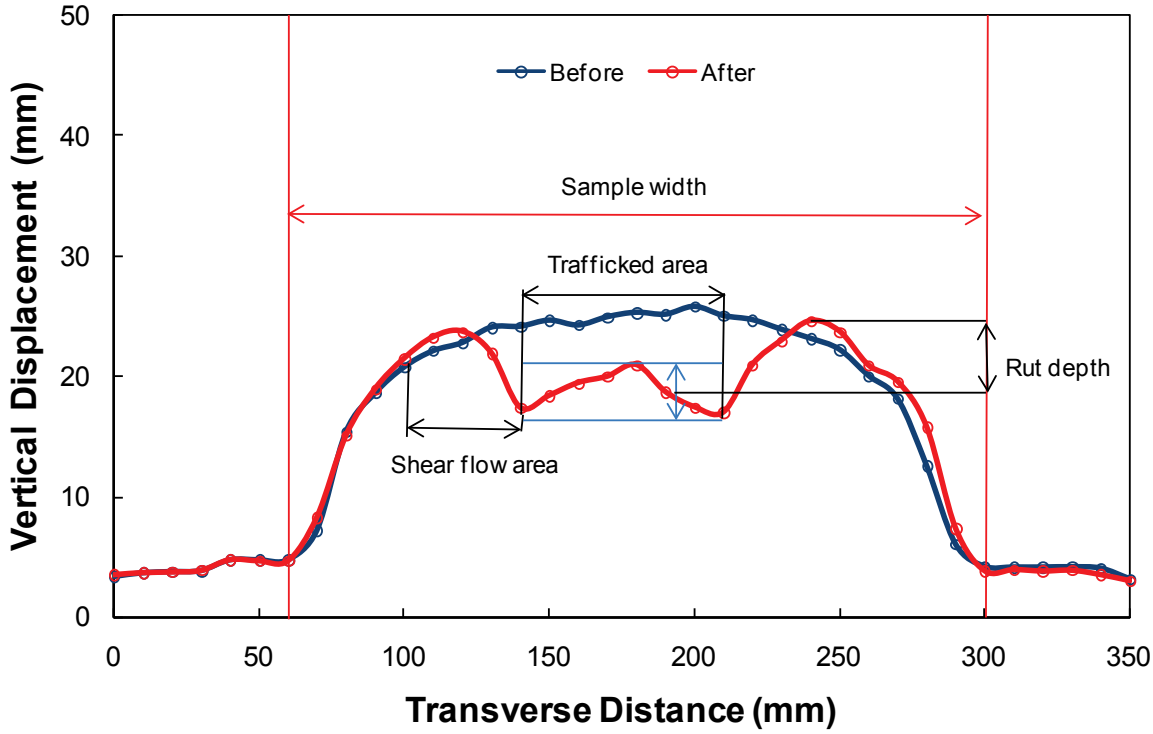

Figure C-10. Schematic diagram of a typical cross-section of a triple seal.

Vialit Test

The Vialit adhesive test uses both gravity and impact to measure the aggregate retention capabilities of a chip seal. The test method is published as British Standard EN12272-3 (2003), and is relatively simple to perform. A sample is fabricated using the ChipSS method. The only difference between the MMLS3 sample fabrication procedure and fabrication procedure for Vialit is that, instead of fabrication on felt paper as with MMLS3, the Vialit samples are fabricated on 203 mm x 203 mm square steel plates. Like the MMLS3 test samples, the Vialit test samples are cured at 35°C for 24 hours before testing. Prior to the test, but after curing the samples, a flip-over test is conducted (ASTM D7000). The purpose of this test is to remove any excess aggregate from the surface. In this procedure, the sample is turned at a 90° angle, and the entire area of the specimen is brushed lightly once with a soft-bristle brush. This process simulates the field sweeping and removal of excess aggregate in field construction.

After the flip-over test, the samples are weighed and conditioned to the proper test temperature. Once a sample has been fully conditioned, it is turned 180° and placed face down in the Vialit adhesion apparatus, shown in Figure C-11. A steel ball (500 ± 5 g) is then released from its resting position so that it falls vertically 500 mm and strikes the back of the sample plate. The most complex part of the test is ensuring that the ball is dropped onto the plate, then reloaded into the holding position above the specimen and then dropped two more

times within the 10-second time limit required for a valid test. After all of the drops have been completed, the sample is re-weighed to determine the amount of aggregate that was lost during the test.

Figure C-11. Vialit test apparatus.

Vialit Testing at Low Temperatures

A modification of the standard Vialit test was also used to quantify chip seal raveling performance at low temperature. The plate used for low temperature Vialit testing is 6.35 mm thick with 12.7 mm lip height, which is different than the standard Vialit plate, and the surface of the plate is roughened, using a sander of a certain pattern and grit level, in order to improve bonding between the emulsion layer and Vialit plate during low temperature testing. This modified Vialit plate was selected based on the recommendations of Jordan and Howard (2011) as they found it to prevent debonding problems often encountered when performing the Vialit test at low temperature using the standard plate. The plate surface area is approximately 200 mm by 200 mm, with a ball weight of 500 ± 5 grams.

Specimen fabrication was performed inside of a 4.88 m by 2.74 m greenhouse built with wood and polycarbonate glass inside of the laboratory. The greenhouse is used to maintain a consistent temperature throughout the entire specimen fabrication process for chip seal surface treatments. To prepare specimens, emulsion and steel plates were preheated inside of an oven at 60°C. Hot emulsion was then poured on the heated plate at the target application rate. The plate with emulsion is then tilted to spread emulsion on the plate uniformly, and allowed to settle for 15 seconds prior to aggregate application. The plate with

emulsion is then placed under the ChipSS spreader to apply oven dried aggregates on the plate.

The compacted specimens were cured at 35°C for 24 hours, following ASTM D7000 recommendations. After curing, specimens are flipped 90° and a soft brush is used to brush away loose aggregate. Lastly, specimens were then placed inside of an environmental chamber at the low test temperature for four hours based on the recommendations of Jordan and Howard (2011). The specimen is then removed from the oven and tested in less than 30 seconds to avoid any significant increase in specimen temperature.

Vialit Height Adjustment Study for Low Temperature Testing

The standard drop height in the Vialit test is 50 cm. Initially, this drop height was used for the low temperature testing of chip seals. However, it was found that the impact was too harsh at this drop height to indicate representative low temperature aggregate loss performance. The result of testing at the standard drop height of 50 cm is shown in Figure C-12, which displays severe aggregate loss and debonding in a chip seal sample tested at the low temperature using the standard Vialit drop height. Based on this finding, a study was developed to determine an appropriate drop height for low temperature testing that captures aggregate loss at the low temperature without significant debonding between the chip seal layer and the Vialit plate. Jordan and Howard (2011) successfully tested chip seals at a low temperature using the standard drop height. However, Jordan and Howard fabricated specimens using 100 pieces of aggregate that were identical in size and then placing these aggregate particles on emulsion in a 10 by 10 aggregate matrix by hand, as observed in Figure C-13(a). However, herein, chip seal samples were prepared to better replicate chip seal specimens with realistic aggregate gradations using the ChipSS aggregate spreader, as shown in Figure C-13(b). The gradation used in this research is the gradation of the granite aggregate that is used extensively for chip seal construction in North Carolina. This difference in the aggregate gradations used in the sample fabrication could have led to the difference in failure mode when a drop height of 50 cm was used.

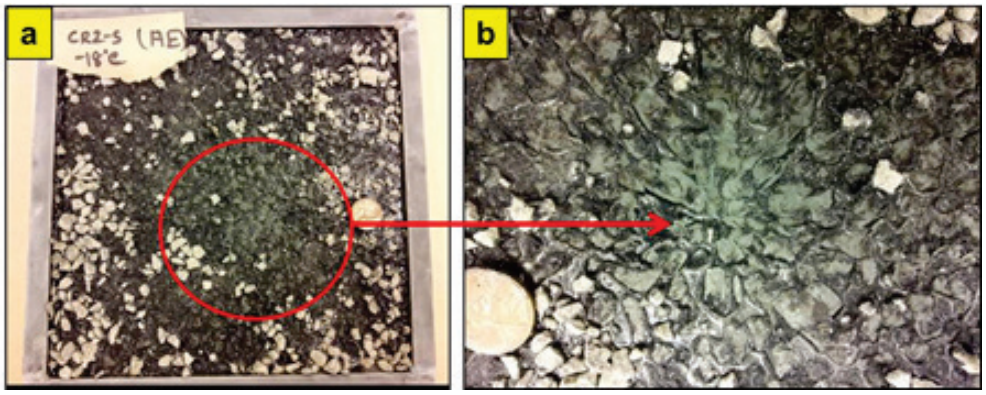

Figure C-12. (a) Tested specimen at -18°C with 50 cm height and (b) close view of tested specimen.

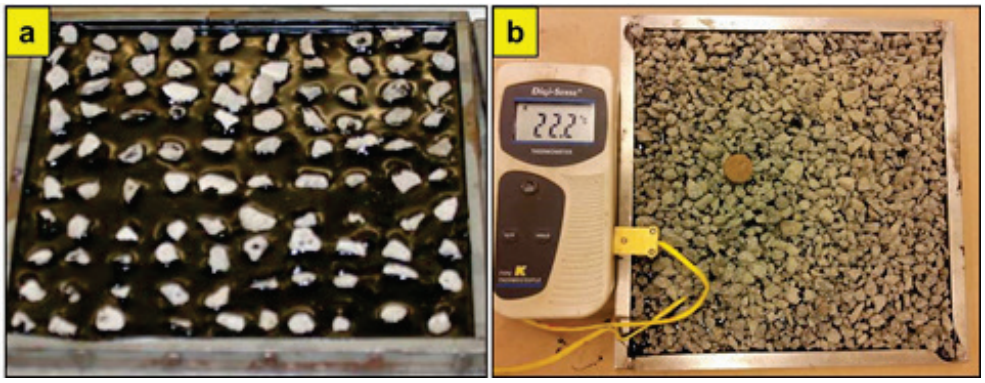

Figure C-13. (a) Specimen with 10 by 10 matrix format and (b) specimen obtained with ChipSS spreader.

In order to determine the appropriate drop height, a systematic study of chip seal specimens fabricated using two emulsions (one modified and one unmodified) where the drop height and temperature were varied was conducted. The resultant failure mechanism under each condition was observed and used to evaluate the drop height. Because the standard drop height of 50 cm resulted in excessive debonding of the chip seal from the Vialit plate, the drop height needed to be lowered in order to eliminate the debonding problem. Therefore, the head in the Vialit test frame was lowered to various heights, as shown in Figure C-14, and tests were conducted using replicate chip seal Vialit specimens. The height was lowered continuously until adhesive failure (or debonding) was no longer observed between the plate and chip seal layer. The results of this study are presented in Figure C-15 and are based on the observed failure mechanisms. The results show that when the Vialit drop height is reduced to 12.5 cm, cohesive failure occurs under all conditions evaluated while the procedure still distinguishes between the raveling performance of the modified and unmodified emulsion types at low temperatures of 0°C and 18°C. Thus, a drop height of 12.5 cm was selected for use in low temperature Vialit testing in this research.

The Vialit height study also served as an initial evaluation of the procedure's ability to capture low temperature raveling. The results shown in Figure C-15 demonstrate expected trends with respect to emulsion type and temperature. The modified emulsion chip seal consistently demonstrated lower aggregate loss than the unmodified emulsion chip seal. In addition, the results demonstrate that aggregate loss increases as the temperature is reduced, which follows intuition, as the binder becomes more brittle when the temperature is reduced and thus is more prone to fracture under impact loading.

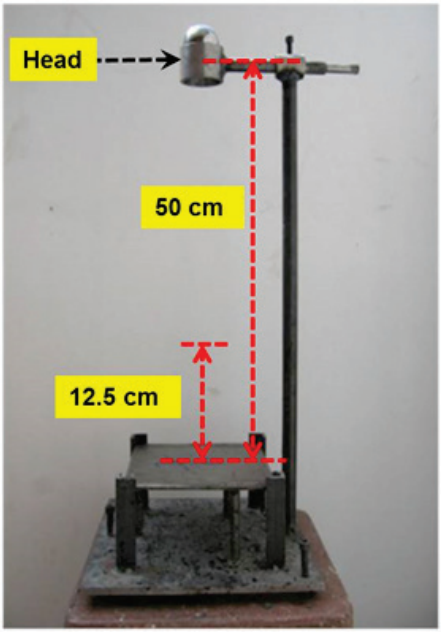

Figure C-14. Vialit test device showing standard height versus modified height used for low temperature testing.

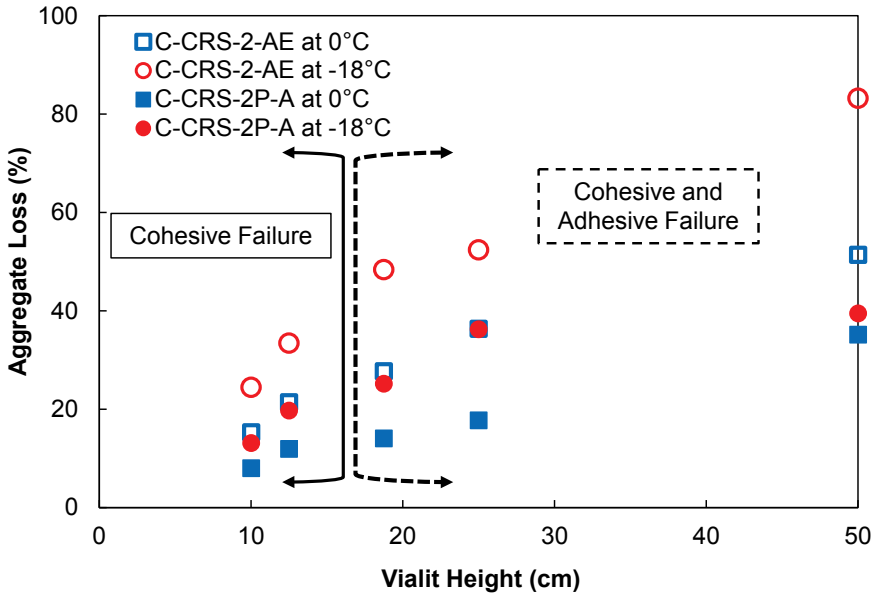

Figure C-15. Vialit test results at different steel ball drop heights and test temperatures.

Microsurfacing Mixture Test Methods

Wet Track Abrasion Test

The wet track abrasion test (WTAT) simulates the in-service traffic loading of micro-surfaces in the laboratory. The test is designed as a wet stripping test, but also can, in theory, be used to quantify dry raveling. The test method itself was developed mainly for microsurfacing testing, but could potentially have applications for chip seal surface treatments as well. This test method is standardized for microsurfacing evaluation as ASTM D3910. In the test, cured samples are placed in a water bath set at 25°C for one hour and then abraded with a rotating rubber hose attached to a planar mixer. This abrasion process lasts five minutes, and afterwards the sample is cleaned and then dried in an oven at 60°C to determine the loss of weight due to abrasion. The test is conducted under water, but it should be noted that the purpose of the submerged specimens is not to increase abrasion, but rather to allow the abraded material to float away. In ISSA TB100, a true moisture damage protocol is suggested. In this method, additional testing on samples soaked in 25°C water for six days is required. At the end of this soaking period the samples are tested the same way as the one-hour soaking samples (i.e., five minutes of abrasion, then specimens are washed, dried, and weighed). Microsurfacing samples for this test are fabricated using the ASTM D3910 procedure described previously, and the chip seal samples are fabricated using the ChipSS method.

According to ISSA TB 100 and Fugro (2004), the acceptable abrasion loss (weight loss) value for a microsurfacing should be less than 807 g/m^2. This loss value was determined from studies conducted by Kari and Coyne (1964) who found that the rate of field wear is highly correlated to in-service performance, and specifically identified the 807 g/m^2 value as a factor for differentiating between good and bad in-service pavements.

In addition, because a micro-surface is a mixture of aggregate, emulsion, mineral filler, and additives, the performance of the mixture depends on the specific combination of these factors. As such, the literature shows that the WTAT is used to evaluate these factors (Andrews et al. 1994). In a study by Andrews et al., the researchers recommend that the abrasion loss obtained from a six-day soak period should be used as an adequate performance parameter. This parameter is suggested over the one-hour soak test because the one-hour soak test results did not show expected trends.

WTAT to Evaluate Raveling

The WTAT is used to assess the raveling resistance of microsurfacing mixtures. Specimens were fabricated for the WTAT following the ASTM D3910 procedure. The specimen fabrication process is shown in Figure C-16 and a cured and tested specimen is shown in Figure C-17.

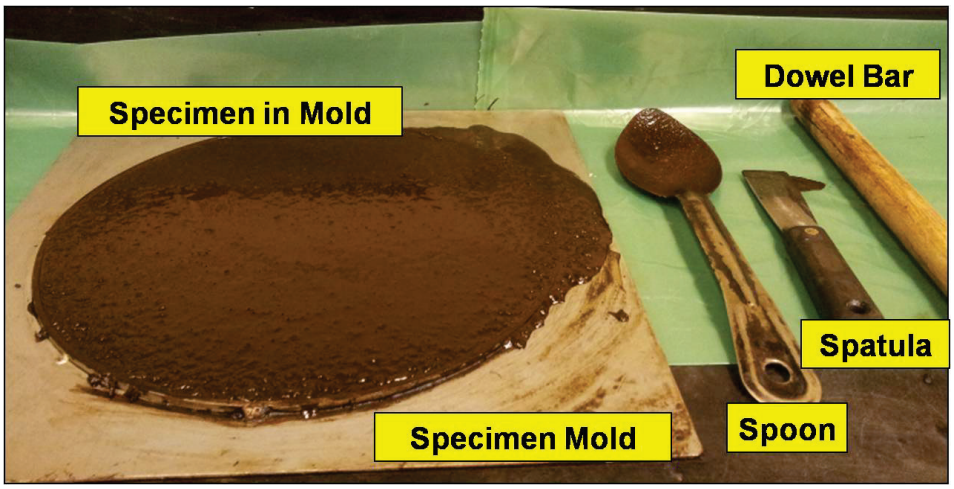

Figure C-16. Specimen fabrication for WTAT test.

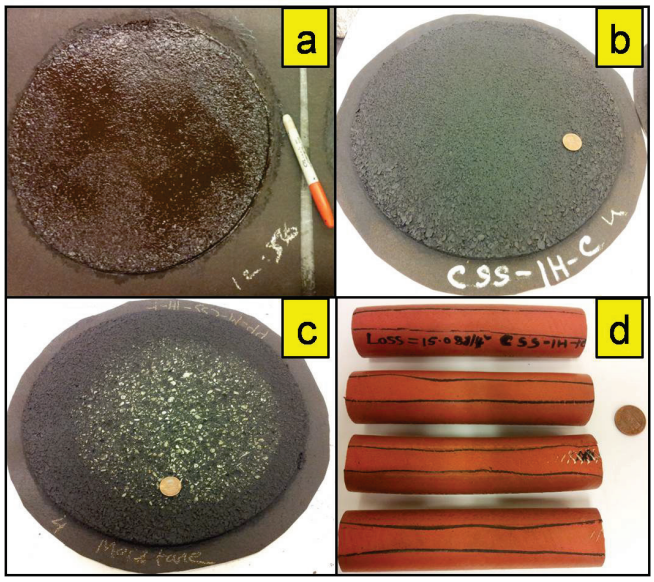

Figure C-17. (a) Specimen before curing, (b) specimen after curing, (c) specimen after testing, and (d) rubber hose after testing.

Prepared specimens are placed on an aluminum pan submerged to a water level at least 6 mm above the specimen surface. The water temperature is set to be equal to the test temperature and the specimen is conditioned in the water for one hour prior to testing. Laboratory investigation confirms that one hour is sufficient for the specimen to reach at desired intermediate test temperature (i.e., 15°, 25°C). After one hour, the specimen is removed and placed in the mixer. Testing is then conducted immediately with the Hobart A-120 mixer while the specimen is submerged under water.

Abrasion is applied to the microsurfacing specimen using a reinforced rubber hose. Application of loading is conducted for 6.7 minutes using a Hobart A-120 mixer at a low

speed. ASTM D3910 recommends using each rubber hose for two specimens rotating by 180° after first test.

After conducting the abrasion test, the specimen is washed with water to get rid of abraded materials from the tested specimen. The specimen is then kept inside of the oven at 60°C for 24 hours to dry it. The mass difference between tested dry specimen and untested dry specimen divided by the abraded area gives the abrasion loss per unit area, which is an indicator of raveling resistance.

In addition, the WTAT is also used to assess resistance to moisture damage. According to the ISSA standard for microsurfacing, a six day soak period at 25°C is recommended to assess moisture damage resistance. Therefore, the six day soak period was used for moisture damage testing in this research. In addition, in order to allow direct comparison with the moisture damage condition for BBS binder testing, 24 hours of moisture conditioning at 40°C (consistent with emulsion residue testing) was used for WTAT as well. To accomplish the moisture damage study, the microsurfacing specimen is submerged under water at 40°C for 24 hours shown in Figure C-18, and then the specimens are removed from the water bath. Next, the specimens are kept inside of Cincinnati Sub Zero (CSZ) oven at 25°C for one hour to allow for thermal equilibration at the test temperature. Finally, WTAT test is carried out under water at 25°C. WTAT test is always conducted on specimens submerged under water to displace abraded materials from the specimen towards the side of the test pan due to wave action of water.

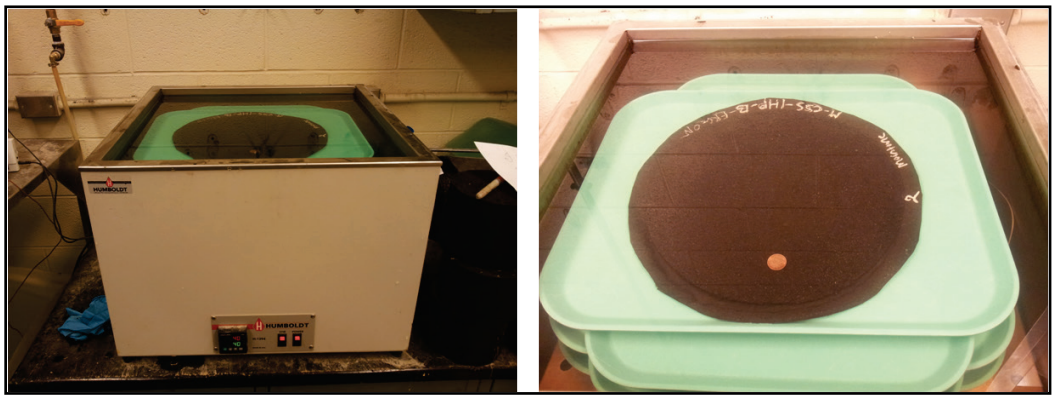

Figure C-18. Moisture damaging of WTAT specimen in the water bath at 40°C.

MMLS3 Testing for Microsurfacing

The MMLS3 device was used to assess the rutting and bleeding of the microsurfacing mixtures at a high temperature for comparison to the MSCR test residue results. The specimen fabrication procedure for MMLS3 testing was consistent with that of the WTAT, in accordance with ASTM D 6372. However, the specimen dimensions differ for the MMLS3 tests. The microsurfacing specimen size for the MMLS3 test is 304.8 mm in length, 177.8 mm in width, and 12.7 mm thickness. The protocol requires 1,400 g of dry aggregate to be mixed with emulsion, water, and cement with the same proportions used for WTAT

specimen fabrication. Prepared specimens were conditioned at 25°C for 24 hours, followed by conditioning at 60°C for 18 to 20 hours to ensure full curing, as specified in ASTM D 6372. An MMLS3 specimen is shown before curing, after curing, and after testing in Figure C-19.

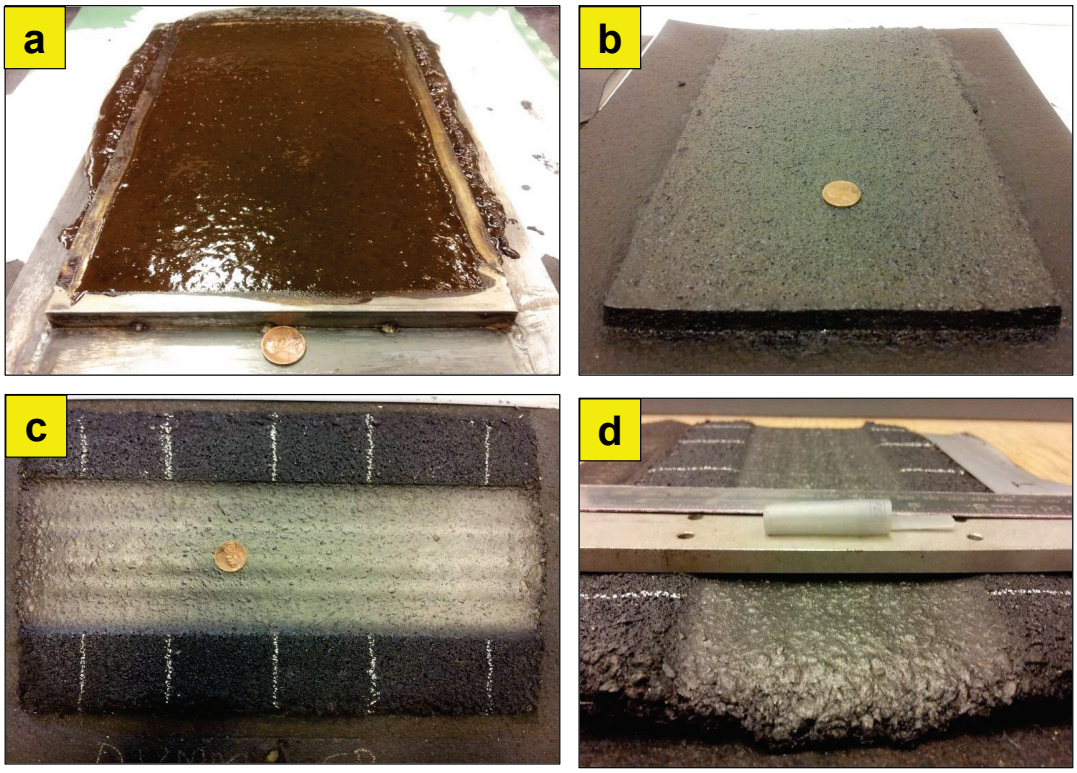

Figure C-19. MMLS3 specimen: (a) before curing, (b) after full curing, (c) after MMLS3 loading, and (d) exhibiting permanent deformation in the wheel-path.

In order to conduct microsurfacing testing at the high temperature, the MMLS3 machine was set inside an environmental chamber. Rutting and bleeding tests were performed at three temperatures corresponding to the three highest Superpave high PG temperatures that are possible within the MMLS3 environmental chamber: 46°C, 52°C, and 58°C. In order to confirm the temperature of the specimen prior to testing, a dummy specimen was set inside the chamber beside the actual test specimen and the temperature was monitored continuously. When the specimen temperature reached the target temperature, the MMLS3 machine was turned on for the desired loading duration (e.g., 30 minutes, 90 minutes, and 180 minutes). After each time interval, specimens were taken out of the MMLS3 and the vertical deformation was measured using a ruler at different locations on the specimen. After measuring the vertical deformation, the specimen was placed in the MMLS3 again and allowed to equilibrate to the target temperature prior to resuming MMLS3 loading. The loading width on the specimen was equal to the tire width, which is 76.2 mm, and the loading area for each specimen was 23,225.76 mm^2.

Bleeding

The MMLS3 test also was used for bleeding assessment. The specimen fabrication procedure, test temperature, and loading conditions were consistent with the rutting test procedures. Two approaches were attempted to quantify the severity of bleeding in micro-surfaces: the sand adhesion method and the glossiness measured using a glossmeter.

Bleeding by Sand Adhesion

The sand adhesion method that is used to quantify bleeding and specified in ISSA TB109 was adapted for the MMLS3. Preheated Ottawa sand at 82°C was applied within a frame to the surface of the samples over the area of wheel loading following MMLS3 trafficking, as observed in Figure C-20 (b). The frame dimensions are 76.2 mm by 203.2 mm. The test protocol is as follows. After the sand is applied, a neoprene rubber sheet is placed on top of the frame. A circular steel plate is then placed on the neoprene rubber and used to compact the sand with three swings, as shown in Figure C-20 (c). The frame is then removed and twenty strokes are applied to the back of the specimen using a circular straight bar to remove excess sand from the specimen. The difference between the specimen weight without sand and with adhered sand divided by the area is interpreted as the sand adhesion. A higher sand adhesion value indicates more severe bleeding.

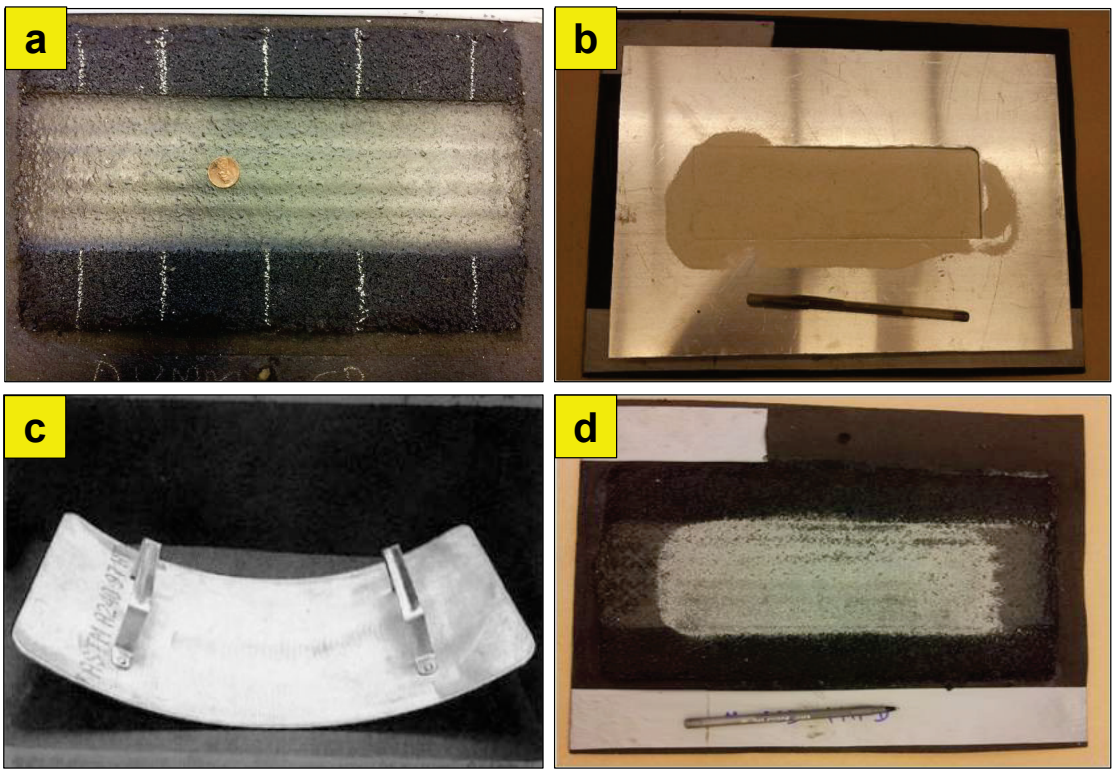

Figure C-20. (a) Tested specimen at high temperature, (b) sand and sand frame on top of specimen, (c) circular plate to apply compactive load on sand, and (d) specimen with adhered sand.

Sand adhesion was measured at each time interval, after which MMLS3 loading was applied for 30 minutes, 90 minutes, and 180 minutes from the beginning. To avoid the effects of sand remaining on the sample during subsequent sand adhesion measurements, the measurements at each time interval of loading were taken at different, non-overlapping sample locations.

Bleeding Measured by Glossmeter

Gloss measurements were implemented as an additional means to assess the bleeding severity of the microsurfacing mixtures. Glossiness has been identified as a possible means to assess bleeding severity, as bleeding leads to emulsion residue migration to the surface, which increases reflectivity. Thus, higher glossiness is expected to indicate greater bleeding.

A glossmeter to measure the glossiness of nonmetallic materials is specified in ASTM D523. Specular gloss is a relative reflectance factor, defined as the ratio between the luminous flux reflection of a specimen and the luminous flux reflection from a standard surface under the same geometric conditions. Gloss is related to the capacity of light reflection from the surface. A glossmeter is a device used to measure the glossiness of a surface and consists of a light source and a receptor. A light beam is applied onto the specimen from a light source at 20°, 60°, and 85° to the vertical axis of the specimen. The reflected light is measured by a receptor from the other side of the vertical axis at angles of 20°, 60°, and 85°, respectively. Among the three geometries, 60° is applicable for most specimens (ASTM D523).

In this study, the ETB-0833 self-calibrating glossmeter was used to measure the glossiness of specimens within the range of 0 to 200 gloss units (GUs). The GU is a measuring unit of the glossmeter and indicates the light reflection index between an experimental surface and highly polished reference black glass. According to glossmeter specifications, this glossmeter is applicable for marble, granite, glass, pottery brick, plastic sheet, printing ink, coating, and woodwork.

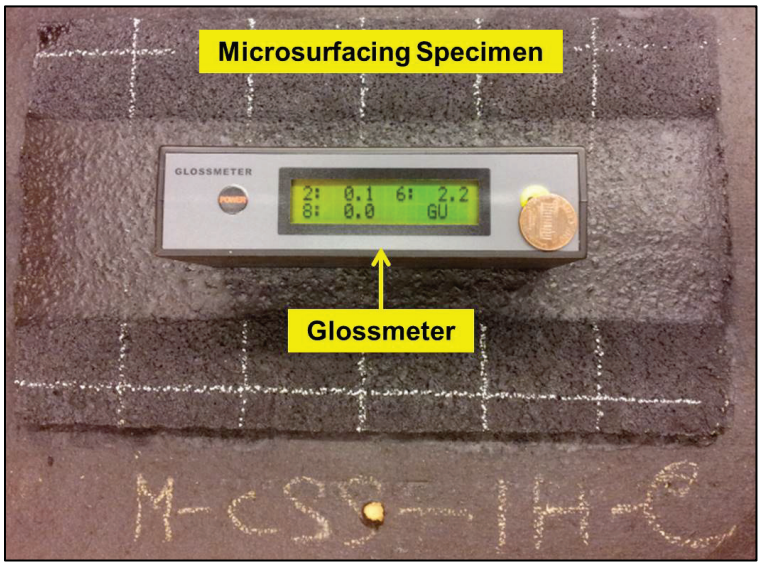

Figure C-21. Glossmeter on a microsurfacing specimen.

The glossmeter is placed on the specimen before and after trafficking by the MMLS3 in order to assess bleeding. Measurements were made by orienting the glossmeter towards the loading direction at three different locations and also perpendicular to the loading direction at four different locations. In order to avoid the effect of surrounding light, the glossmeter was used in a dark room. Because the specimen is deformed due to MMLS3 loading (i.e., rutting), the glossmeter cannot be placed in direct contact with the specimen when the glossmeter is oriented perpendicular to loading direction. That is, the length of the glossmeter is greater than the width of the loading area and the light is emitted in the longitudinal direction of the glossmeter. So, the light emitted from the light source of the glossmeter may scatter outside of the glossmeter through the open area between the glossmeter and the specimen.

Skid Resistance Test Methods and Microsurfacing study

Microsurfacing increases the skid resistance of the pavement; however, skid resistance is reduced over time due to abrasion loss, which is a safety concern. For measuring skid resistance in the laboratory, the British Pendulum Tester (BPT) has been used according to ASTM E 303. The BPT is shown in Figure C-22 (b). This device consists of a pendulum arm with a rubber pad underneath. The pendulum arm moves freely from a horizontal position and the rubber pad slides across the specimen surface or pavement surface. Before the free movement of the arm across the test surface, water is sprayed onto the surface to simulate the critical conditions in the field due to rainfall. The BPT value is measured using the BPT measuring scale attached to the device and ranges from 0 to 140. A higher BPT value indicates greater skid resistance.

The Locked Wheel Skid Tester (LWST), shown in Figure C-22a, is another skid resistance measuring device used in the field. The LWST utilizes a full-scale tire attached to

a truck following ASTM E 274. The truck moves on the pavement at a speed of 40 mph and brakes instantaneously with water spray in front of the test tire prior to applying the brake. Spraying water simulates the critical condition of the placement due to rainfall. The vertical and horizontal forces applied by the wheel are determined based on electrical sensors. The skid number is calculated by multiplying 100 to the ratio of the horizontal force applied to the tire and the dynamic vertical force on the test wheel.

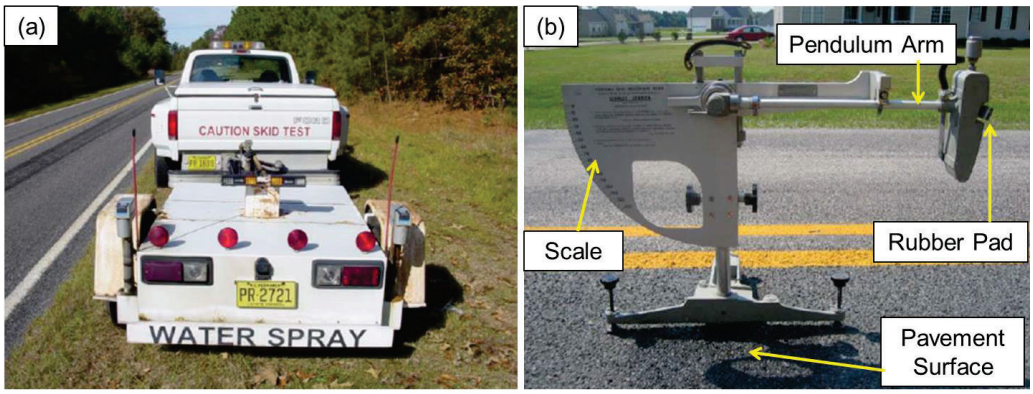

Figure C-22. Skid resistance measurement devices: a) LWST and b) BPT.

The BPT was used in the laboratory on MMLS3-loaded microsurfacing specimens and the measured BPT values were converted to skid number (SN) measured by LWST for which threshold values have been established. Jayawickrama et al., (1996) developed recommended limits for skid resistance of bituminous pavement using LWST followed by ASTM E 274 to ensure safety as shown in Table C-2.

Table C-2. Typical Skid Number for Bituminous Pavements (Jayawickrama et al. 1996)

Skid Number	Comments
< 30	Take measures to correct
≥ 30	Acceptable for low volume roads
31-34	Monitor pavement frequently
≥ 35	Acceptable for heavily traffic roads

In this study, the BPT values of microsurfacing mixtures were measured after 180 minutes of loading at high temperature performance grades of 52°C and 58°C. Next, the BPT values were converted to SN. The minimum SN values at 52°C and 58°C were found to exceed the minimum criteria of 35 for high volume roads (Jayawickrama et al., 1996). Figure C-23 and Figure C-24 summarizes the LWST skid numbers obtained for the BPT-tested microsurfacing mixtures.

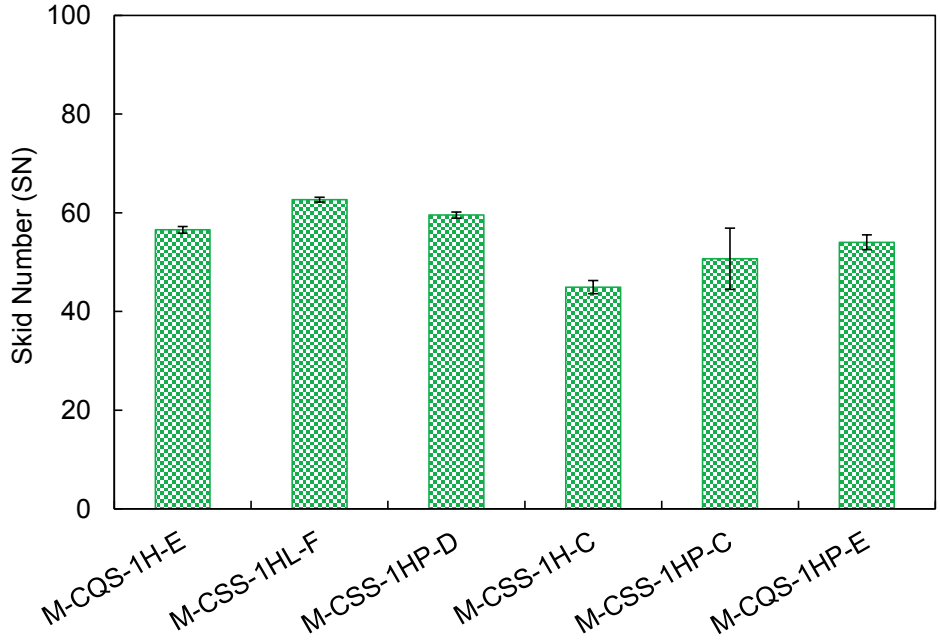

Figure C-23. SN of microsurfacing mixtures after 180 minutes MMLS3 loading at 52°C.

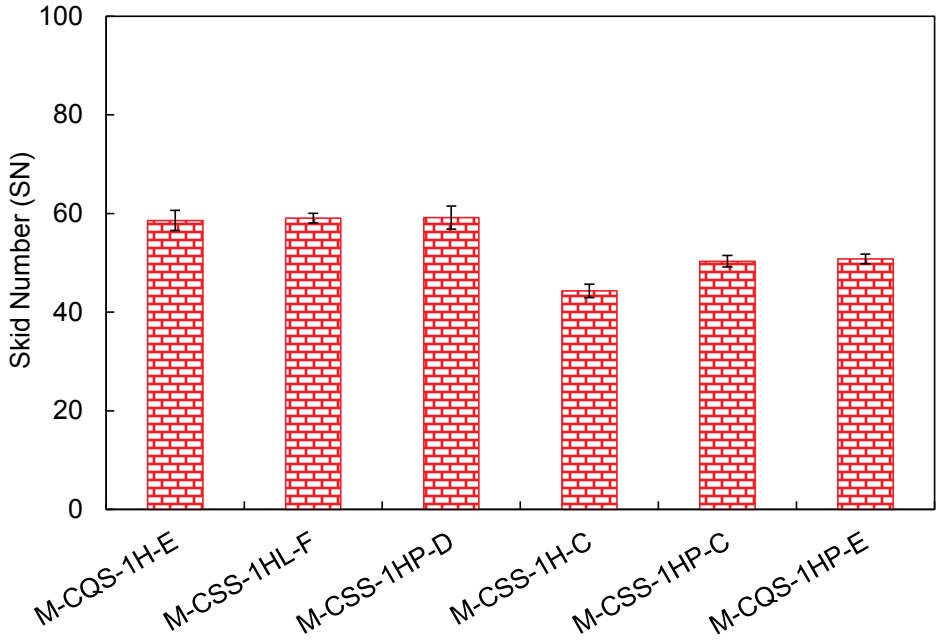

Figure C-24. SN of microsurfacing mixtures after 180 minutes MMLS3 loading at 58°C.

Bleeding is a concern in surface treatments because it reduces the skid resistance of the pavement surface. However, the test results displayed in Figure C-23 and Figure C-24 indicate that sufficient skid resistance was retained in the microsurfacing mixtures despite subjecting the microsurfacing mixtures to the climatic and traffic loading conditions of the MMLS3 bleed test. The MMLS3 bleeding test conditions used on the micro-surfaces were the same conditions that produced significant bleeding in some chip seal mixtures. Therefore, bleeding does not appear to be a performance concern for the microsurfacing mixtures tested. Based on these results, it is postulated that bleeding is more related to the residual asphalt binder rate of microsurfacing mixtures as opposed to binder properties. For the microsurfacing mixtures tested in this research the residual asphalt amount was kept consistent between emulsion types. Thus, specifications were not developed for bleeding of microsurfacing treatments in this research.

Single-Edge Notched Bend (SENB) Test to Evaluate Thermal Cracking Resistance in Microsurfacing Mixtures

The single-edge notched beam (SENB) test was utilized at a low temperature to quantify thermal cracking performance.

SENB mixture test specimens were prepared using the same dimensions that were used for fabricating SENB binder samples: 6.25 mm × 12.5 mm × 102 mm with 3-mm notch depth. Because the microsurfacing samples contain only fine aggregate, the use of small samples still satisfies the representative volume element constraint. SENB tests were conducted at three different temperatures: -16°C, -22°C, and -28°C in a BOSE ElectroForce test system with a loading rate of 0.01 mm/sec.

Although testing microsurfacing mixtures using the SENB test has not been conducted prior to this study, Marasteanu et al. (2009) studied the bending beam rheometer (BBR) test using the binder BBR geometry for asphalt concrete mixtures at a low temperature. They proposed a BBR-SENB mixture test to predict compliance as a surrogate method for the indirect tensile (IDT) test at a low temperature due to the widespread availability of the BBR test system and ease of conducting the test. Their results demonstrated that the test could be used successfully to capture large-scale IDT results.

SENB Fabrication Procedure for Microsurfacing Mixture

In the field, micro-surfaces are spread onto the surface of a pavement without compaction. However, micro-surfaces densify under traffic loading. So, for this study, initially, laboratory-produced micro-surfaces were prepared without compaction for SENB testing. However, it was found that the air void contents of the specimens were highly variable, and thus, the test results were highly unrepeatable. To produce more uniform specimens and better replicate micro-surfaces in the field, which are densified under traffic loading, microsurfacing mixtures were compacted in the Superpave Gyratory Compactor (SGC) following curing in an uncompacted state.

The specimen fabrication procedure developed to produce microsurfacing mixture SENB specimens involved the following considerations:

- The microsurfacing mixture should not be heated to more than 135°C to avoid aging of the mixture and not to disintegrate the polymer or latex inside the mixture.
- The required amount of microsurfacing mixture should be reasonable and realistic because the mixture curing takes about two days. At the same time, the number of SENB test specimens should be sufficient to execute the test matrix successfully.
- Air void contents should reflect typical field conditions.

Reincke et al. (1989) collected field cores from microsurfacing sections and measured the air void contents of the microsurfacing layer that had been separated from the asphalt layer. Reincke et al. (1989) found that micro-surfaces with air void contents in the range of 9 percent to 11 percent performed adequately after one year of placement. Therefore, in this study, a target air void content of 10 percent was utilized.

Reincke et al. also attempted three procedures for the laboratory compaction of microsurfacing mixtures. In one procedure, the aggregate particles were mixed with the emulsion and filler and cured at 60°C overnight. The cured mixtures were broken into small pieces and compacted with 25 blows in the Marshall Compactor after heating at 137.8°C, after which an 8,000-lb static load was applied for further compaction. In a second procedure, the emulsion was mixed with aggregate particles until the emulsion broke. The mix was then cured at ambient temperature for three days and subsequently compacted at 137.8°C by the Marshall compactor. In a third procedure, a mix of emulsion and aggregate was placed in a perforated mold that allowed water to drain out overnight at 60°C. Then, the mixture was compressed to a target density at 60°C and cured at 60°C until the constant weight of the mixture was achieved, indicating that the curing process was complete.

The required amount of microsurfacing mixture was obtained from microsurfacing rectangular specimens that were fabricated for rutting and bleeding tests. The preparation of rectangular specimens of microsurfacing mixtures prior to compaction follows the general guidelines of ASTM D 6372. Specimens were cured at 25°C for 24 hours and then 24 hours at 60°C. Then, the mixture was broken into small pieces, and approximately 5,000 g of microsurfacing mixture was separated for production of a 67-mm (height) gyratory-compacted specimen and for maximum specific gravity (G_{mm}) measurements.

Prior to production of the compacted specimens, the theoretical maximum specific gravity (G_{mm}) was measured according to ASTM D2041 so that the air void contents of the compacted specimens could be calculated. Per the standard, 1,500 g of material was utilized for the G_{mm} determination. The G_{mm} values for two micro-surfaces using CSS-1H-C and CSS-1HP-C emulsions were found to be 2.447 and 2.462, respectively.

It was critical to establish a specimen fabrication compaction procedure to allow for SENB test specimens with well-controlled air void contents. Therefore, initial compaction trials were conducted to determine the required quantity of material to meet the target SENB specimen air void content of 10 percent given a target specimen height. Before compaction in the gyratory compactor, the microsurfacing mixtures were heated in an oven for one hour at

135°C and mixed thoroughly with a spatula. It is important to note that gyratory-compacted specimens do not contain uniform air voids. Rather, the specimen air void contents are highest at the periphery and then are more or less constant within the central portion of the specimen. Thus, in this study it was important to differentiate between the bulk specimen air void content and the SENB test specimen air void contents. The SENB test specimens were extracted from the central portion of the gyratory-compacted specimens after cutting the top and bottom and all four sides of the specimen.

Several 67-mm high specimens were compacted using different weights of microsurfacing mixture in an attempt to develop a procedure to meet the target of 10 percent air void content in the final SENB test specimens. Figure C-25 presents the air void contents of the gyratory-compacted specimens produced using different quantities of mix with the CSS-1H-C and CSS-1HP-C emulsions. The results include the bulk specimen and beams extracted from the inner portion of the specimen. All the results correspond to mixtures compacted to a height of 67 mm. The figure shows that the air void contents of the bulk specimen are consistently higher than those of the extracted SENB specimens, which matches expectations. It can also be observed that the air void content increases as the material quantity decreases, which also follows expectations. Based on the results presented, 2,550 g of CSS-1H-C mix is required to meet the target air void content of 10 percent for SENB test specimens with CSS-1H-C emulsion, whereas 2,575 g of mix is required to reach 10 percent air void content for the CSS-1HP-C emulsion. Based on these results, 2,550 g of mix were utilized to produce unmodified microsurfacing mixtures and 2,575 g were used to produce modified microsurfacing mixtures, compacted to a height of 67 mm. However, these two mixture weights are very close to each other.

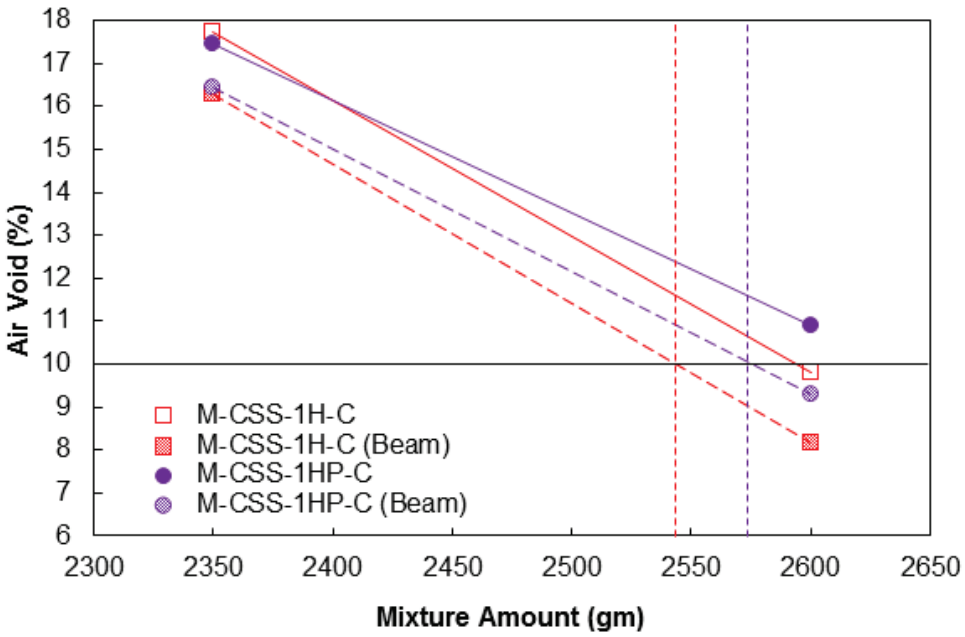

Figure C-25. Gyratory compacted specimen with 67 mm height and 150 mm diameter.

Figure C-26 shows a comparison between the number of gyrations required to compact the CSS-1HP-C and CSS-1H-C microsurfacing mixtures to a height of 67 mm with different amounts of mixture shown on the x-axis. It can be seen that greater compactive effort is required for the modified mixture than for the unmodified mixture.

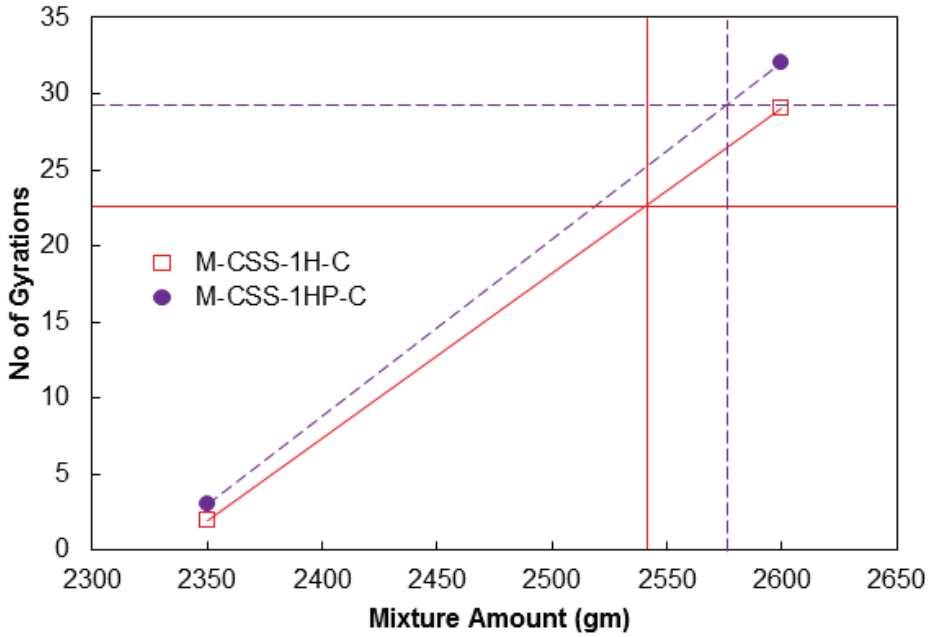

Figure C-26. Number of gyrations for gyratory-compacted specimens with different amounts of microsurfacing mixture.

The fabricated gyratory-compacted specimens were sawn to produce SENB test specimens with a notch cut into the specimen center. Sections I, II, III, and IV were cut from the sides of a gyratory-compacted specimen to obtain the rectangular Section V, as exhibited in Figure C-27 (a). Then, 12.5 mm thick sections were sliced from the top and bottom (shown in Figure C-27 (b) and (c)) of the specimen. Next, the specimen was sawn according to the depiction in Figure C-27 (a) of the plan view of a specimen to obtain a rectangular block of 127 mm x 84 mm x 42 mm (L x W x D), which, based on analysis of air void variability within specimens, represents the portion of the specimen with uniform air voids. The rectangular block (Section V) was then sliced to produce SENB test specimens of the required dimensions.

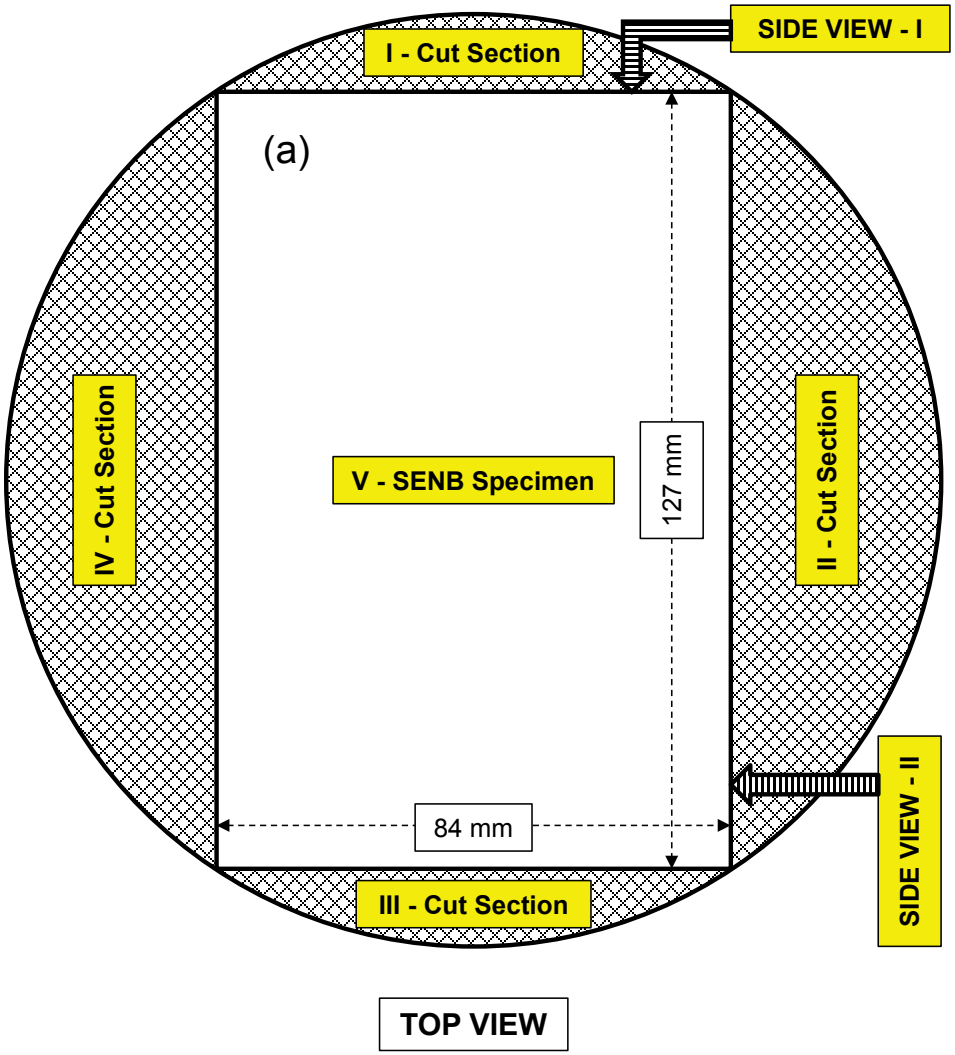
SIDE VIEW - I
I - Cut Section
(a)
IV - Cut Section
V - SENB Specimen
127 mm
II - Cut Section
SIDE VIEW - II
84 mm
III - Cut Section
TOP VIEW

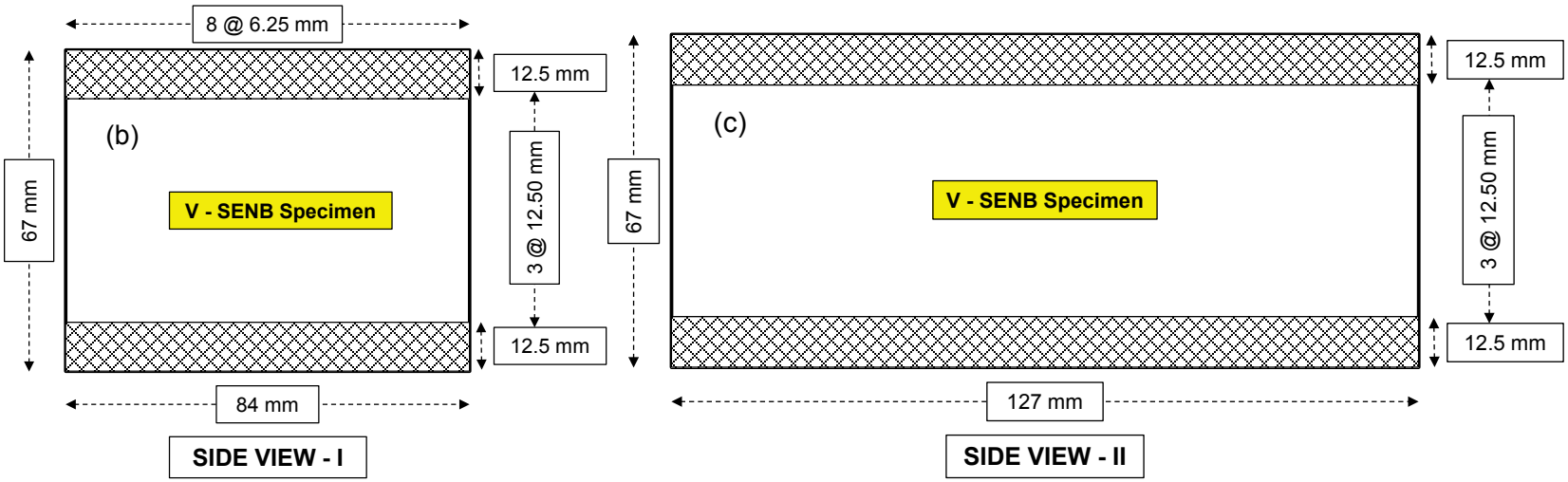

Figure C-27. Schematic of SENB test specimen fabrication steps: (a) top view of gyratory-compacted specimen, (b) side view-I, and (c) side view-II.

After the beam specimens were sawn and dried, the notch was cut into the beam. Beam specimens without notches are shown in Figure C-28 (a). A 3-mm deep notch was cut using the saw set-up shown in Figure C-28 (b). In this set-up, the beam specimen is placed on a steel base against a supporting steel frame. The supporting frame keeps the specimen vertically straight. The supporting frame along with the specimen is pushed across the saw to make a notch 3-mm deep. Note that the saw is configured in such a way that the saw tip remains exposed 3 mm above the steel base. After sawing, the specimens are kept at room temperature under a fan to dry. Testing was always conducted the day after specimen preparation in this study.

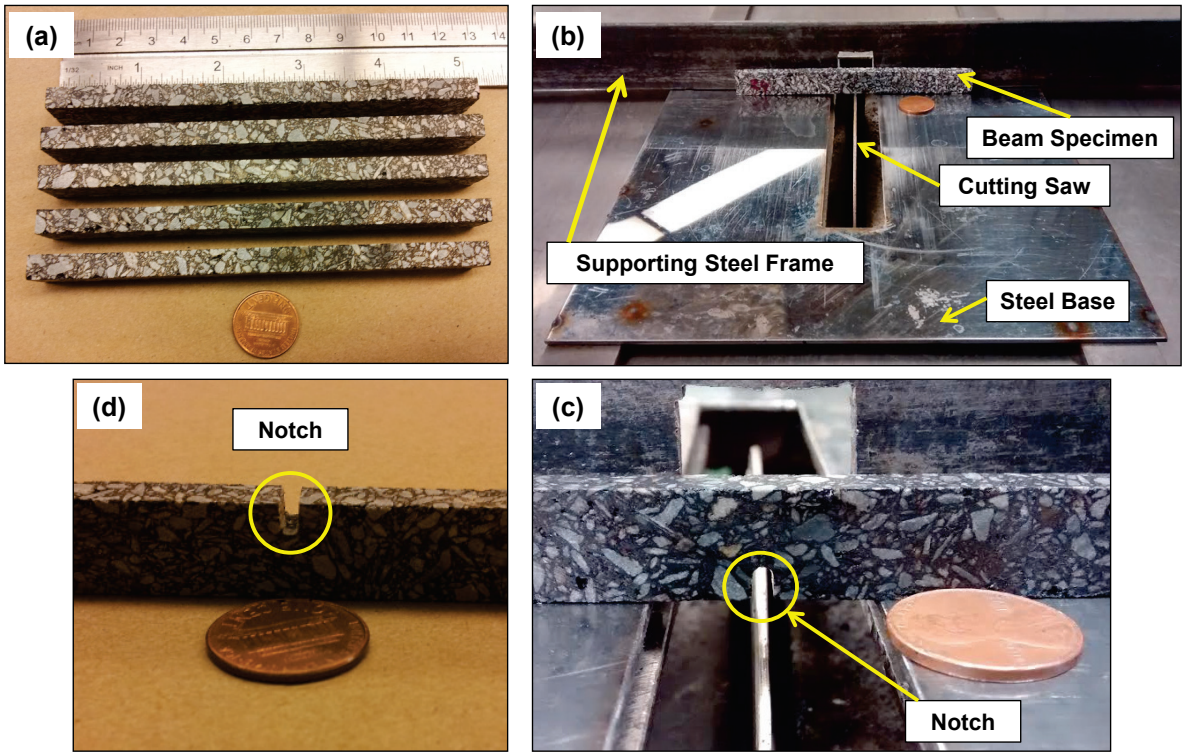

Figure C-28. Notch insertion procedure showing: (a) beam specimens prior to notch insertion, (b) beam specimen on the sawing base, (c) specimen after making the notch, and (d) close view of notch in the specimen.

The microsurfacing mixture SENB tests were conducted inside a BOSE ElectroForce Test System with a constant displacement rate of 0.01 mm/sec. The SENB test specimens were conditioned at the test temperature for one hour prior to testing for consistency with the binder tests. Laboratory studies in which a thermocouple is inserted into a sample indicate that only 15 to 20 minutes is required for thermal equilibration and, thus, the one-hour conditioning time is conservative.

REFERENCES

Adams, J. and Y.R. Kim, "Mean Profile Depth Analysis of Field and Laboratory Traffic-Loaded Chip Seal Surface Treatments," International Journal of Pavement Engineering. Vol. 15, Nos. 7-8, 2013, pp. 645-656.

Andrews, E. M., R. E. Smith, C. K. Beatty, and J. W. Button. *Evaluation of Microsurfacing Mixture Design Procedures and the Effects of Material Variation on the Responses.* Report No. FHWA/TX-95/1289-1, 1994.

ASTM. Standard D 7000: *Standard Test Method for Sweep Test of Bituminous Emulsion Surface Treatment Samples*. West Conshohocken, PA: ASTM International, 2004.

Caltrans Division of Maintenance. *Micro-Surfacing*, Chapter 9, MTAG Volume I Flexible Pavement Preservation, 2nd Edition, 2009.

ISSA. Standard TB 100: *Test Method for Wet Track Abrasion of Slurry Surfaces.* ISSA, Washington, D.C., 1990.

ISSA. Standard TB 109: *Test Method for Measurement of Excess Asphalt in Bituminous Mixtures by Use of a Loaded Wheel Tester and Sand Adhesion.* ISSA, Washington, D.C., 1990.

Jayawickrama, P.W., Prasanna, R., and S. P. Senadheera. Survey of State Practices to Control Skid Resistance on Hot-Mix Asphalt Concrete Pavements. Transportation Research Record 1536, Transportation Research Board, National Research Council, Washington, D.C., 52-58.

Jordan, W.S., and I. L. Howard. *Applicability of Modified Vialit Adhesion Test for Seal Treatment Specifications*. Journal of Civil Engineering and Architecture, 5(3), 2011, pp. 215-223.

Kari, W. J. and L. D. Coyne. Emulsified Asphalt Slurry Seal Coats. *Proceedings of Asphalt Pavement Technologists*, 1964.

Kim, Y. R. and J. Adams. *Development of a New Chip Seal Mix Design Method*. Publication HWY-2008-04, N.C. Department of Transportation, 2011.

Kim, Y. R., S. Lee, Y. Seo, and O. El-Haggan. *Impact of Price Reductions on the Long-Term Pavement Performance of HMA Mixes in North Carolina*. Final Report to NCDOT, FHWA/NC/2005-09, 2005, pp. 53-54.

Lee, J. and Y. R. Kim. *Quantifying the Benefits of Improved Rolling of Chip Seals*. HWY-2006-06. FHWA, U.S. Department of Transportation, 2008.

Lee, J. and Y. R. Kim. Performance-Based Evaluation of Asphalt Surface Treatments Using the Third Scale Model Mobile Loading Simulator. North Carolina State University, Raleigh, NC. 2007.

Marasteanu, M., Velasquez, R., Cannone Falchetto, A., and A. Zofka. A Development of a Simple Test to Determine the Low Temperature Creep Compliance of Asphalt Mixture, IDEA Program Final Report NCHRP 133, Transportation Research Board of the National Academies. 2009.

Reincke, G., Ballou, W. R., Engber, S. L., and T. M. O'Connell. Studies of Polymer-Modified Microsurfacing Materials in Highway Maintenance," in Proceedings of the ISSA, International Slurry Seal Association, February 1989, pp. 45-83.

Transit New Zealand. *Chipsealing in New Zealand.* Transit New Zealand, Wellington, New Zealand, 2005.

Appendix D. EPG Specifications Development Background

CONTENTS

LIST OF FIGURES

LIST OF TABLES

CHAPTER D-1. FRESH EMULSION EPG SPECIFICATION TEST RESULTS

Fresh emulsion property characterization is necessary to determine the constructability and stability of emulsions. After production, all emulsions are stored in a tank and transported to the construction site. When the emulsion is inside the tank, the emulsion is stirred at a low shear rate to maintain uniformity and to avoid emulsion settlement inside the tank. After that, during the construction of chip seals and spray seals, the emulsion is sprayed through nozzles at a high shear rate. For microsurfacing construction, however, the emulsion is not sprayed like chip seal or spray seal emulsions. The microsurfacing emulsions are mixed with aggregate, mineral filler, additive, and water inside of a pug mill and then applied to the pavement through a spreader box. In order to determine the emulsion properties during storing, mixing, and draining out, a storage stability test and three-step shear tests are proposed.

This chapter provides test data for the five parameters are proposed to specify fresh emulsions in the EPG: the separation ratio (R_s), stability or degradation ratio (R_d), sprayability, drainout, and mixability. Among these five parameters, the separation ratio and degradation ratio characterize the emulsion conditions inside the storage tank. Sprayability, drainout, and mixability are proposed for workability during emulsion application. Sprayability, drainout, separation ratio, and stability ratio are the parameters applicable for chip seal and spray seal emulsions, whereas the separation ratio, degradation ratio, and mixability are the material performance parameters for microsurfacing emulsions. In this study, the separation ratio, stability ratio, and mixability were measured using the storage stability test. Sprayability and drainout were measured using the three-step shear test at a high shear rate and low shear rate, respectively.

Table D.1. Emulsion Performance Parameters and Test Methods

Treatment Type	Test Method	Performance Measurement	Performance Parameter
Chip Seal	Storage Stability Test	Emulsion Stability	(a) Separation Ratio (R_s) (b) Stability Ratio (R_d)
Spray Seal			
Microsurfacing			
Chip Seal	Three Step Shear Test	Workability	(a) Sprayability (b) Drainout
Spray Seal			
Microsurfacing	Storage Stability Test		Mixability

Storage Stability Test Results

The storage stability test results are presented in Figure D-1, Figure D-2, and Figure D-3. The separation ratio is ideally 1.0 or close to 1.0, indicating no separation of the water and

asphalt during storage of the emulsion. A separation ratio less than 1.0 indicates settlement of the asphalt in the emulsion. A separation ratio greater than 1.0 indicates creaming or thickening of the asphalt at the top of the emulsion. A stability ratio greater than 1.0 indicates loss of water from the emulsion during storage. The separation and stability of emulsions depend on the amount of residue content, open surface area of the storage tank, shipping procedure, and environmental conditions during shipping.

For the chip seal emulsions (Figure D-1), the measured separation ratio values range from 0.7 to 1.7 and the stability ratio values range from 0.2 to 2.1, excluding the poor performing emulsions. Note that, although the poor performing emulsions were fabricated to be intentionally poor performing, they were not necessarily fabricated by the supplier to be poor performing with regard to the particular parameter being measured. Therefore, poor performing emulsions were excluded from the analysis except in the instances where the emulsion was intentionally made to be poor performing for the parameter being measured. For the microsurfacing emulsions (Figure D-2), the separation ratio values range from 0.3 to 1.2 and the stability ratio values range from 0.9 to 2.0, excluding the poor performing emulsions. For the spray seal emulsions (Figure D-3), the separation ratio values range from 0.6 to 1.3 and the stability ratio values range from 0.5 to 2.6.

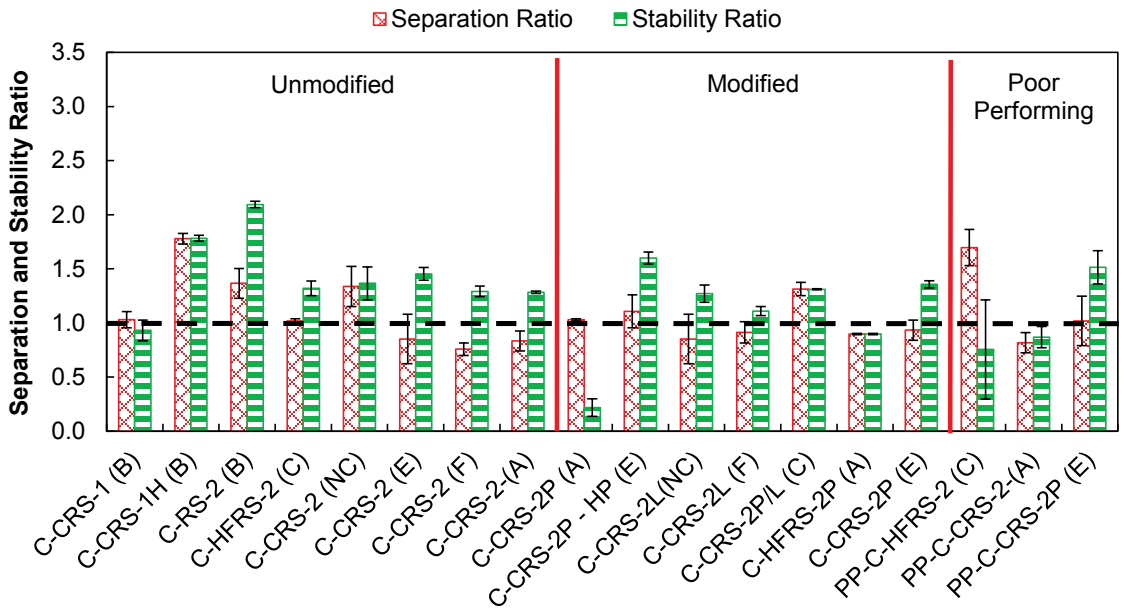

Figure D-1. Storage stability test results for chip seal emulsions at 60°C.

Figure D-1 displays the storage stability results for the chip seal emulsions. The separation ratio for the modified (CRS-2L and CRS-2P) emulsions is close to 1.0, indicating minimal settlement during storage. However, the separation ratio for the CRS-2 (NC) emulsion is 1.4, indicating that the emulsion is likely to have experienced some settlement during storage. Conversely, the CRS-2 (E), CRS-2 (F), and CRS-2 (A) emulsions demonstrate a reverse trend; that is, the separation ratio is well below 1.0, indicating that the emulsion may have thickened near the top of the emulsion cylinder. However, the storage stability test results for all the emulsions are not consistently close to 1.0, which is the reason that statistical analysis has been implemented to set the specification limits.

The stability ratios of the microsurfacing emulsions are 1.0 or close to 1.0, excluding the poor performing emulsions, as shown in Figure D-2. The only exception is the M-CSS-1H-F emulsion. The reason for the relatively good stability ratio values for the microsurfacing emulsions compared to those for the chip seal emulsions is that the emulsions are slow-setting emulsions or quick-setting emulsions as opposed to chip seal emulsions that are rapid-setting, indicating lower stability. Again, the separation ratio of the microsurfacing emulsions is less than 1.0 except for the poor performing emulsions and M-CSS-1H-A emulsion, indicating that the emulsions may have thickened near the top of the emulsion cylinder.

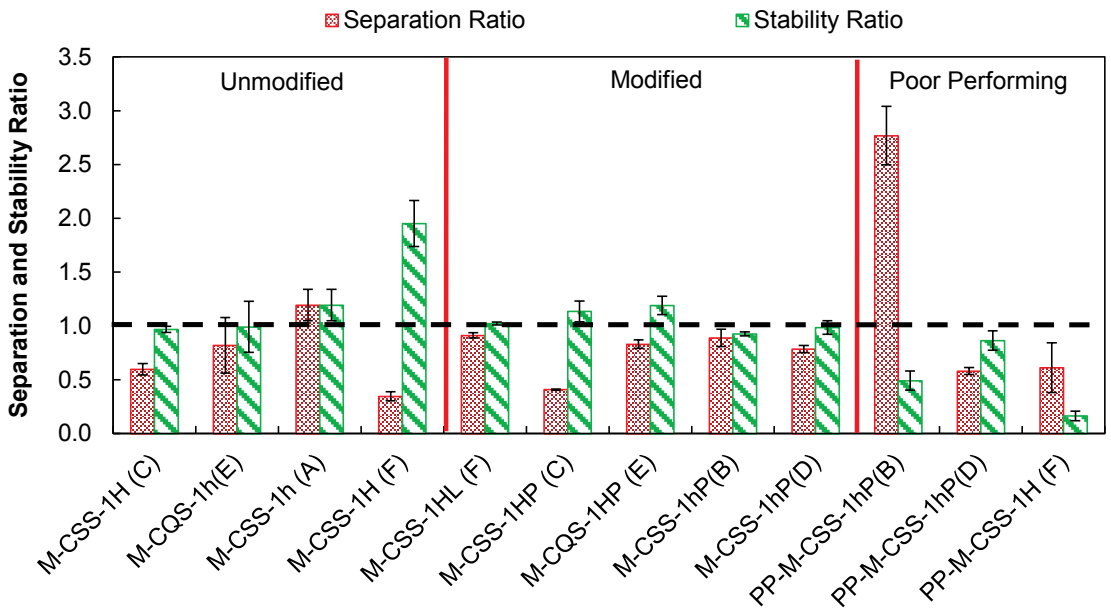

Figure D-2. Storage stability test results for microsurfacing emulsions at 25°C.

The separation ratios and stability ratios of the spray seal emulsions are shown in Figure D-3. The results indicate considerable variability in the separation ratios and stability ratios among the emulsions. It is speculated that the high variability is caused by the different dilution rates used for the different emulsions.

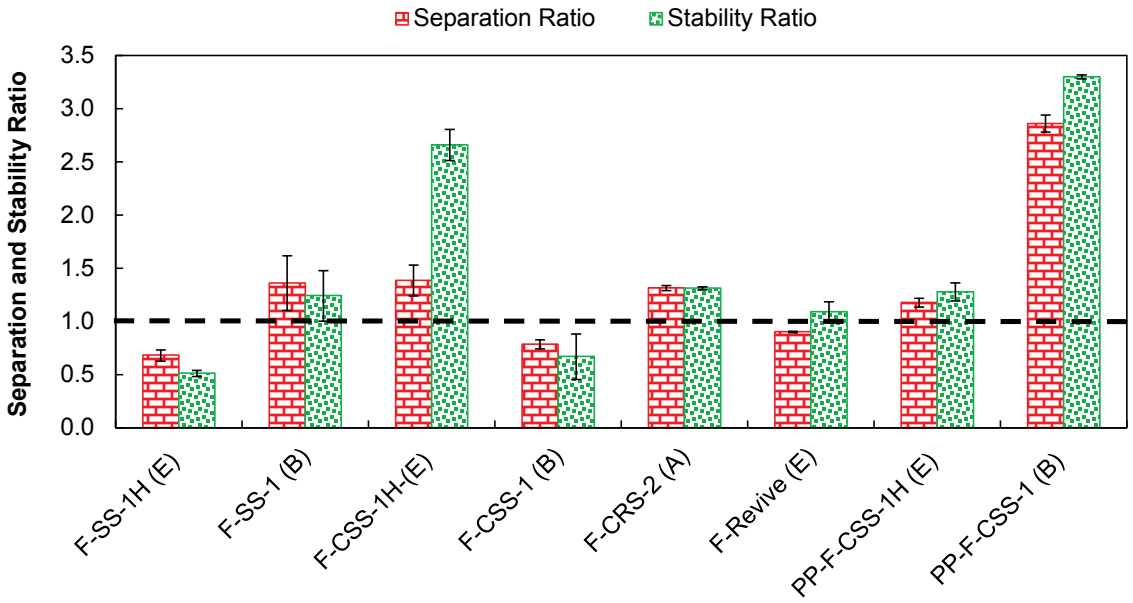

Figure D-3. Storage stability test results for spray seal emulsions at 25°C.

Microsurfacing Constructability

For the microsurfacing emulsions, the mixability parameter was used to indicate the constructability. This mixability parameter was determined based on fresh emulsion viscosity. The mixability of the microsurfacing emulsions is shown in Figure D-4 and indicates the viscosity of fresh emulsions measured at a low shear rate at 25°C. Among all the mixability values, the PP-M-CSS-1H (F) emulsion has the highest mixability rating, because it was made to be poor performing by increasing the emulsifier content to five percent. The standard emulsifier content of emulsions should be 0.1 percent to 2.5 percent.

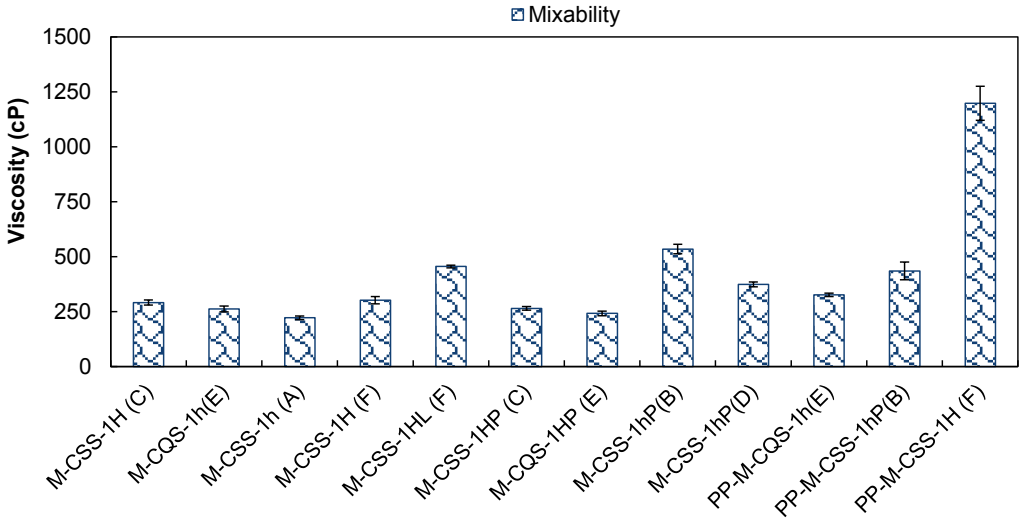

Figure D-4. Mixability of microsurfacing emulsions.

Three-Step Shear Test Results

Three-step shear testing is proposed to define the sprayability and drainout of the chip seal and spray seal emulsions using the viscosities at high and low shear rates, respectively. Figure D-5 and Figure D-6 present the chip seal sprayability and drainout results, respectively. Figure D-7 and Figure D-8 present the spray seal sprayability and drainout results, respectively. The results indicate that the drainout viscosity is always higher than the sprayability viscosity, which makes sense as asphalt emulsions are shear thinning material. This phenomenon is the reason that the viscosity at a high shear rate (sprayability) is less than the viscosity at a low shear rate (drainout). The sprayability and drainout viscosity values vary from emulsion to emulsion, indicating that the three-step shear test is able to discriminate between the different emulsions. The viscosity values of the modified, unmodified, and poor performing emulsions cannot be differentiated based on sprayability and drainout viscosity values, however, indicating that constructability is not significantly affected by modification and the emulsions included were not made poor performing by altering their viscosity. Statistical analysis was implemented again to specify the values for the sprayability and drainout for both chip seals and spray seals.

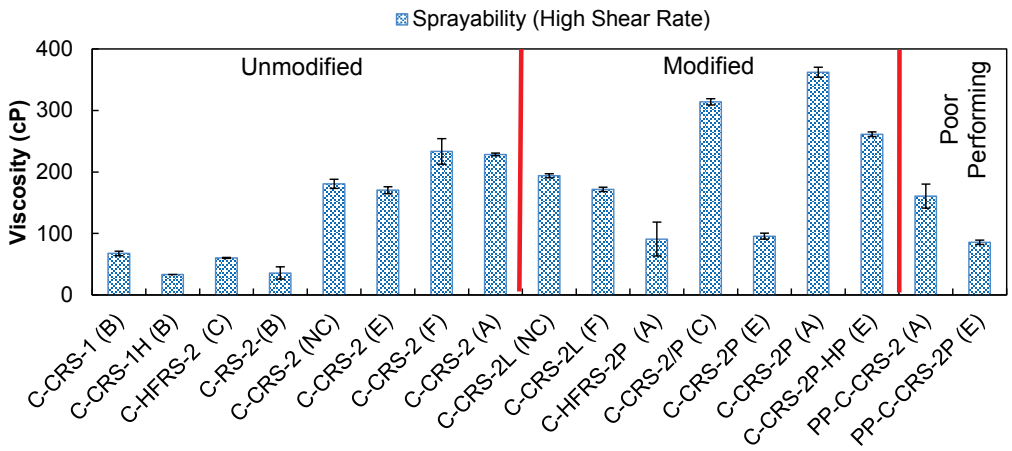

Figure D-5. Sprayability of chip seal emulsions.

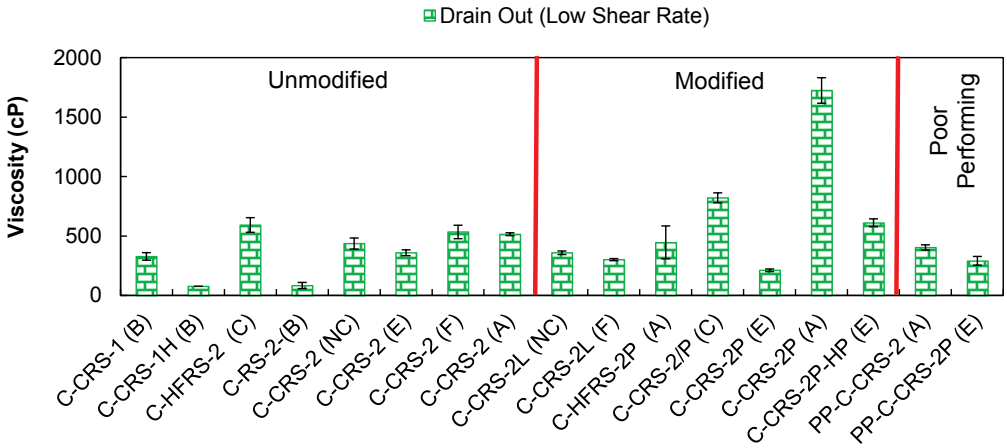

Figure D-6. Drainout of chip seal emulsions.

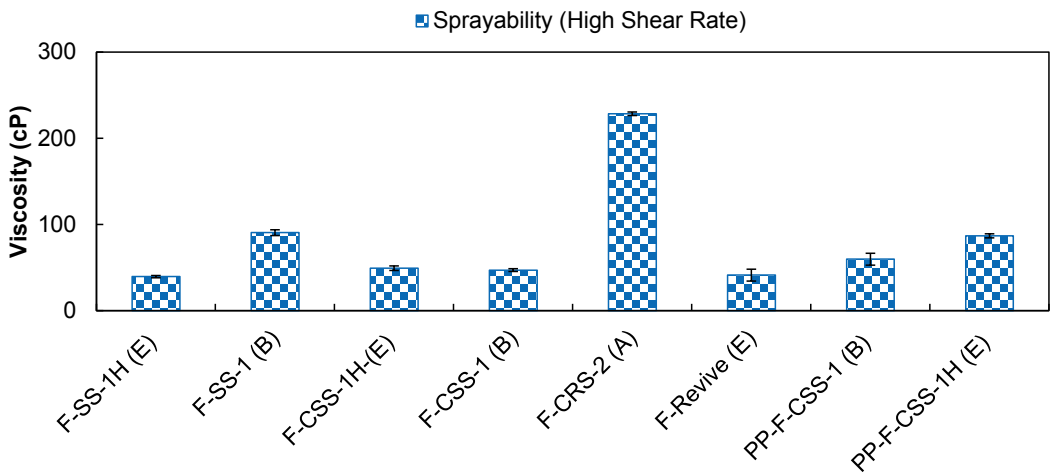

Figure D-7. Sprayability of spray seal emulsions.

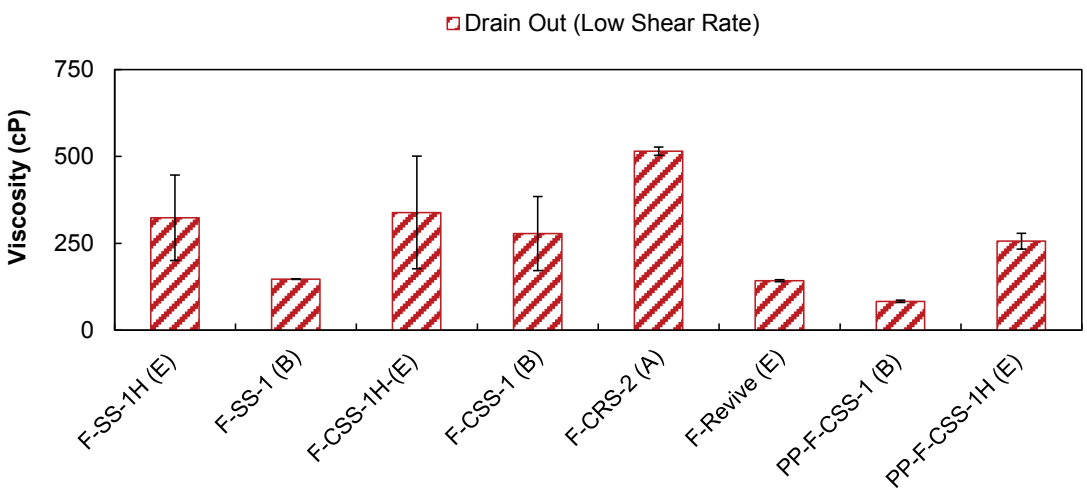

Figure D-8. Drainout of spray seal emulsions.

CHAPTER D-2. EPG SPECIFICATION DEVELOPMENT AT HIGH TEMPERATURE PERFORMANCE GRADES

High Temperature EPG Specification Framework Concept

For the development of the EPG specification limits at high temperatures, the relationship between the material binder properties that directly relate to critical surface treatment mixture performance had to be established. This high temperature relationship was developed with consideration for the effect of traffic level on performance, as the developed EPG specifications are intended to grade the binders according to the appropriate traffic situations for which they apply. For the development of the specification limits at different traffic levels, fully cured surface treatments were subjected to a variety of MMLS3 traffic loads, and the high temperature

mixture performance was measured. The mixture results were then compared to those of the binder test, i.e., multiple stress creep and recovery (MSCR) test, for the same asphalt materials in order to determine the appropriate specification limits at different traffic levels.

In order to determine the equivalent MMLS3 loads that correspond to each level of field traffic in the EPG specifications, a conversion method based on certain assumptions was needed, as the complexities of field traffic loading demands nationwide could not be replicated solely using MMLS3 tests in the laboratory. Using the low, medium, and high traffic classes defined in the main body of this report, a traffic conversion was utilized to translate the field average annual daily traffic (AADT) for each traffic class to the equivalent laboratory MMLS3 loading conditions to determine the high temperature EPG specification limits. This conversion is detailed in the following section.

Assumptions for Traffic Conversion for the High Temperature EPG Specifications

For the development of the EPG specifications at high temperatures, MSCR binder testing was conducted at temperatures of 46° to 70°C (at 6°C increments as in the HMA performance grade specifications). That is, EPG specification testing was conducted under climatic conditions where the surface treatment is most susceptible to the distresses being measured, which are bleeding and rutting for the high temperature range. For a direct comparison to the high temperature binder properties measured from the MSCR test, chip seal and microsurfacing mixture specimens also were subjected to high temperatures up to 58°C (the maximum temperature the MMLS3 chamber is capable of maintaining) for all applied MMLS3 wheel loading.

For the mixture testing using the MMLS3, bleeding and rutting were measured at 990, 2,970, 9,810, and 17,820 MMLS3 wheel loads so that the effect of traffic on high temperature mixture performance could be examined. These specific numbers of MMLS3 wheel applications, at which bleeding and/or rutting measurements were recorded, correspond to specific test times for the MMLS3, as summarized in Table D.2.

Table D.2. MMLS3 Loading Time vs. Applied Wheel Loads

MMLS3 Loading Time (minutes)	MMLS3 Wheel Loads
10	990
30	2970
90	9810
180	17820

In order to use the MMLS3 mixture performance test results to develop the high temperature specification limits at multiple traffic levels, a relationship was needed to correlate the AADT volumes that correspond to the low, medium, and high traffic classes to the corresponding MMLS3 wheel loads for the development of the high temperature EPG specification. This conversion is summarized in Figure D-9.

AADT	average annual daily traffic, in vehicles
X 365	days/year
X 2	avg. # of applied wheels per vehicle
X 7/365	days out of the year surface is exposed to 7 day max pavement temp.
X 3/24	hours out of the day surface is exposed to max pavement temp.
X 3	conservative design life for a typical surface treatment, in years

Estimated MMLS3 Equivalent Wheel Passes

Figure D-9. Conversion of field AADT to MMLS3 equivalent wheel passes.

The first step shown in Figure D-9 is to convert the field AADT to annual field wheel loads by first acknowledging that, for a given vehicle, each axle will essentially have one wheel that crosses the wheel path. The assumption is that, for a typical car or truck, the typical surface treatment experiences two applied loadings on average, i.e., one when the front axle passes and a second when the back axle passes, as each vehicle moves longitudinally across the surface treatment section. It should be noted that large trucks can sometimes have more than two axles, but the number of these types of trucks would vary from location to location so an assumption had to be made. Any necessary adjustments to the developed EPG specification to account for trucks with more than two axles will be addressed in the long-term validation plan. The long-term validation plan will include obtained vehicle counts separated into Federal Highway Administration (FHWA) vehicle class for each field validation section constructed. This information will provide data about the average number of axles per vehicle for further investigation into any additions/adjustments that may be needed in the EPG specification to account for the effect of multiple field axle configurations of heavy vehicles. The AADT (in vehicles) times two wheel loads per vehicle equals the number of field wheel loads applied to the pavement each day. That result multiplied by 365 days per year yields the annual number of field wheel passes.

Another consideration that was needed in order to estimate the equivalent MMLS3 wheel loads is that all MMLS3 applied wheel applications occur at the seven-day average annual maximum pavement temperature for which the binders are graded, although this is not the case for the annual field traffic. The MMLS3 specimens were tested in a climate-controlled chamber within +/-1°C of the high temperature grade being considered. Therefore, when converting the field traffic to equivalent MMLS3 traffic, only the field wheel loadings that occur when the pavement surface is exposed to maximum pavement temperatures are considered. The annual number of field wheel passes reflects the number of wheel passes over the course of the entire year at the various temperatures that a location experiences within that time. The field pavement surface temperature varies greatly from the average annual seven-day maximum pavement temperature for which the binder is specified. In converting the field wheel passes to the equivalent MMLS3 wheel passes for the high temperature bleeding analysis, the loads that occur, for example, during the winter, which does not represent the temperature conditions under which bleeding initiates and propagates, should not be included. Therefore, the number of field wheel loads needs to be adjusted to capture the loading that occurs during the times of maximum pavement temperature exposure, or the seven hottest consecutive days of the year when bleeding

is most likely to initiate. This scenario more accurately reflects the temperature conditions under which the MMLS3 tests were conducted in the development of the EPG specification. Thus, the number of annual field wheel loads is multiplied by 7/365 days that represent the average seven-day maximum pavement temperature used to determine the high temperature performance grade for these EPG specifications.

Likewise, during each day of the seven days that constitute the average seven-day maximum pavement surface temperature, the temperature decreases greatly at certain times (e.g., night and morning hours), and therefore, the maximum temperature is not maintained for 24 hours. Thus, assumptions needed to be made in order to estimate the exposure time of the pavement surface to the maximum temperatures that are represented by the high temperature grade. The duration that the maximum pavement temperature is maintained can vary between climatic regions and also between each of the seven different days that comprise the average seven-day maximum pavement surface temperature in the EPG specification. Therefore, the assumption was made that the maximum pavement temperature should be maintained for approximately three hours per day on average (based on a preliminary investigation into hourly air/pavement temperatures in Raleigh, NC, Wisconsin, Phoenix, AZ, and Death Valley, CA). Because the time that the maximum pavement surface temperature is sustained varies as a function of location, this assumption is intended as a reasonable starting point for estimating the percentage of field traffic loads that occur during the period of daily maximum pavement temperature exposure.

The assumptions regarding the maximum pavement temperature exposure used in converting the field traffic to equivalent MMLS3 traffic were not made without consideration of the fact that bleeding can also occur at slightly lower pavement surface temperatures than the maximum temperature for which the binders are graded. However, in translating the field traffic to MMLS3 traffic for the purposes of developing the high temperature EPG specification limits, an approximation of the percentage of the field wheel loads that occur at a temperature matching the continuous high temperature condition of the MMLS3 chamber during testing was used, simply to establish a starting point for the analysis to be validated in the long-term validation plan for different climatic regions.

The final assumption made was that each field wheel load is equal to one MMLS3 wheel load for the purposes of this traffic conversion. This assumption was determined to be reasonable for surface treatments under MMLS3 loading, as previous findings have clearly shown that the changes in surface texture for a chip seal under MMLS3 loading are similar to the changes in surface texture of the same chip seal under field traffic loading (Adams 2013). These changes in surface texture are related to bleeding performance, in that a bled or flushed surface will exhibit less surface texture depth, represented by a very low mean profile depth (MPD), than a non-bled surface. A non-bled surface will retain some of the natural surface texture of the aggregate structure, as the residual binder will not negate the surface roughness that the aggregate provides. This phenomenon results in a higher measured MPD value and a seal with more skid resistance for braking vehicles. The MPD is reduced as a function of increased wheel applications as the aggregate reorients to its least dimension and is further embedded into the binder. Likewise, as the residual binder is forced to the surface during bleeding, or if excessive aggregate loss leaves bare spots, the MPD would be reduced as an indicator of this distress. Similarities observed with regard to the changes in surface texture between the laboratory specimens and the field-loaded specimens indicate that both the field and laboratory traffic methods impacted the chip seals similarly in the study. The changes in surface texture due to field traffic levels that correspond to medium and high traffic in these EPG specifications were found to be not significantly different

from the changes in texture due to MMLS3 traffic loading in the study by Adams (2013). Therefore, the research team decided to use a simple ratio of one field wheel load to one MMLS3 wheel load as a starting point for the developed EPG specification, because the changes in surface texture were proven to be similar between the field traffic and MMLS3 traffic within the traffic range covered by the developed specifications. Ultimately, the true effects of field traffic on surface treatment performance will be validated for all of the traffic categories during the execution of the long-term validation plan prior to implementation of the EPG specifications.

After completing the conversion from field AADT to equivalent MMLS3 loads using the aforementioned assumptions, the following number of MMLS3 loads was determined to correlate to the field traffic volumes (in AADT) associated with the low, medium, and high traffic grades in the EPG specifications. These traffic equivalencies are summarized below:

- 3,000 MMLS3 wheel loads equal approximately 500 AADT
    - Representative of traffic at the low traffic upper limit
- 13,000 MMLS3 wheel loads equal approximately 2,500 AADT
    - Representative of traffic at the medium traffic upper limit
- 18,000 MMLS3 wheel loads equal approximately 3,500 AADT
    - Representative of traffic within the high traffic range

These equivalent MMLS3 traffic levels were used to develop the high temperature binder performance limits at all three traffic levels in the EPG specifications. Hereafter in this writing, the MMLS3 equivalent loads evaluated for EPG specification development are represented by the three traffic levels of the EPG specifications, as follows:

- Low traffic (L): 3,000 MMLS3 wheel loads
- Medium traffic (M): 13,000 MMLS3 wheel loads
- High traffic (H): 18,000 MMLS3 wheel loads

Development of Specification Limits – High Temperature

In the development of the high temperature specification limits for low, medium, and high EPG specification traffic levels, the relationship between the material binder property, i.e., the nonrecoverable creep compliance (J_{nr}) and the percentage of bleeding (% bleeding) for the mixtures was used. For developing these limits, a critical maximum allowable bleeding threshold of 80 percent, found based on previous research, was utilized to determine the maximum allowable J_{nr} value for each traffic level in the specifications.

Background for 80 Percent Bleeding Limit

In order to utilize the bleeding test results at different traffic levels to establish J_{nr} values for the specifications, a bleeding limit was needed that clearly defines unacceptable performance. Bleeding test results from the dissertation by Jusang Lee (2007) were used to obtain the 80 percent bleeding threshold for chip seal surface treatments. In his bleeding study, Lee studied bleeding as a function of changes in the material application rate at 50°C. The results from Lee's study of bleeding performance are summarized in Figure D-10.

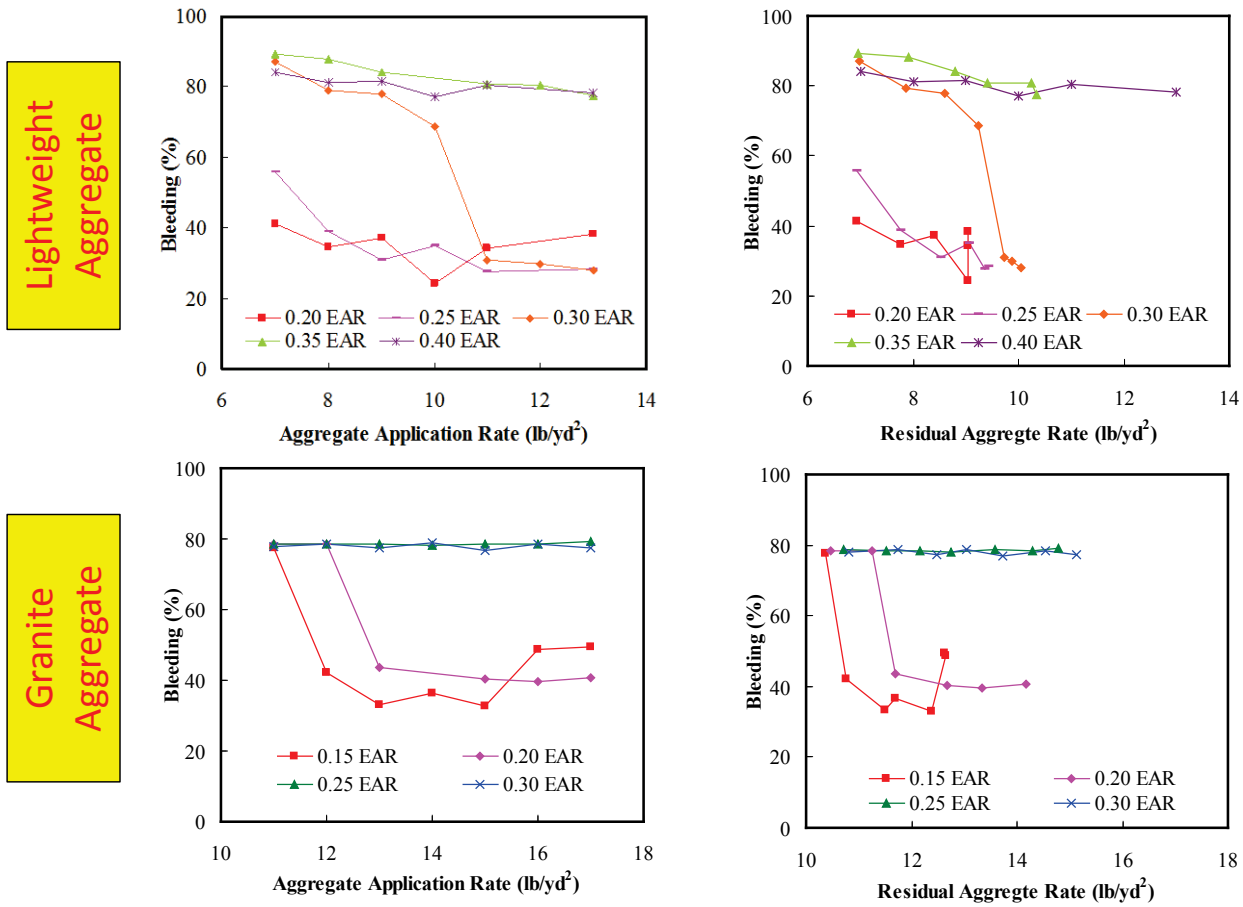

Figure D-10. Bleeding vs. material application rates for granite and lightweight aggregate types and CRS-2 emulsion (Lee 2007).

The 80 percent critical bleeding limit defines the bleeding performance that, when exceeded, is clearly unacceptable for surface treatment performance. In Lee's study, the material application rates were varied and each condition was tested under MMLS3 loading. The aggregate and emulsion application rates (AARs and EARs) used in chip seal design are the most critical factors that influence bleeding performance. Essentially, if the EAR is too high in a chip seal (a phenomenon referred to as flushing), the chip seal mixture will exhibit bleeding issues regardless of binder type. Conversely, if the AAR is too low, there may be insufficient aggregate to provide skid resistance for the surface treatments and the chip seal surface will display bare spots, which is another cause of bleeding. The results show that an extremely high EAR and low AAR is a combination that maximizes the bleeding susceptibility of chip seal mixtures and that chip seals consistently exhibit bleeding of 80 percent or higher. Therefore, if a binder used in a well-designed chip mixture (i.e., for a performance-based design to find an optimal EAR and AAR) has 80 percent bleeding or higher, it is safe to say that the binder is not acceptable for use under those climatic/traffic loading conditions. Essentially, this 80 percent limit definitively identifies unacceptable performance in chip seal mixture testing.

For specification purposes, the maximum bleeding threshold used for the EPG specification limit determination should not be so restrictive (i.e., too low a bleeding limit) that it fails all of the commercial binders included in this research at the low traffic level for typical high temperature grades, as all of the binders included in the EPG specification development are

already in service nationwide under at least the low traffic level. The 80 percent bleeding limit allows a relatively high level of confidence that any binder unable to pass this 80 percent bleeding limit would have a very high risk of bleeding problems in the field at the tested traffic level and temperature.

However, the premise that a mixture that exhibits 75 percent bleeding (which would pass the 80 percent maximum bleeding threshold) can perform acceptably is worth further discussion. Here, it is important to note that the MMLS3 tests for multilayered seals for the high temperature EPG specification development used harsh test conditions, which caused increased bleeding. For the high temperature EPG specification developmental testing, the wandering feature on the MMLS3 was turned off in order to capture both rutting and bleeding simultaneously. The wandering feature simulates the natural wandering of a vehicle that occurs perpendicular to the direction of traffic. The reason for turning off the wandering feature on the MMLS3 for these tests was so the rut depth could be measured as the height difference between the trafficked and untrafficked area of the sample while at the same time acquiring images for assessing bleeding performance as a function of applied wheel loads. However, by turning off the wandering feature, the specimen experienced a high number of wheel passes in the loading area spanning the width of the tire. If the wandering feature had been turned on, the tire would wander across the entire 175-mm sample width, thereby distributing the wheel loads during loading. The effective loading area for this test covers only approximately 87.5 mm of the 175 mm in the sample width with the wandering feature turned off. Figure D-11 shows the loading area of a specimen tested under MMLS3 loading without wandering, as acquired from laser scan data of the surface of a chip seal specimen.

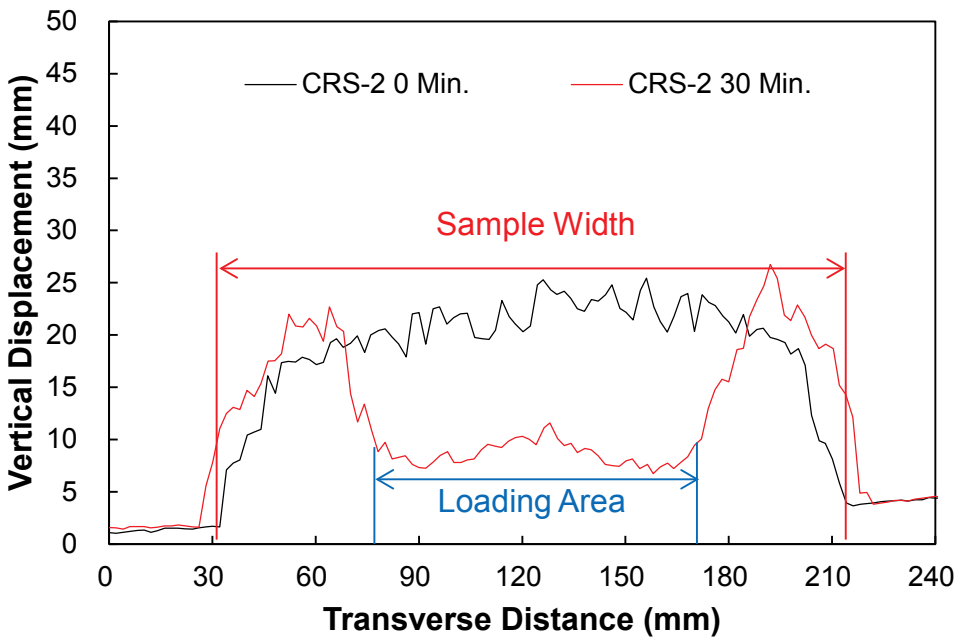

Figure D-11. Laser scan data showing chip seal specimen in original condition and after 30 minutes of MMLS3 loading.

Due to this lack of wheel wandering, there was also less recovery time for the binder than it typically would have experienced in service under field traffic loading where natural vehicle

wandering in the transverse direction occurs. Although the MMLS3 provides an accelerated loading condition (applying 990 wheel loads in just 10 minutes), the number of loading cycles experienced by the area of a single MMLS3 tire width of the chip seal specimen is even greater when the wandering is turned off. Under field traffic loading at high temperatures, asphalt binders recover during the rest period between traffic loads applied from passing vehicles. During this recovery period, the elasticity of the binder allows it to recover from some of the non-permanent deformation that it experienced due to the loading stress. In the MMLS3 test without wandering, the binder is not allowed this recovery time due to the highly accelerated nature of loading onto the same location of the specimen. Due to these factors, a conservative maximum bleeding threshold was established that takes into account the possibility of higher magnitudes of '% bleeding' for MMLS3 testing than might have been observed under field traffic loading.

Rutting Performance

For multilayered seals, rutting is also a performance characteristic that is used in the evaluation of surface treatments. Although surface treatments provide no structural strength and rutting performance can be heavily dependent on the structural integrity of the underlying layers, resistance to rutting within a multilayered seal is still desirable.

Rutting performance was measured using the MMLS3 device with the wandering feature disabled so that the specimen was trafficked continuously along a defined wheel path while other portions of the sample remained untrafficked outside of the wheel path. Figure D-12 shows the laser scan data from an untrafficked chip seal specimen and the same specimen scanned after 30-minute and 90-minute loading times. The figure shows neat, latex-modified, and polymer-modified emulsions.

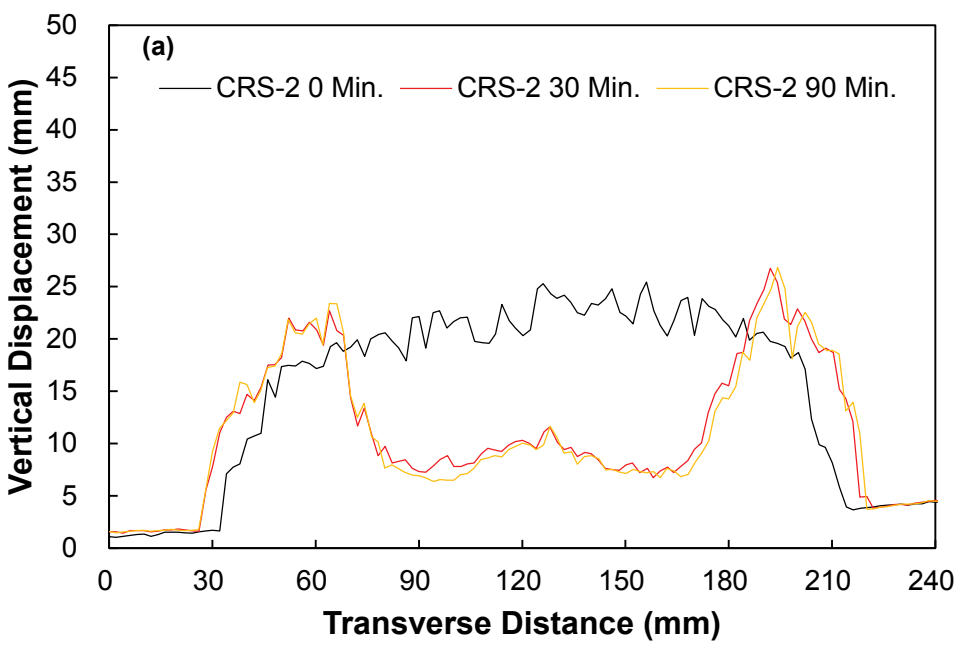

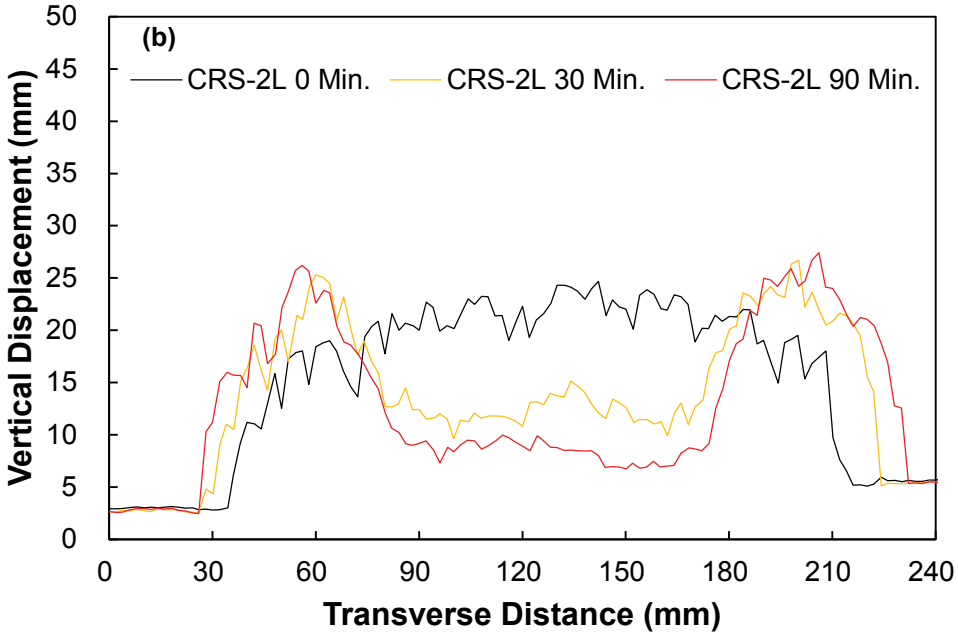

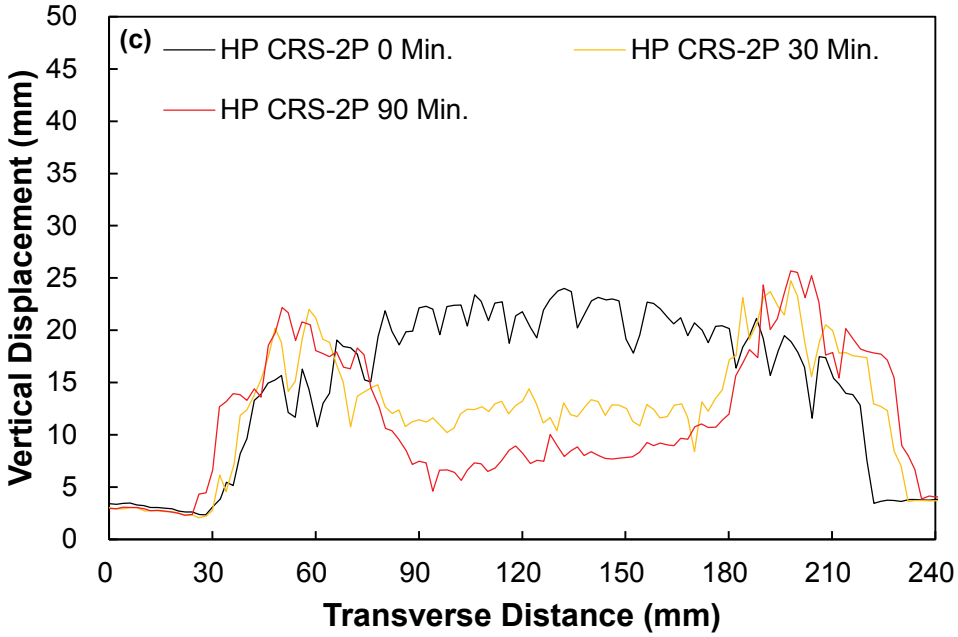

Figure D-12. Effect of binder modification on MMLS3 rutting performance shown after MMLS3 loading times of 0, 30, and 90 minutes for: (a) CRS-2, (b) CRS-2L, and (c) HP-CRS-2P emulsions.

Figure D-12 shows the effects of binder modification on rutting performance at high temperatures. The results show that the rate of rutting is slowed by the effect of binder modification. The 30-minute rutting results for both modified binders displayed in Figure D-12 (a) and (b) exhibit slower rut depth growth than the unmodified CRS-2 emulsion, which immediately reached its ultimate rut depth within the first 30 minutes of loading. From the MSCR binder tests for the EPG specification it has been observed that modified binders have

lower measured J_{nr} values and exhibit less nonrecoverable deformation than unmodified binders, which is confirmed by the higher resistance to rutting in the chip seal mixture specimens.

The findings from the rutting analysis are provided in Figure D-13 and show that the resistance to rutting in the chip seal mixture correlates with the high temperature binder parameter, J_{nr}.

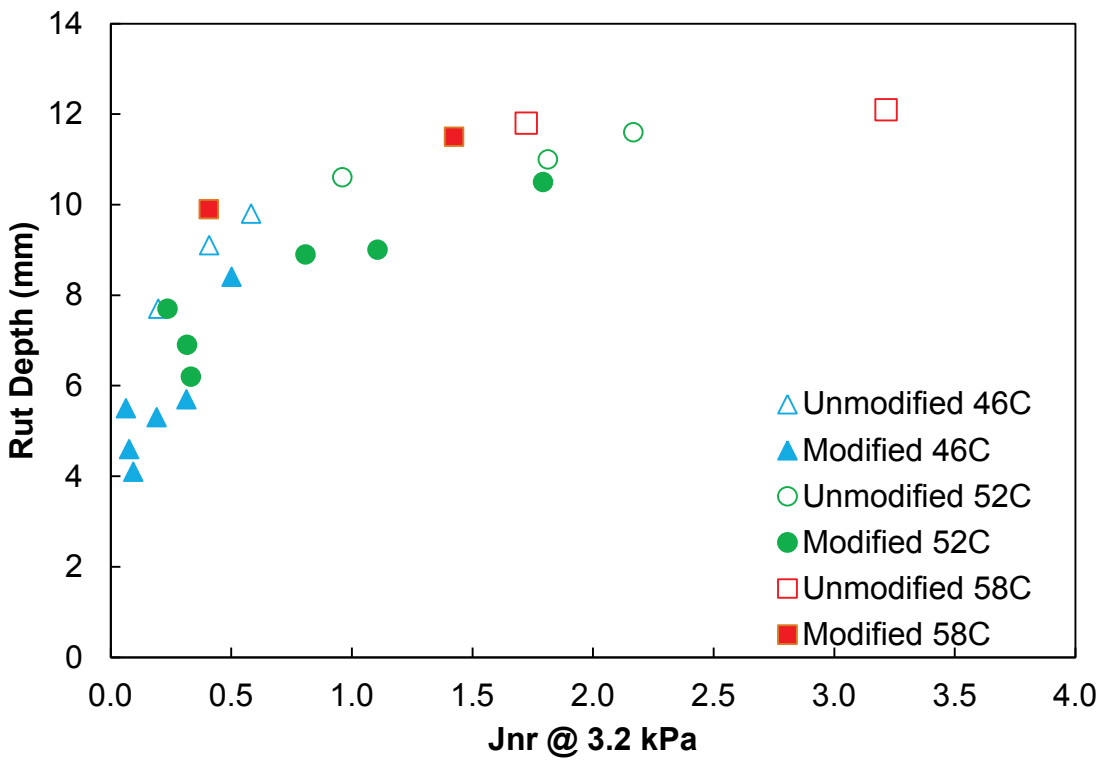

Figure D-13. High temperature rutting performance for modified and unmodified binders at 990 MMLS3 wheel passes.

The results from the rutting performance tests show that a relationship exists between the rut depth and J_{nr} at 3.2 kPa at multiple high temperatures. Binders that have lower measured J_{nr} values, or less residual strain after repeated creep and recovery testing, show a greater resistance to rutting. Conversely, binders that have higher J_{nr} values show significantly less resistance to rutting. The mixtures composed of modified binders show greater resistance to rutting than the mixtures with the unmodified binders at all temperatures tested. The increased stiffness of the modified binder materials increases their resistance to permanent strain, whereas the increased elasticity of these materials helps them recover better under stress loading. These material properties of modified binders translate to better resistance to rutting in chip seal mixtures.

Bleeding vs. Rutting Correlation

For chip seal treatments, bleeding is the more critical distress compared to rutting for characterizing high temperature chip seal performance, and therefore, bleeding is the major distress utilized in the development of the EPG specification. Nonetheless, a relationship exists between bleeding and rutting such that the resistance of the binder to rutting can be reasonably predicted based on the bleeding performance of multilayered seals. The relationship observed

between bleeding and rutting at high temperatures (46°C, 52°C, and 58°C) for 2,970 and 17,820 MMLS3 wheel passes is shown in Figure D-14, which indicates a solid relationship exists between bleeding and rutting performance in chip seal treatments.

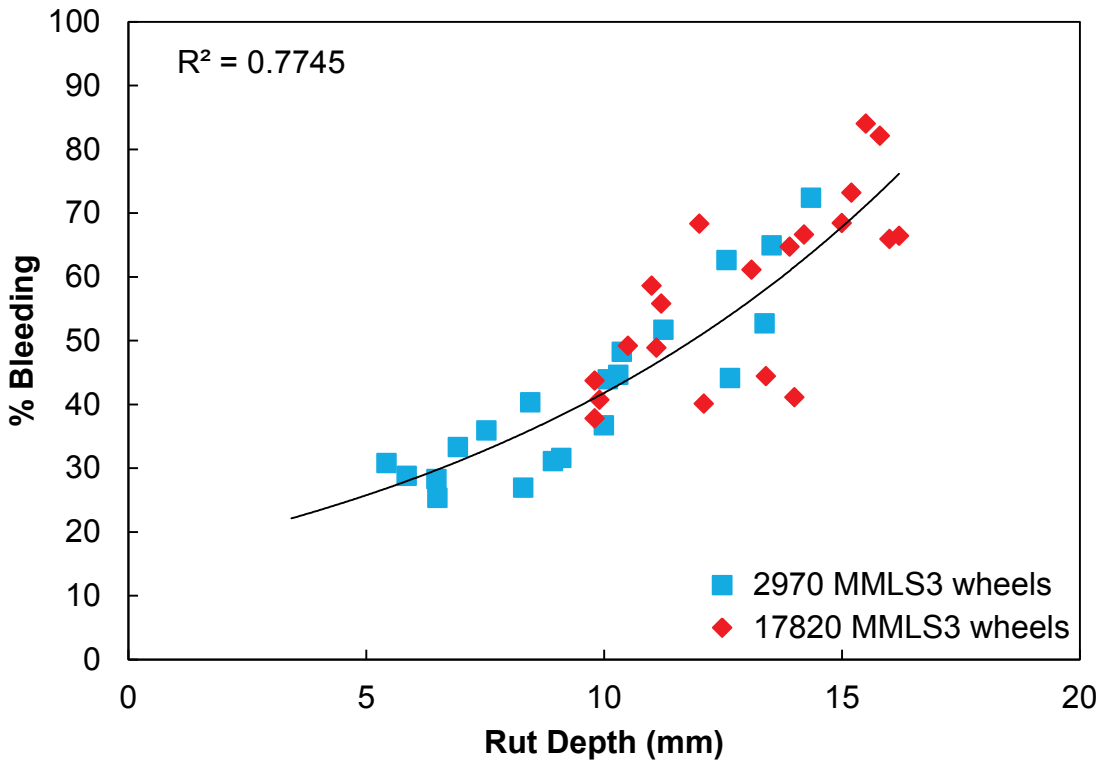

Figure D-14. Correlation between bleeding and rutting at multiple high temperature grades.

The results presented in the figure show that the same binder mechanisms govern resistance to both bleeding and rutting. The high temperature stiffness of the binder as well as the elastic recovery capabilities of the material translate to mixture performance in terms of both bleeding and rut depth propagation.

CHAPTER D-3. CHIP SEAL EPG RECOMMENDATION DEVELOPMENT AT INTERMEDIATE TEMPERATURE

This section provides additional research conducted on chip seal emulsions at intermediate temperature which the EPG recommends be tested during the mix design, and not in the EPG. At intermediate temperatures aggregate loss is the major distress type for chip seal treatments, as the loss of aggregate chips dislodged due to traffic loading can cause damage to passing vehicles. Also, excessive aggregate loss can lead to bare spots that contribute to bleeding in chip seal treatments at high temperatures. The EPG recommends that the BBS test methods described in this chapter are conducted during the mix design phase instead of during emulsion grading phase since the component aggregate materials are unknown at the time of grading for measuring compatibility. The BBS test, a modification of AASHTO TP91, was used to assess raveling at intermediate temperature grades. The BBS test measures the stress that is required to detach a

binder specimen that is adhered to an aggregate substrate (i.e., bond strength) and is used for quantifying the emulsion residue's resistance to aggregate loss. The BBS test checks the ability of an emulsion to resist both adhesive and cohesive failure under loading at two stages in the critical early life of the seal. The first test is conducted after four hours and measures early raveling resistance, thus simulating the bond strength that the seal has developed by the time a chip seal is typically opened to traffic. The test helps ensure that each emulsion develops strength fast enough to avoid early raveling loss when opened to field traffic. The second BBS test is conducted on an untested sample after it has been fully cured, as a chip seal should show sufficient bond strength to resist late raveling after curing is complete. The BBS test is also used to test the ability of the binder to resist stripping due to moisture damage when exposed to rainfall early in the life of the seal. Using the bitumen bond strength (BBS) test, the ability of an emulsion to resist both adhesive and cohesive failure under loading at various stages in the critical early life of the seal can be determined. The development of the protocol for these test methods as well as key findings are outlined in subsequent sections.

Development of Curing and Moisture Conditioning Protocol for BBS Testing

The developed curing and conditioning procedures used to characterize early, late, and wet raveling for both the binder and mixture specimens tested in this research are described in the following sections. For the development of the recommended mix design test protocol at intermediate temperatures, studies were also conducted to examine if BBS testing on emulsion in uncured, wet, and fully cured conditions appropriately captured the raveling potential of the mixture.

Determination of Curing Times for BBS Test

The curing times at which the chip seal emulsions and mixtures were tested for the BBS tests are four hours and 21 hours. The four-hour curing time test represents the early raveling susceptibility in the emulsion or the likelihood of early aggregate loss in the chip seal mixture when the newly constructed chip seal is initially opened to traffic. The 21-hour curing time test represents the late raveling that occurs once the emulsion in the chip seal has cured significantly and has been allowed to develop a level of bond strength that approaches its maximum strength. Figure D-15 displays findings from the dissertation by J. K. Im (2013) that was conducted using CRS-2L emulsion cured on an aggregate substrate using the COR method.

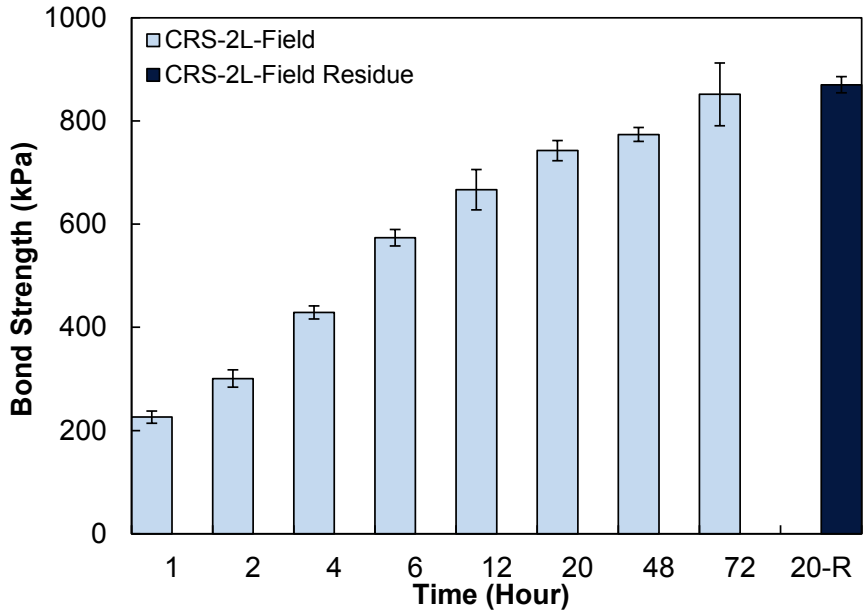

Figure D-15. Bond strength development for a typical chip seal emulsion as a function of curing time (Im 2013).

The Im study results show that after 20 hours of curing, the bond strength observed from the BBS test is over 90 percent of the maximum value obtained after 72 hours of curing. Also, the difference between the 20-hour and 72-hour results is almost statistically insignificant based on the standard error associated results. Therefore, the bond strength after 21 hours of curing was determined to be enough time to characterize late raveling potential in chip seal emulsions using the BBS test. This curing time was selected considering that the specimen curing time required for the BBS test should be practical for mix design purposes. However, curing tests can be conducted on the specific emulsion material to be used in the design to ensure full curing prior to late raveling tests.

Moisture-Conditioning Procedure for Wet BBS and Wet Vialit Tests

The wet BBS test evaluates the ability of the binder to resist moisture damage that causes stripping, or moisture-induced aggregate loss, in a chip seal mixture. After fabrication, specimens undergo four hours of dry curing in a forced-draft oven at the temperature specified as the intermediate performance grade. Then, the specimen is placed in a heated water bath at 40°C, which is the temperature used to characterize the effect of moisture damage of asphalt binders (Moraes et al. 2011). This moisture conditioning lasts for 16 hours before the specimen is removed from the water bath and allowed to dry for one hour prior to testing. The premise behind waiting four hours to begin the moisture-conditioning procedure is that chip seals are normally cured under dry (i.e., no rain) condition. Because chip seal construction should never take place in rainy conditions, the moisture-conditioning procedure should not be started immediately after specimen fabrication. Typically, the weather forecast is monitored in an attempt to finish the entire chip seal construction process and open the road to traffic while conditions remain dry. Therefore, the initial four-hour curing stage should be completely dry for the simulation of field construction conditions, followed by the aforementioned moisture-conditioning procedure that simulates rainfall during the summer season.

Figure D-16 displays the wet and dry BBS test results for the different chip seal emulsions. The results show the effect of moisture damage on the bond strength measured using the BBS test. These results indicate that the moisture-conditioning procedure for the wet BBS test effectively induces moisture damage within the binder. For both the modified and unmodified binders, the measured bond strength values for the moisture-conditioned wet BBS specimens are significantly lower than the dry bond strength values. The results show that the polymer-modified binder (CRS-2P-E) had the highest dry bond strength values and the highest wet bond strength values after moisture conditioning.

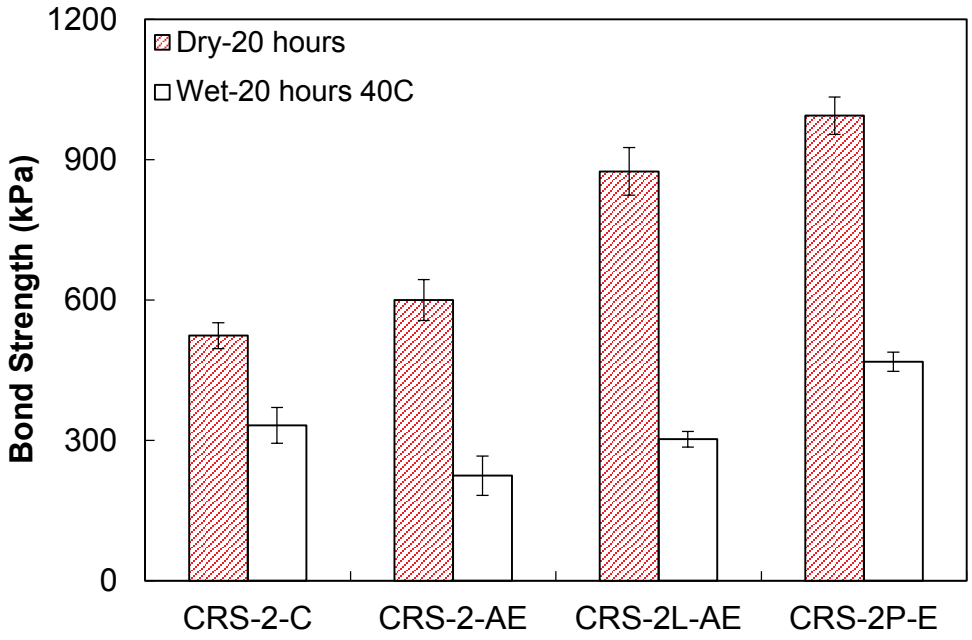

Figure D-16. Dry vs. wet BBS test results for chip seal emulsions.

Summary of BBS and Vialit Mixture Test Results

For assessing chip seal raveling resistance, BBS tests were conducted at 15°C and 25°C for late raveling and at 25°C for early raveling. Vialit mixture testing was conducted using the same curing times, temperatures, and moisture conditioning procedures as the BBS binder tests to obtain a direct comparison to the BBS test results. The BBS binder test results were compared to the Vialit mixture test results to determine if the BBS test would capture the binder's effect on the chip seal's aggregate loss resistance. Figure D-17, Figure D-18, and Figure D-19 show the relationships observed for late raveling, early raveling, and wet raveling, respectively.

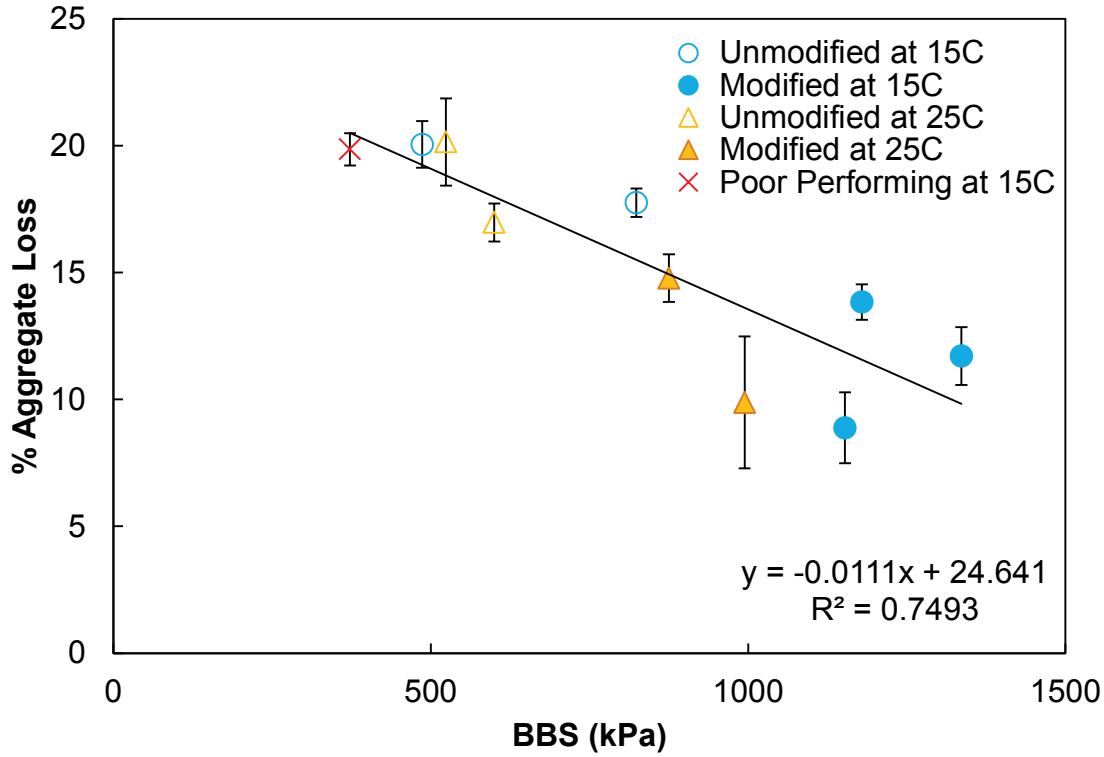

Figure D-17. Minimum 21-hour bond strength limits.

The results in Figure D-17 indicate that a relationship exists between the aggregate loss and BBS that is independent of the test temperature. The relationship appears to have a linear trend for the emulsions tested. The modified and unmodified binders tested at 25°C have a negative linear slope that is different from the slope of the plotted trend line shown in Figure D-17. However, additional data are needed to determine if a separate trend truly exists for the modified or unmodified binders tested at 25°C. Due to the standard error for emulsions tested at 25°C, it is unclear whether the deviation of those data from the trend line represents the material's behavior or scatter due to error within the data.

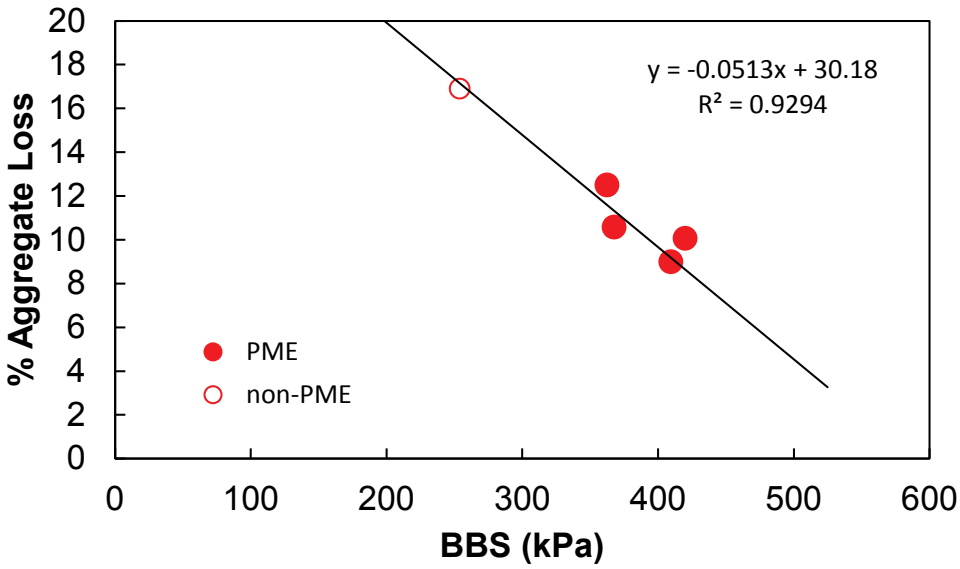

Figure D-18. Early raveling relationship between BBS and percent aggregate loss after four hours of curing.

The results, presented in Figure D-18, show a linear relationship between BBS and mixture aggregate loss, despite the limited number of unmodified emulsions available for testing.

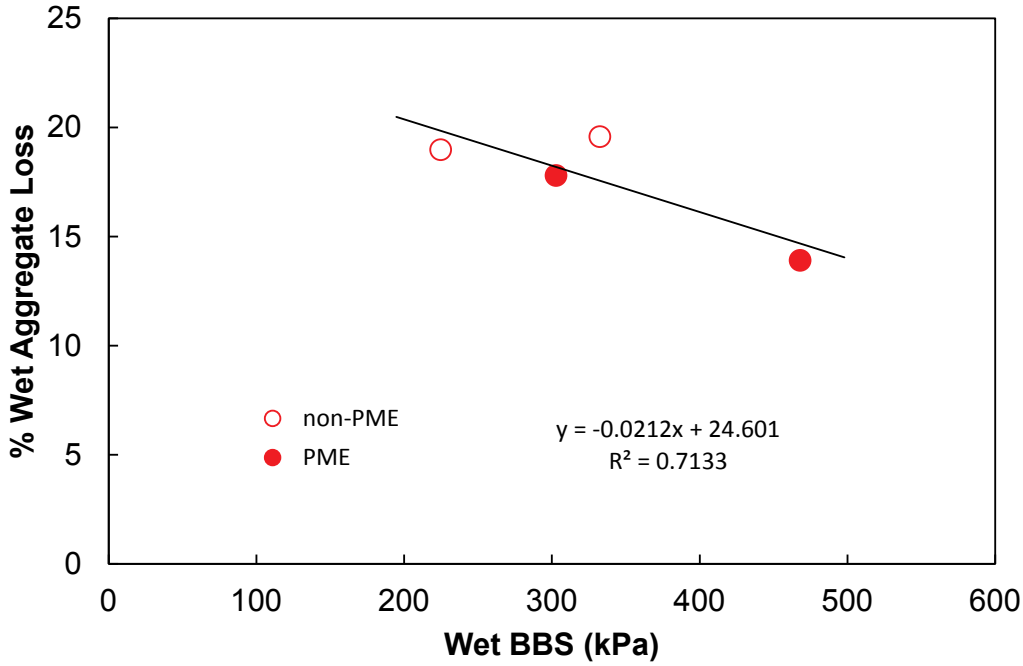

Figure D-19. Wet raveling relationship between wet BBS and percent wet aggregate loss.

The data show a solid correlation between the wet BBS and percentage of wet aggregate loss, demonstrating the potential for wet BBS to characterizing wet raveling resistance, for multiple emulsion types.

CHAPTER D-4. MICROSURFACING EPG RECOMMENDATION DEVELOPMENT AT INTERMEDIATE TEMPERATURE

At intermediate temperatures, raveling and reflective cracking were identified as the most critical distress types in microsurfacing treatments. However, the raveling of microsurfacing mixtures was determined to be driven by the chemical interaction between the emulsion and other mixture constituents (i.e., aggregate, cement, lime). Thus, raveling resistance cannot be linked to the quality of the binder alone. Reflective cracking is related to the pavement structure and is driven largely by the condition of the underlying pavement surface and, thus, is also not related directly to binder quality. Therefore, the microsurfacing EPG specification does not include any provisions for testing at intermediate temperatures. However, the specifications recommend conducting the Wet Track Abrasion Test (WTAT) after combining the emulsion with the aggregate to ensure adequate raveling resistance. The following sections detail the WTATs conducted during this research.

Wet Track Abrasion Test (WTAT) Findings

Prior to proceeding with the WTATs for the microsurfacing emulsions, a preliminary specimen-to-specimen variability study was conducted to determine the required number of replicates for testing. To assess variability comprehensively, six to eight replicates of WTATs were conducted using microsurfacing mixtures produced with several emulsions. The results of the variability study are shown in Figure D-20. These results demonstrate that the running average loss becomes constant after four specimens have been tested. Thus, four replicate specimens were tested for each condition in the remaining WTAT study.

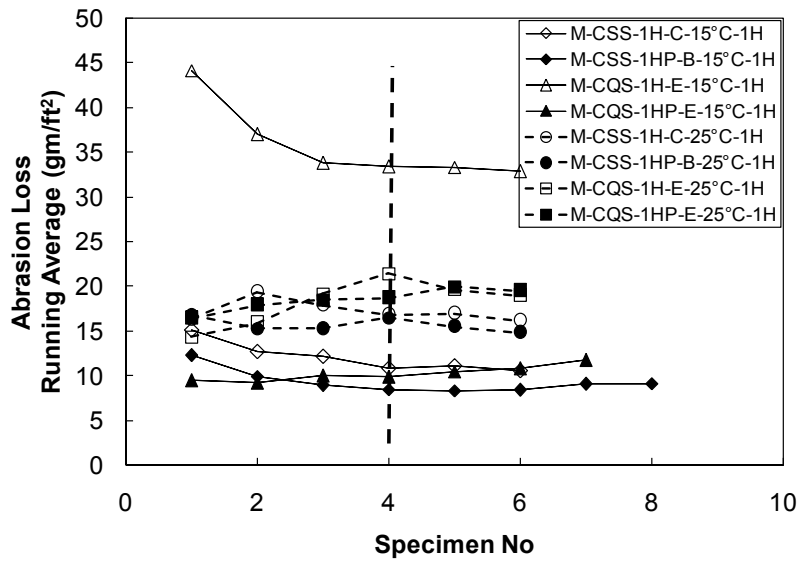

Figure D-20. Variability study for Wet Track Abrasion Test.

Initially, WTATs were conducted using a one-hour soak period at both 15°C and 25°C along with a moisture-conditioning procedure, i.e., 24 hours moisture conditioning at 40°C and tested at 25°C. Figure D-21 shows the results of the WTATs. The results indicate that the WTAT was able to detect the poor performing emulsions, as indicated by the high abrasion loss of the poor performing (PP) emulsion tested. This poor performing emulsion was expected to exhibit poor raveling performance due to its high emulsifier content of five percent. A high emulsifier

content increases the viscosity during mixing, leading to poor coating and poor bonding of the emulsion with the aggregate. The poor mixability performance of this emulsion was captured using viscosity test methods.

The WTAT abrasion losses for the modified and unmodified emulsions do not follow any specific trend. The International Slurry Surfacing Association (ISSA) specification limit for abrasion loss at 25°C after the one-hour soak period is 50 gm/ft^2. The results demonstrate that this specification is met with the exception of the poor performing emulsion (PP-M-CSS-1H-F).

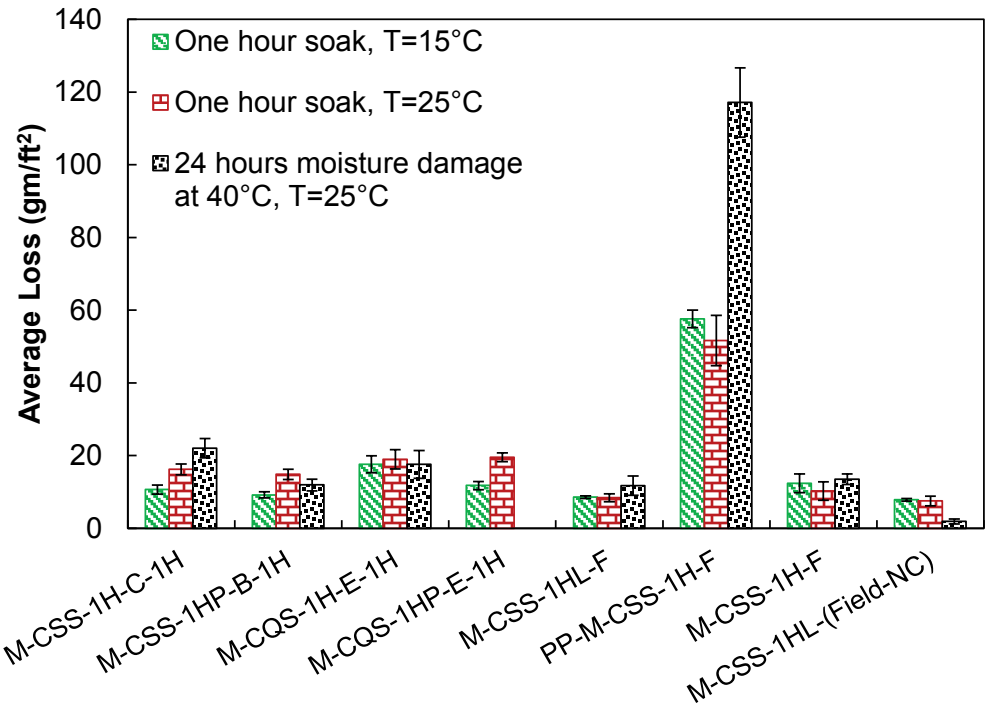

Figure D-21. WTAT results at 15°C and 25°C and moisture damage at 40°C.

Additional WTATs were conducted using the six-day soak period specified by ISSA. To further evaluate the sensitivity of the WTAT, two mix designs were tested with 6.5 percent residue content and 9 percent residue content to see if the WTAT could capture the difference in performance as a result of changing residue content.

Figure D-22 displays the WTAT results for four different emulsions using the additional test conditions. The results indicate that the WTAT was able to capture the effect of residue content on raveling resistance. The WTAT also can capture moisture sensitivity, as evidenced by the difference in results at the same residue content with a different moisture conditioning history. The WTAT abrasion loss results for the one-hour soak period and six-day soak period are within ISSA specified limits for all emulsions, with the exception of the poor performing emulsion. Based on these results, it is concluded that the WTAT is an effective performance test that can be used to capture the raveling resistance of microsurfacing mixtures.

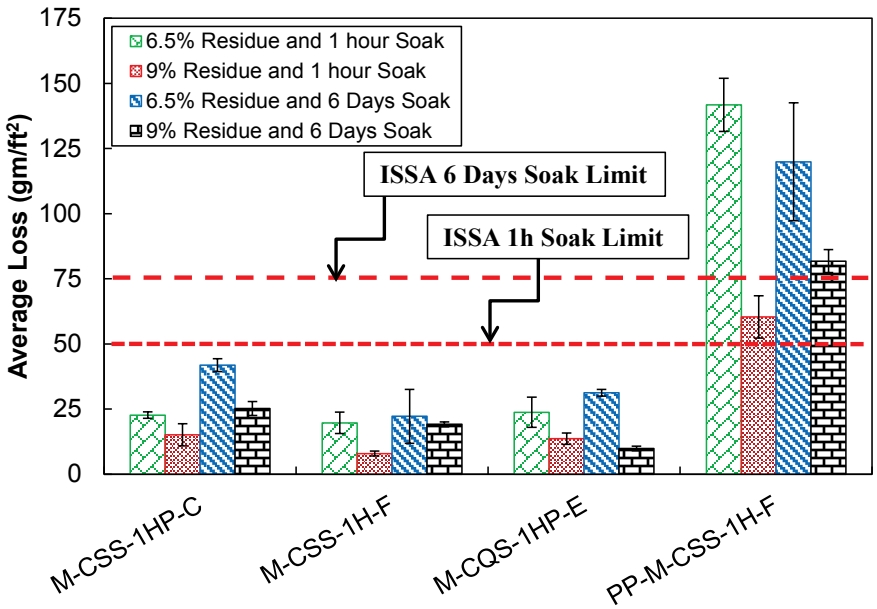

Figure D-22. WTAT results with different residue contents and different test conditions.

Comparison of Bitumen Bond Strength (BBS) Test and WTAT Results

WTAT vs. BBS Test for Residue on Rock (ROR)

The comparison between the bitumen bond strength (BBS) tests where recovered residue was applied to the substrate, i.e., the residue on rock (ROR) method, and the initial WTATs using the one-hour soak period and moisture-conditioning procedure that matches that of the BBS test is presented in Figure D-23. Figure D-23 demonstrates that there is no clear relationship between the WTAT and BBS test results, and thus, relationships between the WTAT and BBS test were investigated further using the expanded WTATs with the six-day soak period results included in Figure D-25.

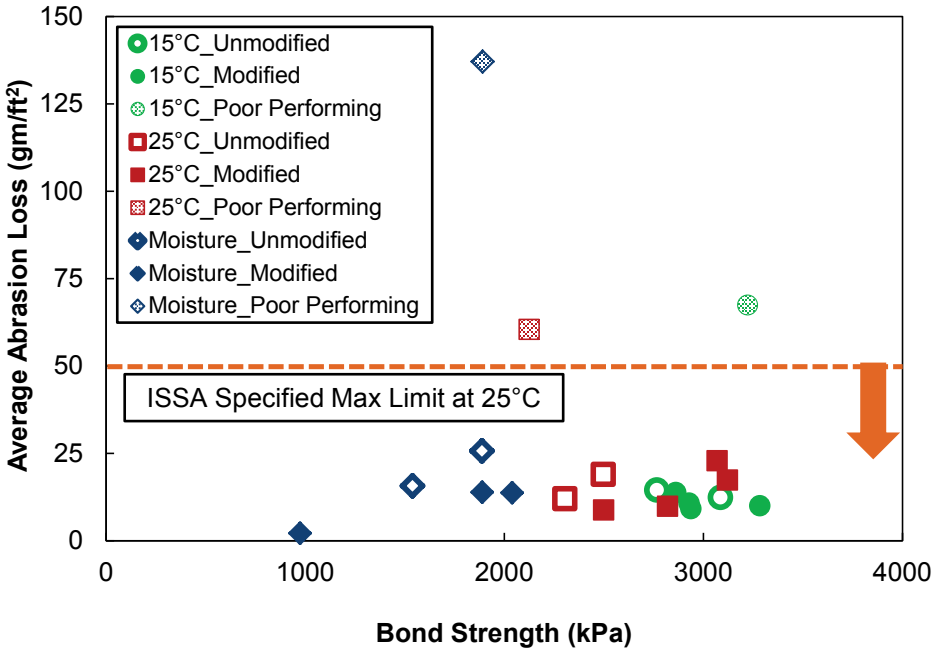

Figure D-23. WTAT results at different test conditions.

Figure D-24 and Figure D-25 present comparisons between the BBS test results using the ROR curing method and the WTAT results using the one-hour and six-day soak periods, respectively. The results demonstrate that there is no clear relationship between the BBS test and WTAT results, indicating that the BBS test is ineffective in capturing the raveling resistance of microsurfacing emulsions.

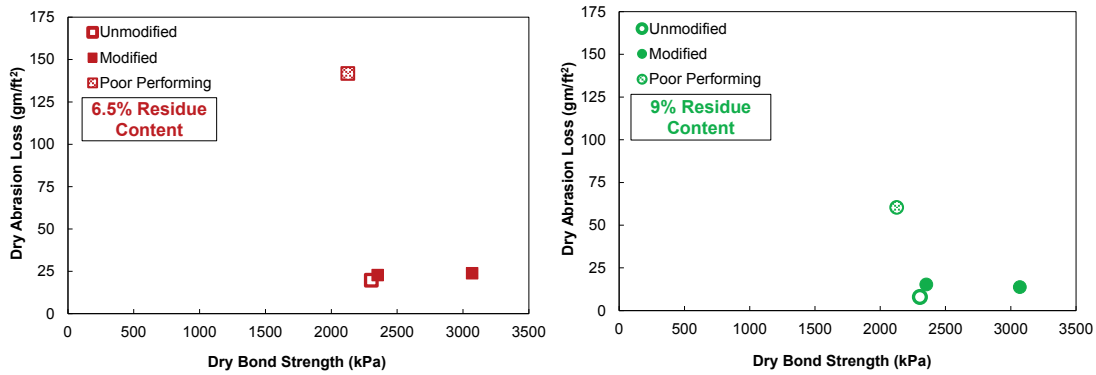

Figure D-24. Comparison of dry WTAT and dry BBS test results.

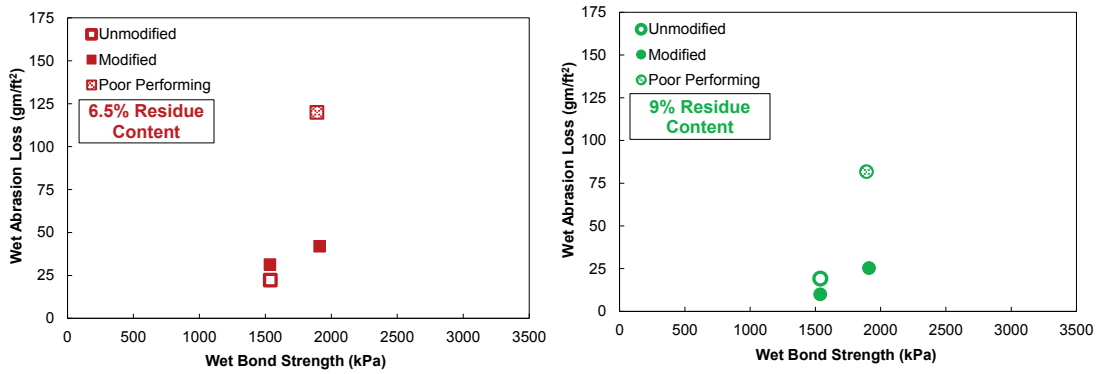

Figure D-25. Comparison of wet WTAT and wet BBS test results.

However, because the ROR was determined not to be an appropriate curing method for simulating the bond development between the emulsion and the aggregate in the BBS tests, further tests were conducted to compare the WTAT to the BBS test using the cured on rock (COR) method that allows for a more natural bond formation than the ROR method.

WTAT vs BBS for Emulsion Cured on Rock (COR)

The comparison between the BBS test results based on COR emulsion and the WTAT results is detailed in this section. Because emulsions are mixed with aggregate the field, curing in the field occurs while the emulsion is in contact with the aggregate, potentially influencing the bond between the emulsion residue and aggregate as the emulsifier is adsorbed onto the surface of the aggregate, neutralizing the surface charge. Figure D-26 and Figure D-27 present comparisons between the BBS test results for COR emulsions cured for 20 hours and WTAT results at 15°C and 25°C, respectively. No correlation between the WTAT results and BBS test results was found. The poor performing emulsion that exhibited poor WTAT results exhibits bond strength that is comparable to that of a standard performing emulsion, with significantly high WTAT results compared to standard emulsions. Thus, the results indicate that the BBS test is incapable of capturing the raveling resistance of microsurfacing emulsions.

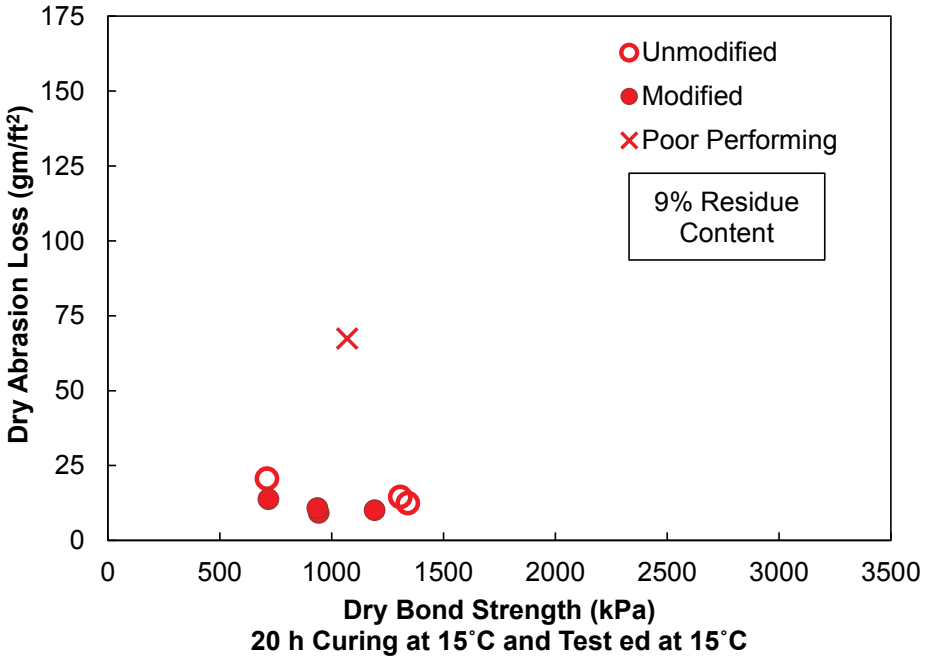

Figure D-26. Comparison of WTAT and BBS test results with emulsions cured on rock at 15°C.

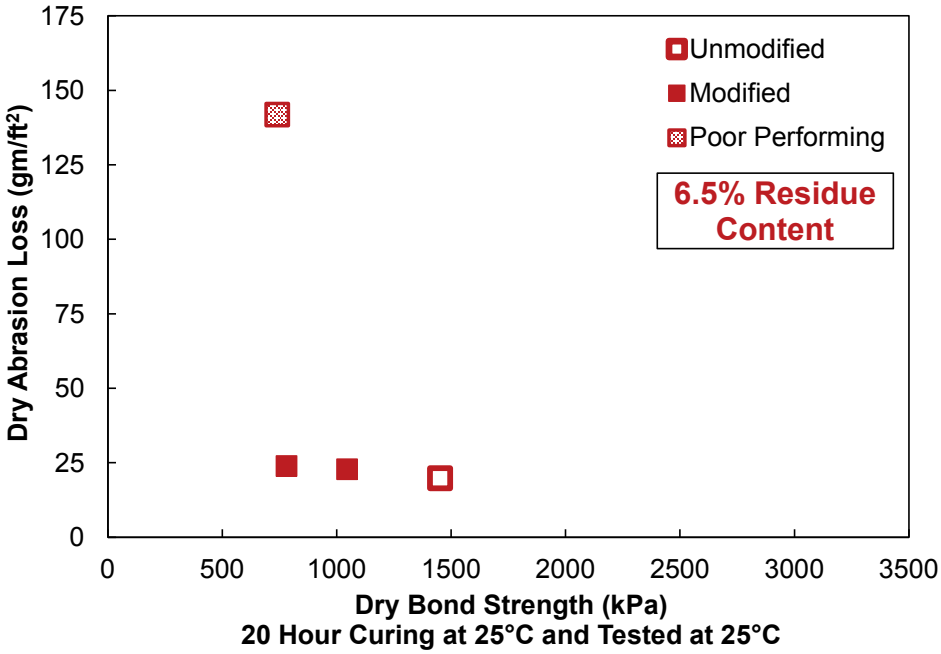

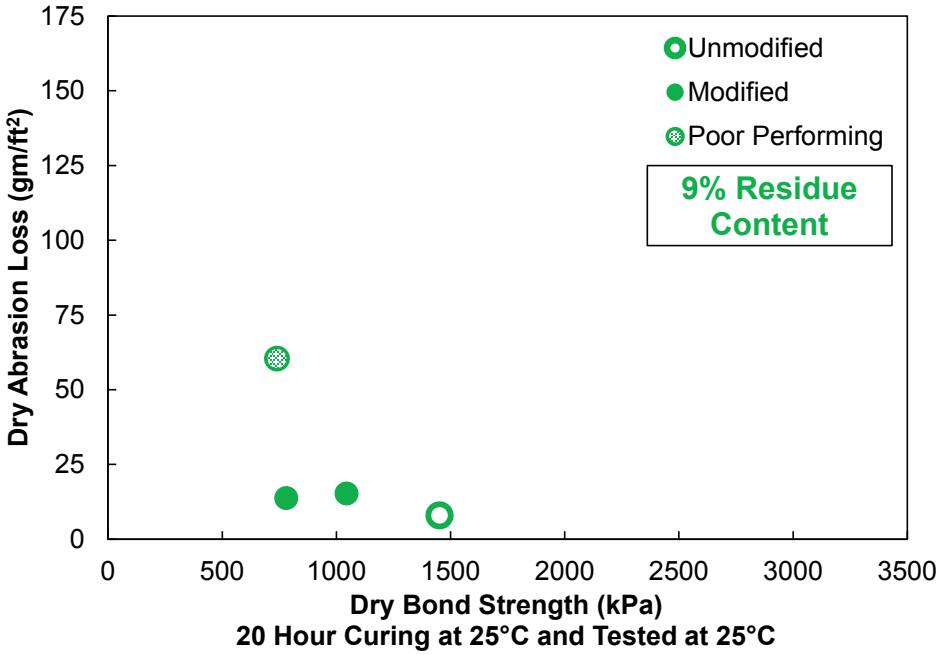

Figure D-27. Comparison of WTATs with different residue contents and BBS tests with emulsions cured on rock at 25°C.

The BBS test fails to correlate with the WTAT because microsurfacing mixture performance is mostly chemistry-driven and aggregate plays an important role in that chemistry. The surface area and surface charge of the aggregate are critical factors for microsurfacing performance. Microsurfacing emulsion suppliers typically formulate an emulsion for compatibility with the specific aggregate source to be used in a particular microsurfacing construction project. In this research, a single aggregate was used for fabricating the microsurfacing mixtures for all the emulsion types, which presents a problem for chemistry-driven microsurfacing mixtures.

Therefore, the EPG specification recommends that WTATs be conducted at intermediate temperatures for microsurfacing emulsions using the specific aggregate source that will be utilized for construction.

CHAPTER D-5. EPG SPECIFICATION DEVELOPMENT AT LOW TEMPERATURE PERFORMANCE GRADES

Aggregate loss is the primary distress in chip seals at low temperatures. Aggregate loss in chip seals was found to occur in a cohesive fracture pattern within the binder during low temperature mixture performance testing. Therefore, it was speculated that chip seal aggregate loss at low temperature is driven largely by the properties of the residual binder rather than the compatibility between aggregate and binder. Thermal cracking is the primary distress in microsurfacings at low temperatures. Thermal cracking in microsurfacings is related to the ability of the residual binder to withstand thermal contraction upon cooling without fracture. The critical low temperature distresses in both chip seals and microsurfacings typically occur during the first winter following construction. Because the low winter temperatures occur only a few months after the initial construction, it was assumed that the low temperature distresses were the most critical distresses before the residue aged significantly. Therefore, unaged residue was used for the low temperature grading.

Chip seal mixture low temperature aggregate loss performance was measured using Vialit tests. Microsurfacing mixture resistance to thermal cracking was quantified using fracture energy measured from Single Edge Notch Beam (SENB) testing. Both fracture mechanics based and rheology based residual binder properties were evaluated for chip seal and microsurfacing low temperature specification. The strength of the relationship between mixture performance and binder properties was to evaluate the appropriateness properties for low temperature specification.

Residual binder fracture properties were obtained from SENB tests conducted at -16°C, -22°C, and -28°C. The SENB test subjects a beam made of binder with a notch at the midpoint to constant displacement and three-point bending. For this study, 6.25 mm x 12.5 mm x 102 mm beam specimens were fabricated with a 3-mm notch at the center. These beams were loaded at a rate of 0.1 mm/s until failure. In a standard Bending Beam Rheometer (BBR) test, ethanol is used as the cooling medium during low temperature testing. However, under field conditions air is the cooling medium, not ethanol. Past research has shown that although linear viscoelastic properties are relatively consistent when specimens are conditioned in air and ethanol, the fracture resistance is greatly diminished in ethanol compared to air (Marasteanu et al. 2012). Because air best replicates field conditions, the use of air as a cooling medium was used herein. SENB test results were used to determine the fracture energy and fracture toughness of residual binders.

Residual binder dynamic rheological properties were obtained from Dynamic Shear Rheometer (DSR) temperature-frequency sweep testing at temperatures ranging from 5°C to 15°C. Temperature-frequency sweep test results were used to construction dynamic shear modulus and phase angle master curves. The Christensen-Anderson-Marasteanu (CAM) model (Marasteanu and Anderson 1999) was applied to provide analytical representations of developed mastercurves. The relationship between numerous rheological parameters and mixture performance were evaluated. Creep domain properties currently used for low temperature PG grading (i.e., stiffness and m-value) as well as frequency domain properties (i.e., functions of dynamic shear modulus (G*) and phase angle (δ)) were evaluated.

Creep rheological properties for microsurfacing residual binders were predicted from DSR frequency sweep test results using the inter-conversion methods developed by Ferry (1980) and Anderson et al. (1994). Creep properties of chip seal residual binders were obtained using Bending Beam Rheometer (BBR) tests (AASHTO T 313). Both temperature dependent properties and temperature independent properties (e.g., iso-modulus based parameters) were evaluated.

Relationship between Mixture Low Temperature Performance and Residual Binder Fracture Resistance

Residual Binder Parameters Evaluated

Both fracture energy and fracture toughness were evaluated as low temperature residual binder specification parameters. Both fracture energy and toughness provide an indication of the ability of a material containing a crack to resist fracture. Fracture energy and fracture toughness were calculated based on force and displacement results of SENB tests. A typical force versus displacement curve obtained from an SENB test is shown in Figure D-28. Fracture energy is calculated as the area under the force – displacement curve up to the point of maximum force (P). Fracture toughness (K_{IC}) is calculated using Equation (9.1).

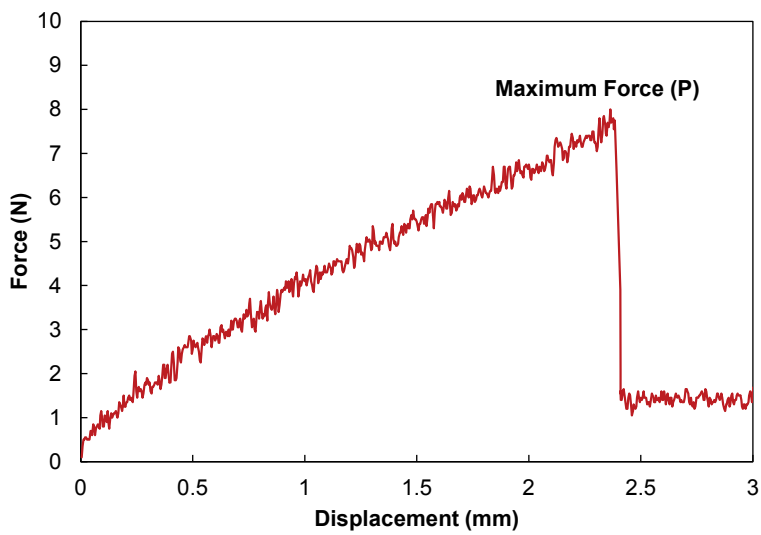

Figure D-28. Typical binder SENB force versus displacement data.

$$K_{IC} = \frac{PL}{BW^{3/2}} f(\frac{a}{W}) \tag{9.1}$$

Where P = Maximum force (N), L = Length of beam (102 mm), a = Depth of notch (~0.3 mm), W = Beam width (12.5 mm), and B = Beam depth (6.25 mm), and

$$f(\frac{a}{W}) = \frac{3(\frac{a}{W})^{1/2}[1.99 - \frac{a}{W}(1-\frac{a}{W})(2.15 - 3.93(\frac{a}{W}) + 2.7(\frac{a}{W})^2)]}{2(1+2\frac{a}{W})(1-\frac{a}{W})^{3/2}} \quad (9.2)$$

Chip Seal Results

The relationships between chip seal mixture aggregate loss and residual binder (a) fracture energy and (b) fracture toughness are shown in Figure D-29. Each data point in the figure represents the average of multiple specimens, and three data points are shown for each residual binder, representing the average of tests conducted at -16°C, -22°C, and -28°C, respectively. Both Figure D-29 (a) and (b) indicate a relationship between binder and mixture performance. However, results in Figure D-29 (a) indicate that the relationship between aggregate loss and binder fracture energy of modified binders (denoted by filled symbols) differs from that of unmodified binders (denoted by hollow symbols), making binder fracture energy inappropriate for use in low temperature specifications. Results in Figure D-29 (a) demonstrate that the relationship between binder fracture toughness and mixture aggregate loss is independent of modification. However, while a relationship between binder fracture and aggregate loss is evident, there is a significant amount of spread in the data with some unexpected trends. It is expected that an increase in fracture toughness would correspond to decrease in aggregate loss for a given binder. However, results of CRS-2-NC, CRS-2-F, and CRS-2P-A do not consistently follow this expected trend, prohibiting reliable use of fracture toughness in specifications.

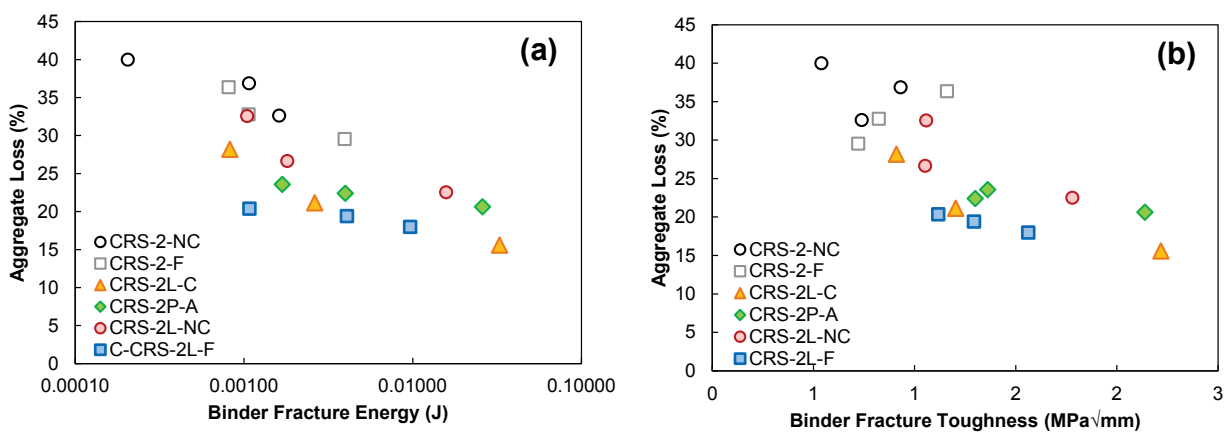

Figure D-29. Correlation between chip seal mixture aggregate loss and residual binder (a) fracture energy, and (b) fracture toughness.

Microsurfacing Results

The relationships between microsurfacing mixture fracture energy and residual binder (a) fracture energy and (b) fracture toughness are shown in Figure D-30. Each data point in the figure represents the average of multiple specimens, and three data points are shown for each residual binder, representing the average of tests conducted at -16°C, -22°C, and -28°C, respectively. Results in Figure D-30 (b) reveal no relationship between mixture fracture energy and binder fracture toughness. Results in Figure D-30 (a) indicate mixture fracture energy and

binder fracture energy are somewhat related. However, the relationship between mixture and binder fracture energies for CSS-1H-C deviates from the remaining emulsions. Therefore, results suggest fracture toughness and fracture energy are not appropriate for low temperature specification of microsurfacing emulsions.

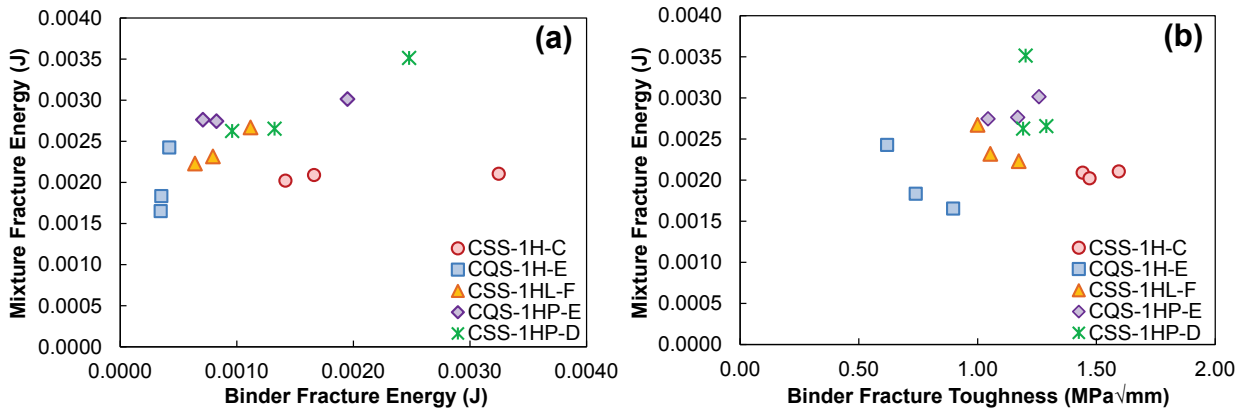

Figure D-30. Correlation between microsurfacing mixture fracture energy and residual binder (a) fracture energy, and (b) fracture toughness.

Relationship between Low Temperature Mixture Performance and Residual Binder Rheological Properties

Relationship between Low Temperature Mixture Performance and Residual Binder Temperature Dependent Properties

Residual Binder Parameters Evaluated

The temperature dependent rheological properties evaluated include G*, δ, G*·sinδ, and the Glover-Rowe parameter ($G^*\cdot\cos^2\delta/\sin\delta$). In addition, BBR stiffness and m-values at low temperature were predicted using DSR results. Analysis of the predicted BBR properties is presented in the main body of the report.

The dynamic shear modulus provides an indication of a material's stiffness and the phase angle provides an indication of a material's tendency towards elastic versus viscous behavior. The parameter G*·sinδ was evaluated because it is currently used in PG specifications to evaluate intermediate temperature performance. The specification was developed under the assumption that a lower dissipated energy implies lower propensity for cracking. Based on the assumption that fracture is a strain controlled phenomenon, it was demonstrated that energy dissipation minimization is accomplished through reducing the parameter G*·sinδ (Hicks et al. 1993). The Glover-Rowe parameter has been proposed as an indicator of binder ductility (Rowe 2011). It has been demonstrated that the Glover-Rowe parameter is correlated with pavement block cracking when evaluated at 15ºC and 0.0008 Hz (0.005 rad/s) (Anderson et al. 2011). Herein, the Glover-Rowe parameter was evaluated at the mixture performance test temperatures (-16ºC, -22ºC, and -28ºC) and anticipated loading frequencies in surface treatments. For chip seals residual binder analysis, a loading frequency of 12 Hz was used. This loading frequency was determined based on the anticipated loading pulse time experienced on at a point on a pavement surface subjected to 30 mph vehicular traffic (Brown 1973). Snow plows induce the majority of raveling at low temperature and 30 mph represents a typical snow plow speed.

Thermal cracking is the critical distress in microsurfacings at low temperature. Thermal loading occurs at a much slower rate than traffic loading. Since the Glover-Rowe parameter was introduced to address block cracking, a form of thermal cracking, the recommended frequency for evaluation of the parameter, equal to 0.0008 Hz, was adopted.

It should be noted that determination of rheological properties at low temperature required significant extrapolation because frequency sweep data was only acquired at intermediate temperatures. Many rheometers use water for cooling, thus making testing at temperatures below 0ºC impractical for specification. Master curves for chip seal and microsurfacing residual binders are shown in Figure D-31 and Figure D-32, respectively. The markers in Figure D-31 and Figure D-32 represent measured data and master curve CAM model predictions are denoted by the solid lines. Additional markers are included to show the location of the critical temperature and frequency conditions for low temperature performance within the master curves. For chip seals, it can be seen that the critical low temperature conditions require significant extrapolation from the measured data. While less extrapolation is required for microsurfacing residual binders because the critical frequency used in analyses is much lower, extrapolation is still necessary for -22ºC and -28ºC analyses.

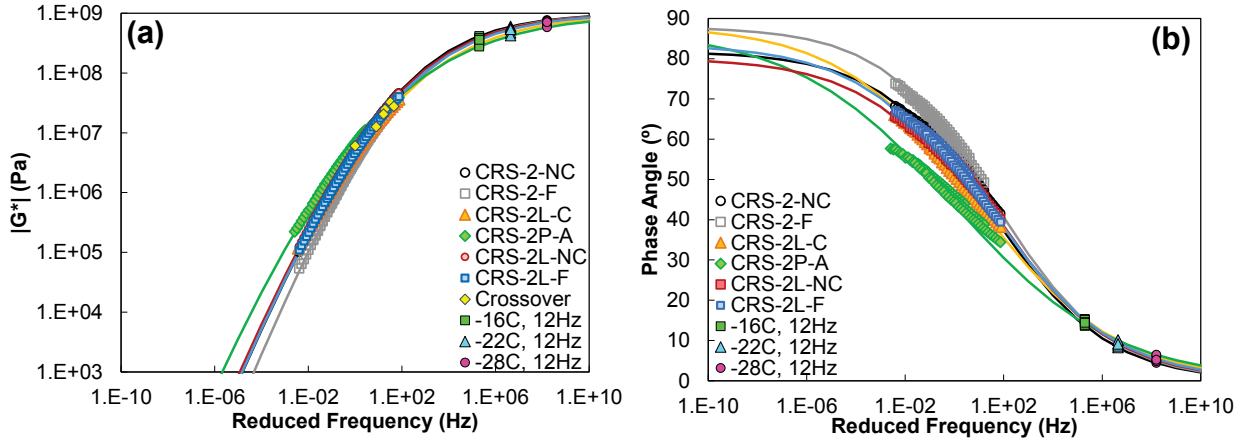

Figure D-31. Chip seal residual binder mastercurves: (a) dynamic shear modulus, (b) phase angle.

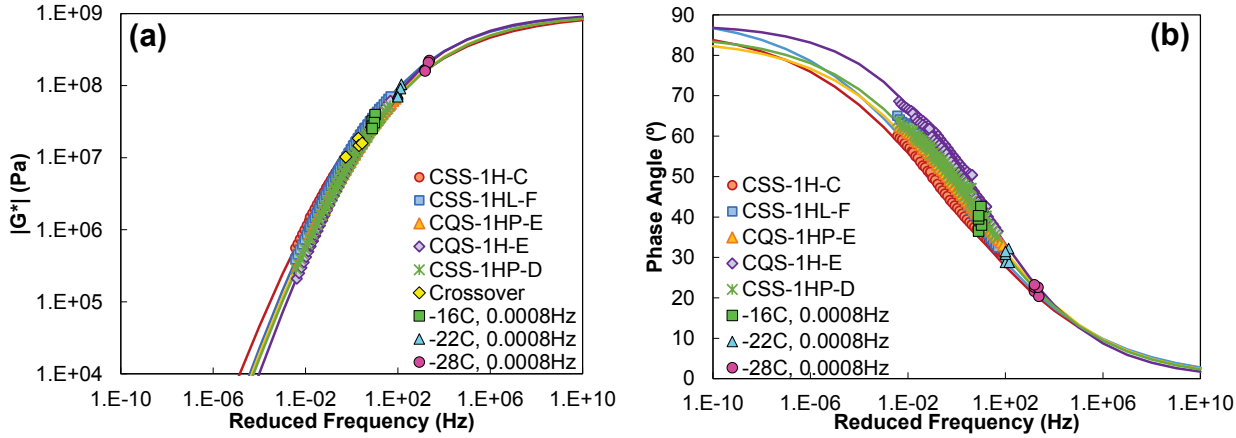

Figure D-32. Microsurfacing residual binder mastercurves: (a) dynamic shear modulus, (b) phase angle.

Chip Seal Results

The relationships between chip seal aggregate loss and temperature-dependent residual binder properties are shown in Figure D-33. Each data point in the figure represents the average of multiple specimens, and three data points are shown for each emulsion, representing the average of results at -16°C, -22°C, and -28°C, respectively. Results clearly demonstrate that the aggregate loss performance of modified binders (denoted by filled symbols) is superior to unmodified binders (denoted by hollow symbols). However, the rheological properties evaluated do not differ significantly between modified and unmodified binders. Consequently, while aggregate loss and the rheological properties evaluated appear to be somewhat related, the relationship is dependent on whether or not the material is modified. In addition, some results exhibit unexpected trends. Trends in Figure D-33 (a) indicate a lower G* is better for resisting aggregate loss at low temperature which is somewhat intuitive as softer materials are generally less prone to fracture. However, results in Figure D-33 (b) defy intuition, indicating a higher phase angle improves aggregate loss performance which indicates phase angle is not the most critical binder property to aggregate loss performance. A higher phase angle implies lower elasticity which is not expected to improve aggregate loss resistance. Furthermore, results in Figure D-33 (c) indicate that $G^* \cdot \sin\delta$ increases with increasing temperature, (due to the increase in phase angle with increasing temperature), whereas aggregate loss always decreases with increasing temperature. Please note that at the intermediate temperatures included in PG specifications, $G^* \cdot \sin\delta$ always decreases with increasing temperature. However, the low temperatures and relatively high frequency (12 Hz) considered herein are near the glassy region where G* is much less sensitive to temperature than at intermediate temperature. Interestingly, while the Glover-Rowe parameter also involves both G* and δ, results in Figure D-33 (d) do not demonstrate the inconsistency in trends observed in $G^* \cdot \sin\delta$ results. Based on the aforementioned factors, the temperature-dependent rheological properties evaluated are not deemed appropriate for specification of low temperature chip seal emulsion performance.

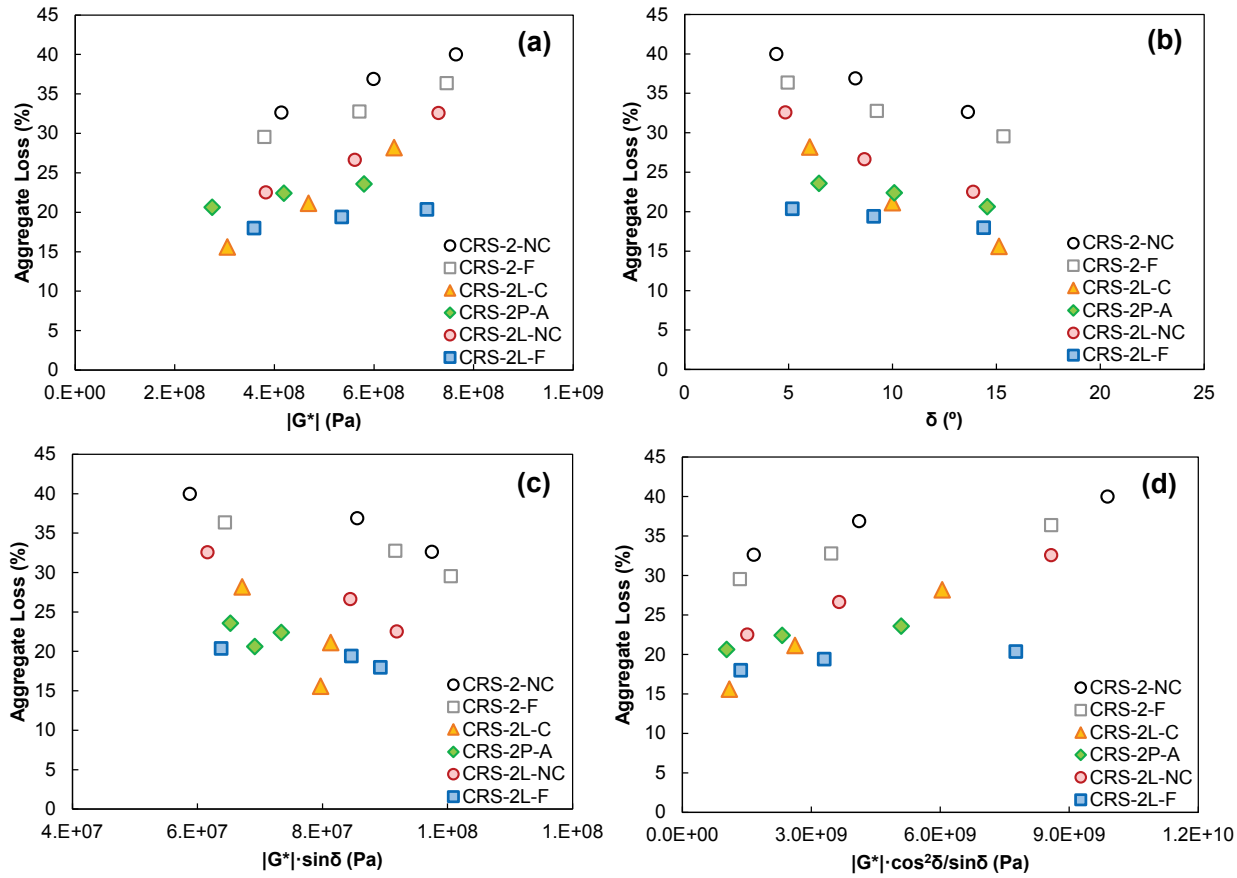

Figure D-33. Correlation between chip seal mixture aggregate loss and residual binder (a) G*, (b) phase angle, (c) G*·sinδ, and (d) Glover-Rowe parameter.

Microsurfacing Results

The relationships between microsurfacing mixture fracture energy and temperature-dependent residual binder properties are shown in Figure D-34. Each data point in the figure represents the average of multiple specimens, and three data points are shown for each emulsion, representing the average of results at -16°C, -22°C, and -28°C, respectively. Results in Figure D-34 demonstrate that none of the rheological properties evaluated is uniquely related to mixture fracture energy. While a relationship between mixture fracture energy and each rheological property evaluated property is observed for each emulsion, the relationship varies with emulsion type. Therefore, the temperature-dependent rheological properties evaluated are not deemed appropriate for specification of low temperature microsurfacing performance.

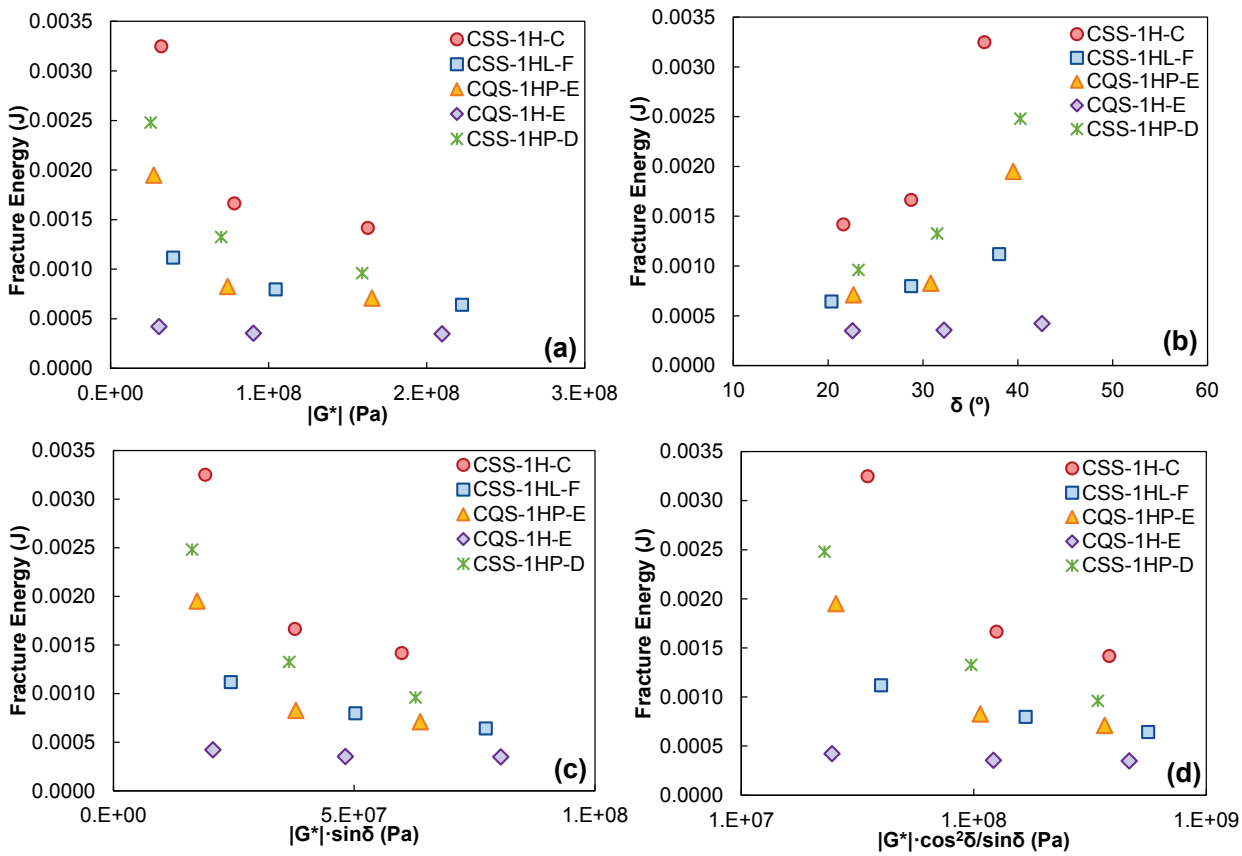

Figure D-34. Correlation between microsurfacing mixture fracture energy and residual binder (a) G*, (b) phase angle, (c) G*·sinδ, and (d) Glover-Rowe parameter.

<u>Relationship between Low Temperature Mixture Performance and Residual Binder Temperature Independent Properties</u>

<u>Residual Binder Parameters Evaluated</u>

Several temperature independent residual binder properties were evaluated because a temperature dependent residual binder property which is uniquely related to mixture performance could not be identified. One temperature independent property was evaluated based on creep domain analysis of rheological results: "delta T critical" (ΔT_c), equal to the difference between the low temperature critical PG specification temperature for m-value and stiffness (Anderson et al. 2011). Several frequency domain temperature-independent properties were also evaluated. The Glover-Rowe parameter at the proposed conditions (15ºC, 0.0008 Hz) was tried. In addition, several CAM model-based parameters were investigated, including the R value and crossover modulus. The CAM model is given in Equations (9.3) and (9.4).

$$|G^*|(\omega_R) = |G^*|_g \left[1 + \left(\frac{\omega_c}{\omega_R} \right)^v \right]^{-\frac{m}{v}} \tag{9.3}$$

$$\delta(\omega_R) = \frac{90 \cdot m}{\left[1 + \frac{\omega_R}{\omega_c}\right]^v} \tag{9.4}$$

Where ω_R is reduced frequency, G^*_g = G* as f → ∞: glassy dynamic modulus, ω_c is the cross-over frequency (reduced frequency where δ = 45°); and m and v =log(2)/R are the shape parameters, dimensionless.

The R value represents the logarithmic distance between the glassy asymptote and G* mastercurve at the crossover frequency (i.e., reduced frequency where phase angle equals 45º). The crossover modulus is the G* value corresponding to a phase angle of 45ºC. The crossover modulus values were always within the measured range of data acquired in frequency sweep testing at temperatures ranging from 5ºC to 15ºC. To evaluate a similar property at conditions representing low temperature conditions for which mixture testing was conducted, the G* values corresponding to a phase angle value of 5º for chip seal binders and 20º for microsurfacing binders were also analyzed.

Chip Seal Results

The relationship between chip seal mixture aggregate loss and residual binder ΔT_c is shown in Figure D-35 for three mixture test temperatures: (a) -16ºC, (b) -22ºC, and (c) -28ºC. Note that while mixture aggregate loss varies as a function of temperature, ΔT_c does not. The parameter ΔT_c is the difference between critical stiffness and m-value PG specification temperatures. Results indicate that ΔT_c is related to aggregate loss performance, with a lower ΔT_c indicative of better aggregate loss performance. These results suggest that if a binder's stiffness is lower for a given m-value, better aggregate loss performance is expected. However, there are outliers which deviate from the majority of results. Results in Figure D-35 (a) and (b), corresponding to aggregate loss test temperatures of -16ºC and -22ºC, demonstrate that CRS-2P-A results deviate from the trend of the other materials. Results in Figure D-35 (c) and (d), corresponding to aggregate loss test temperatures of -22ºC and -28ºC also demonstrate that CRS-2L-F results deviate from the trend of the other materials, with the greatest deviation at -28ºC. Note that the aggregate loss of chip seal mixtures containing CRS-2L-F did not vary significantly with temperature unlike the other materials which may explain these observations.

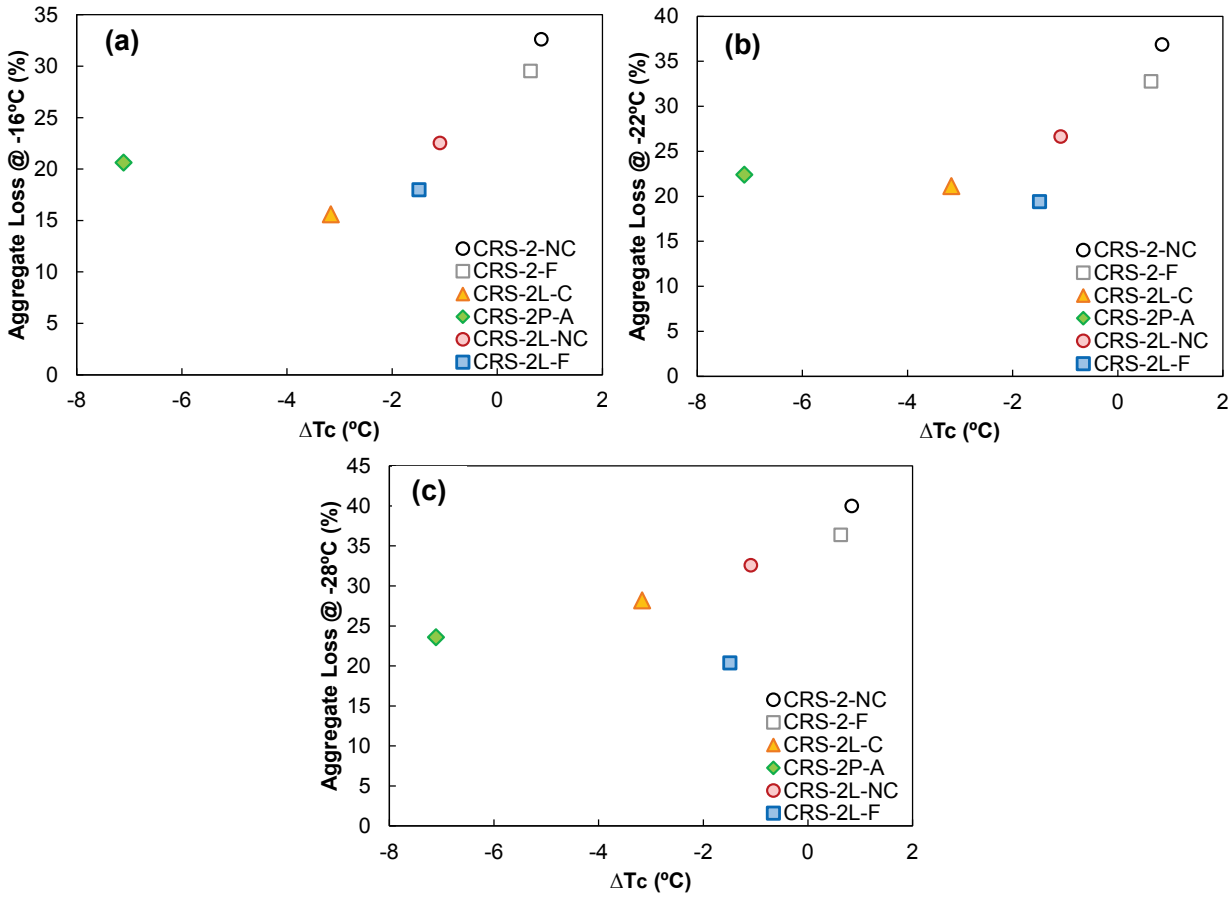

Figure D-35. Relationship between residual binder ΔTc and chip seal mixture aggregate loss at (a) -16ºC, (b) -22ºC, and (c) -28ºC.

The relationship between chip seal mixture aggregate loss and residual binder Glover-Rowe parameter is shown in Figure D-36 for three mixture test temperatures: (a) -16ºC, (b) -22ºC, and (c) -28ºC. Irrespective of mixture test temperature, the Glover-Rowe parameter was evaluated at 15ºC and 0.0008 Hz. Result reveal that the Glover-Rowe parameter evaluated at 15ºC and 0.0008 Hz is not related to mixture aggregate loss.

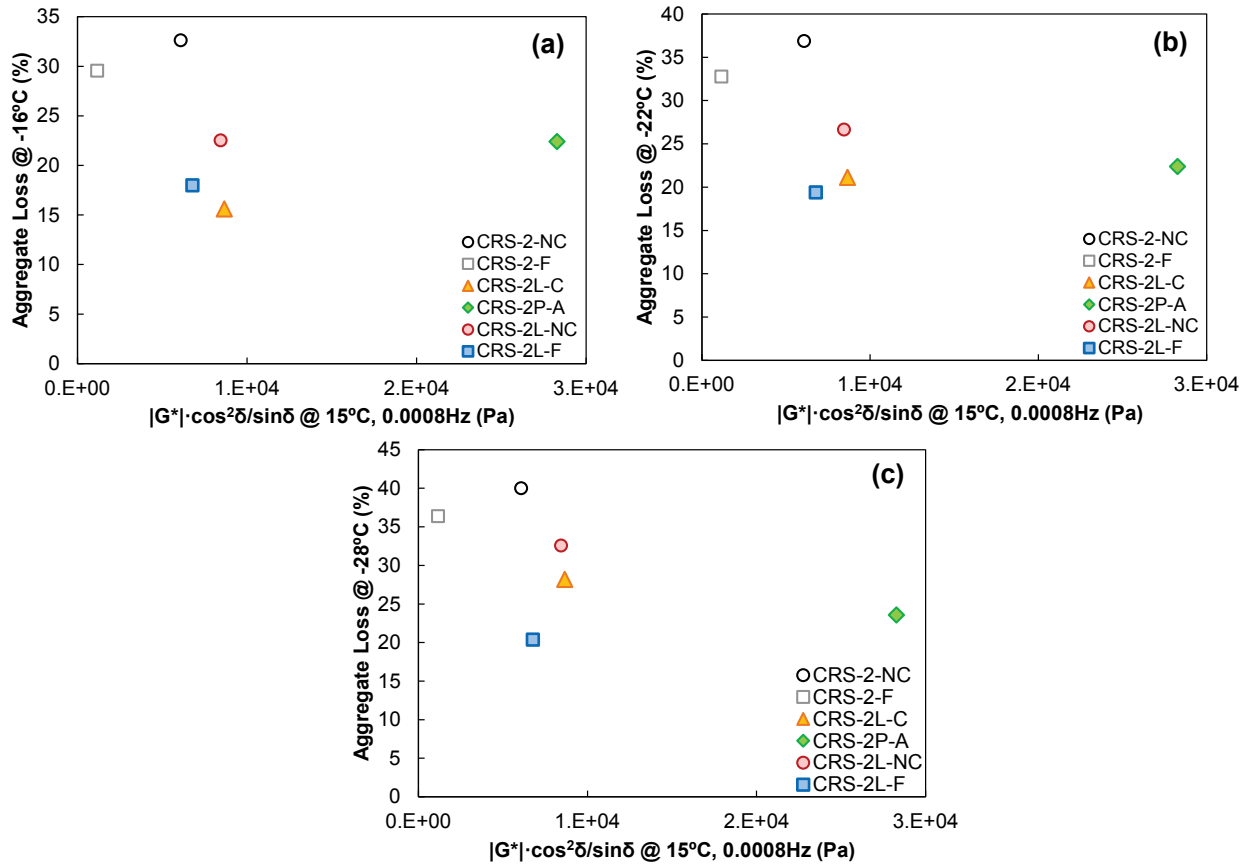

Figure D-36. Relationship between residual binder Glover-Rowe Parameter evaluated at 15ºC, 0.008 Hz and chip seal mixture aggregate loss at (a) -16ºC, (b) -22ºC, and (c) -28ºC.

The relationship between chip seal mixture aggregate loss and residual binder R-value is shown in Figure D-37 for three mixture test temperatures: (a) -16ºC, (b) -22ºC, and (c) -28ºC. Note that while mixture aggregate loss varies as a function of temperature, the R-value is a unique property of a given binder. Results indicate that R-value is related to aggregate loss performance. Results generally indicate a higher residual binder R-value leads to better aggregate loss resistance. As discussed, the R-value represents the distance between the G* master curve and the glassy modulus at the reduced frequency where phase angle equals 45º. For the majority of binders, the glassy modulus is approximately 10^9 Pa (Christensen and Anderson 1992). Thus, results generally imply that a lower modulus value at the reduced frequency where phase angle equals 45º is desirable. However, there are outliers which deviate from the majority of results. These outliers are generally consistent with the outliers observed in ΔT_c results presented in Figure D-35. Results in Figure D-37 (a) and (b), corresponding to aggregate loss test temperatures of -16ºC and -22ºC, respectively, demonstrate that CRS-2P-A results deviate from the trend of the other materials. Results in Figure D-37 (d), corresponding to aggregate loss test temperature of -28ºC demonstrates that CRS-2L-F results deviate from the trend of the other materials.

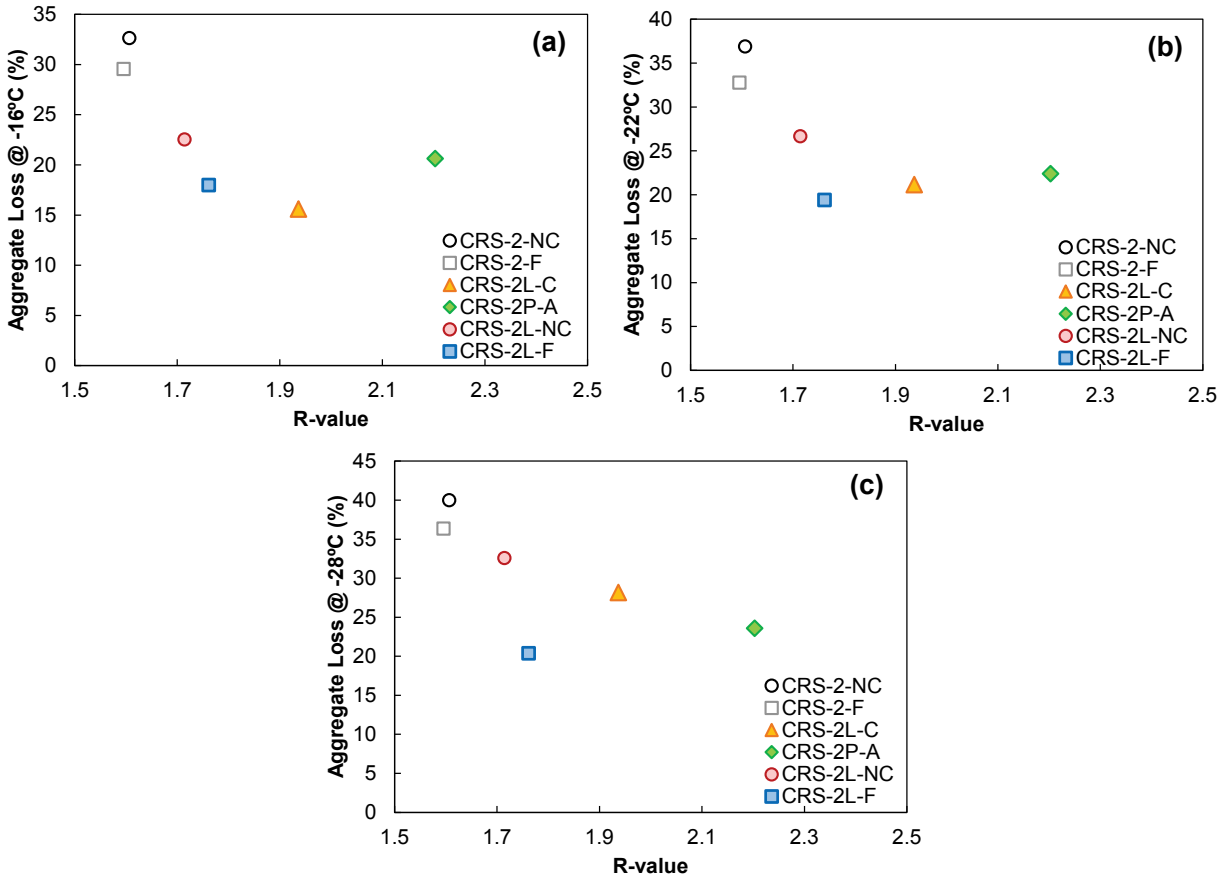

Figure D-37. Relationship between residual binder R-value and chip seal mixture aggregate loss at (a) -16ºC, (b) -22ºC, and (c) -28ºC.

The relationship between chip seal mixture aggregate loss and residual binder crossover modulus is shown in Figure D-38 for three mixture test temperatures: (a) -16ºC, (b) -22ºC, and (c) -28ºC. Note that while mixture aggregate loss varies as a function of temperature, crossover modulus values are unique to a given binder. Crossover modulus is defined as the G* value at the reduced frequency where phase angle equals 45º. Thus, the crossover modulus is closely related to the R-value previously discussed for a given binder. Results indicate that crossover modulus is related to aggregate loss performance. Several outliers exist in results which match those observed in R-value results: CRS-2P-A at both -16ºC and -22ºC and CRS-2L-F at -28ºC.

Results generally indicate a lower residual binder crossover modulus leads to better aggregate loss resistance which matches intuitions. At reduced frequencies lower than the crossover frequency (i.e., higher temperature or slower rates), the loss (viscous) component of the dynamic shear modulus exceeds the storage (elastic) component. In the study of polymers and other viscoelastic materials, it has been postulated that the crossover modulus is an indicator of intermolecular forces comprising a material's microstructure (Winter 1987). At temperatures below (frequencies above) the crossover point, the excitation applied to the material is insufficient to overcome the forces of molecular interaction contained within the material's microstructure. However, once the crossover point is exceeded, (either by increasing temperature or decreasing rate), the excitation applied overcomes the forces of the material's microstructure and hence, a tendency towards fluid behavior ensues. Thus, a lower crossover modulus in asphalt binders, theoretically, implies a higher degree of compatibility (i.e., less structured). Materials

which are structured are inherently more brittle and susceptible to cracking than more compatible materials.

It should also be noted that the findings that both ΔT_c and crossover modulus are related to aggregate loss performance is not surprising. The parameter ΔT_c is related to stiffness at an m-value of 0.300. If stiffness is significantly lower than the PG specification limit of 300 MPa at the temperature where m-value equals 0.300, ΔT_c will be highly negative because the PG critical stiffness temperature will be significantly lower than the critical m-value temperature. The m-value represents the slope of the logarithmic stiffness versus time plot. The slope of the G* master curve is equal to δ/90 (Anderson and Marasteanu 2010) and thus, findings that a lower G* corresponding to a phase angle of 45ºC will lead to better aggregate loss is consistent to finding that a lower (more negative) ΔT_c will lead to better aggregate loss.

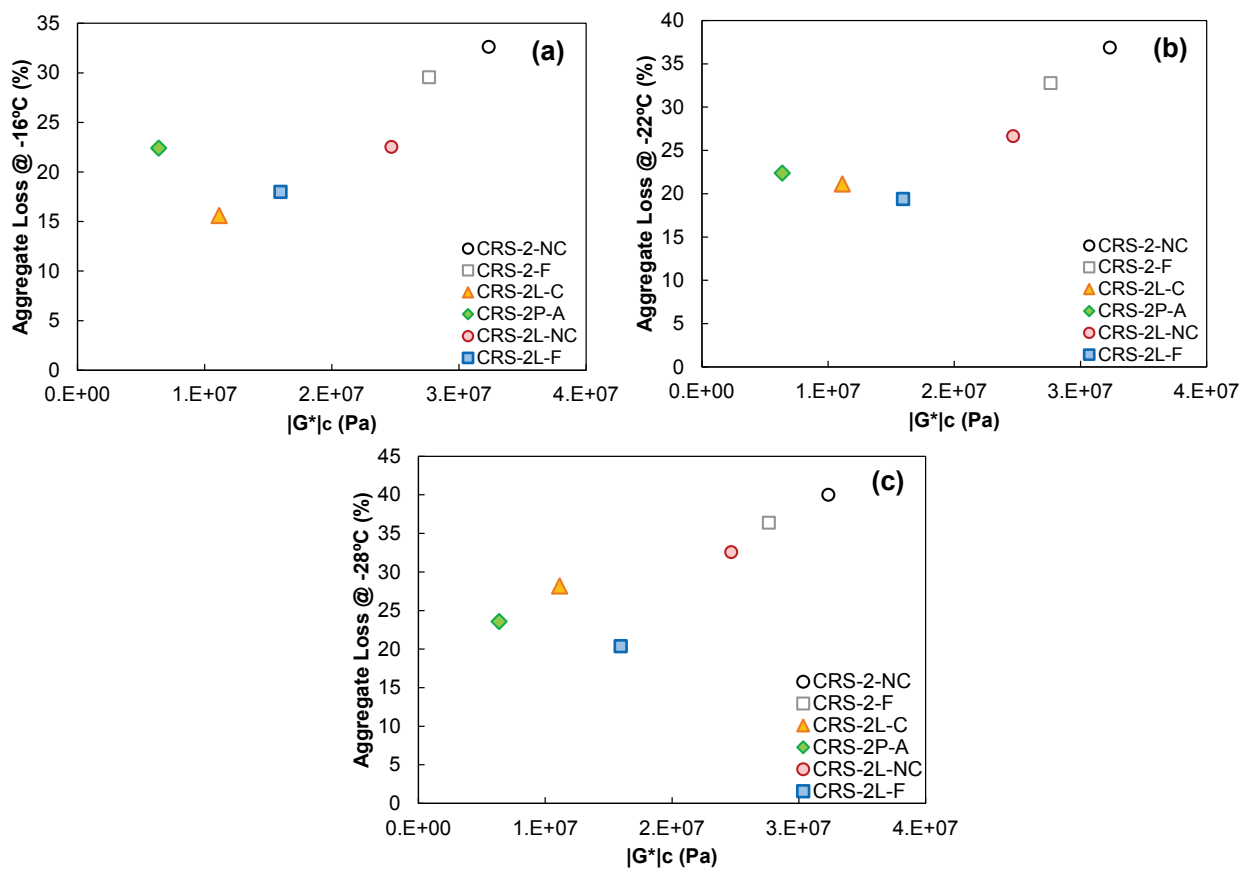

Figure D-38. Relationship between residual binder crossover modulus and chip seal mixture aggregate loss at (a) -16ºC, (b) -22ºC, and (c) -28ºC.

For all binders evaluated, the crossover point occurred within the range of measured data acquired from temperature-frequency sweep testing at temperatures ranging from 5ºC to 15ºC (See Figure D-31). Thus, crossover moduli were determined via interpolation of data. However, at the reduced frequency where low temperature performance is deemed most critical, phase angle values are much lower than 45º. Phase angle results at the low temperatures used in mixture testing and a frequency of 12 Hz, (which as previously discussed corresponds to the expected rate of loading induced by snow plow traffic), were generally close to 5ºC (See Figure D-33 (b)). Therefore, to evaluate a similar property at conditions representing critical low

temperature conditions, the G* values corresponding to a phase angle value of 5º were also analyzed.

The relationship between chip seal mixture aggregate loss and residual binder G* values corresponding to a phase angle of 5º is shown in Figure D-39 for three mixture test temperatures: (a) -16ºC, (b) -22ºC, and (c) -28ºC. Results match crossover modulus trends shown in Figure D-38. Thus, results indicate no advantage in relating binder and mixture results by using an iso-phase angle condition corresponding to low temperature.

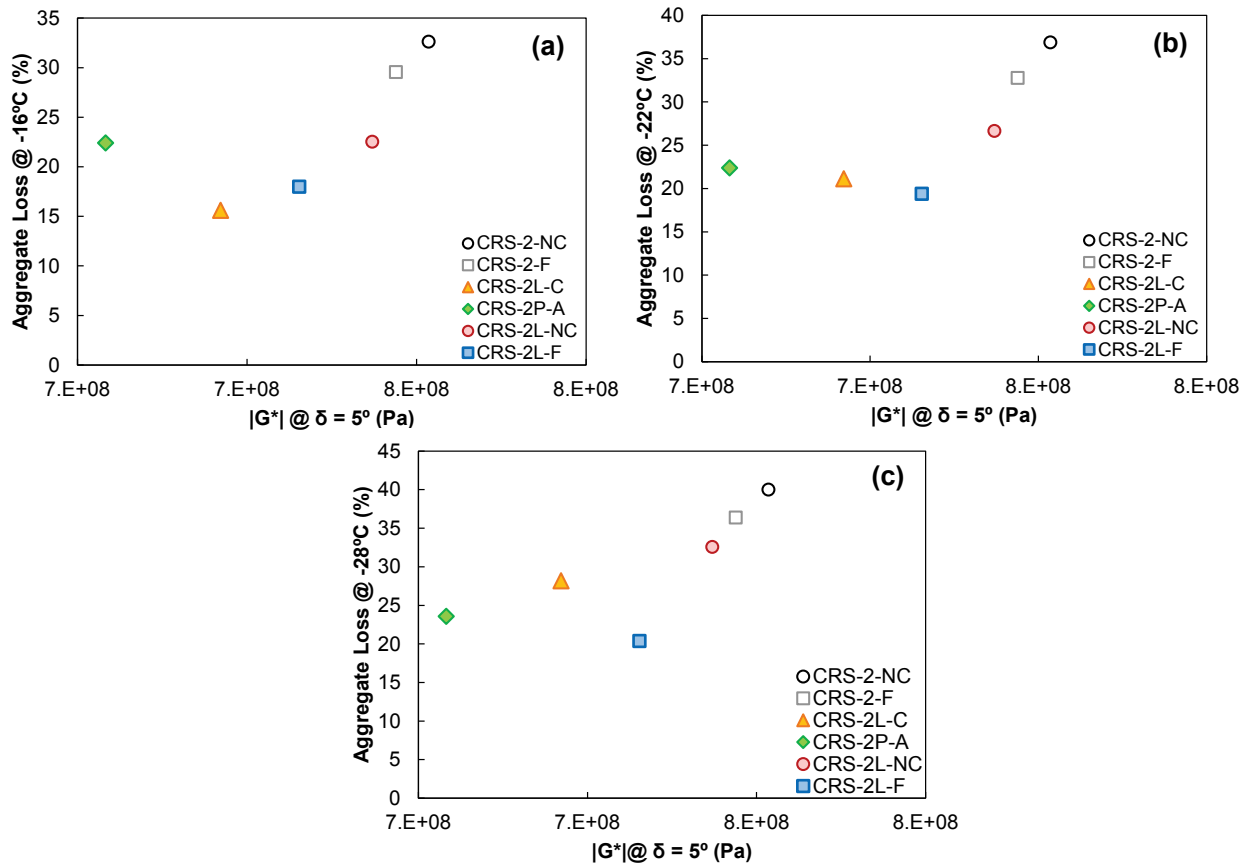

Figure D-39. Relationship between residual binder G* values corresponding to a phase angle of 5º and chip seal mixture aggregate loss at (a) -16ºC, (b) -22ºC, and (c) -28ºC.

Microsurfacing Results

The relationship between microsurfacing mixture fracture energy and residual binder ΔT_c is shown in Figure D-40Figure D-35 for three mixture test temperatures: (a) -16ºC, (b) -22ºC, and (c) -28ºC. Results indicate that ΔT_c is related to microsurfacing mixture fracture energy, with a lower (more negative) ΔT_c indicative of better performance. These findings match findings of chip seal results presented in Figure D-35.

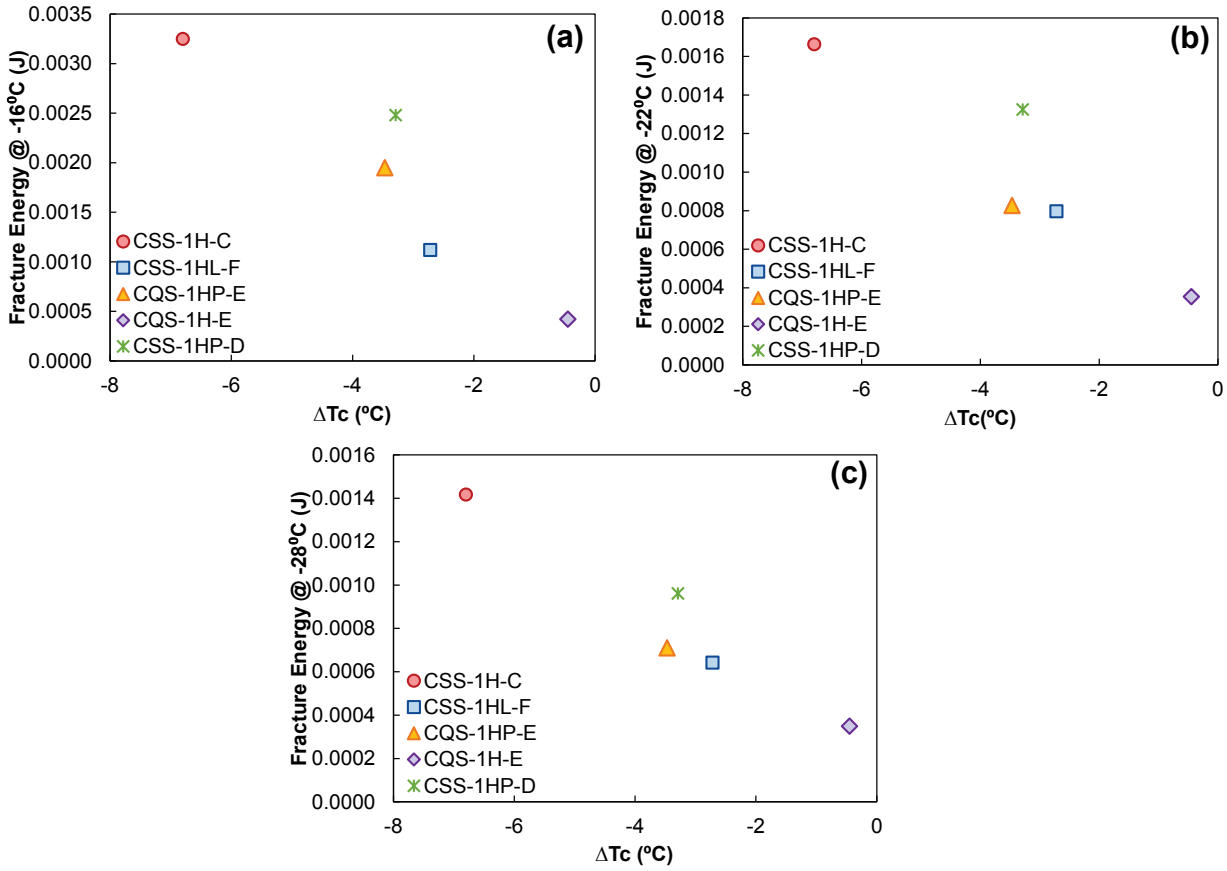

Figure D-40. Relationship between residual binder ΔTc and microsurfacing mixture fracture energy at (a) -16ºC, (b) -22ºC, and (c) -28ºC.

The relationship between microsurfacing mixture fracture energy and residual binder Glover-Rowe parameter is shown in Figure D-41 for three mixture test temperatures: (a) -16ºC, (b) -22ºC, and (c) -28ºC. Irrespective of mixture test temperature, the Glover-Rowe parameter was evaluated at 15ºC and 0.0008 Hz per the methodology used by Anderson et al. (2011). Result reveal that the Glover-Rowe parameter is only weakly related to microsurfacing fracture energy.

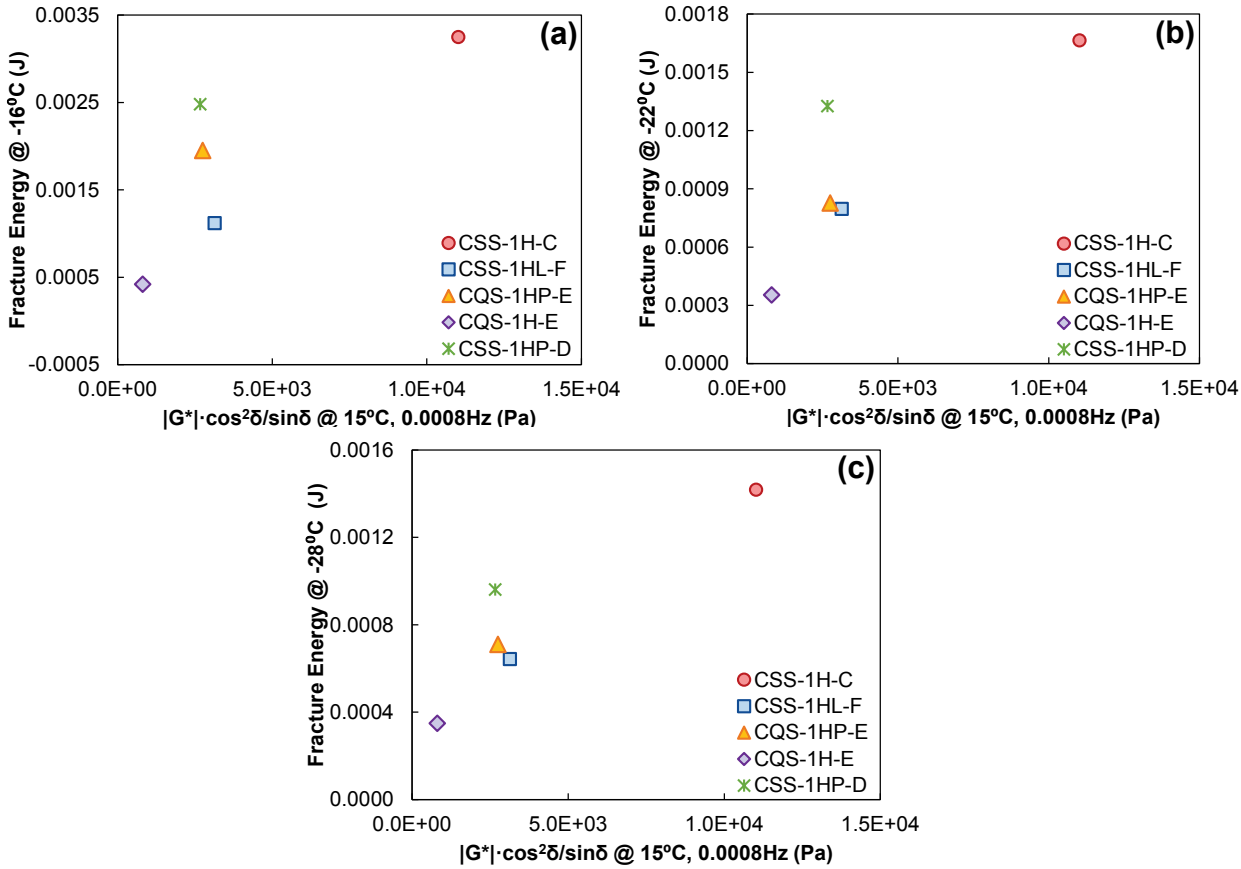

Figure D-41. Relationship between residual binder Glover-Rowe Parameter evaluated at 15ºC, 0.008 Hz and microsurfacing mixture fracture energy at (a) -16ºC, (b) -22ºC, and (c) -28ºC.

The relationship between microsurfacing mixture fracture energy and residual binder R-value is shown in Figure D-42 for three mixture test temperatures: (a) -16ºC, (b) -22ºC, and (c) -28ºC. Results indicate that R-value is related to aggregate loss performance, with a higher R-value indicative of improved fracture resistance. These findings are consistent with the findings of chip seal R-value analysis presented in Figure D-37.

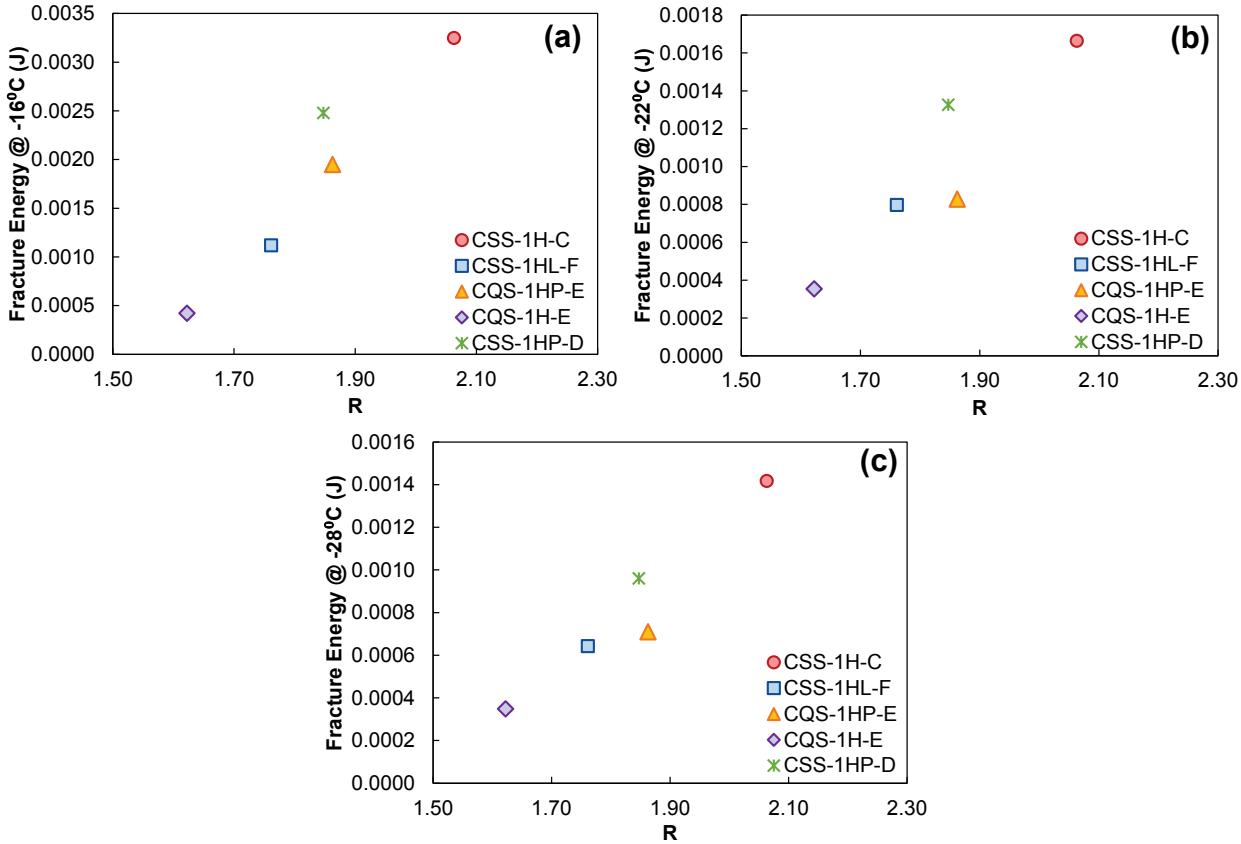

Figure D-42. Relationship between residual binder R value and microsurfacing mixture fracture energy at (a) -16ºC, (b) -22ºC, and (c) -28ºC.

The relationship between microsurfacing mixture fracture energy and residual binder crossover modulus is shown in Figure D-43 for three mixture test temperatures: (a) -16ºC, (b) -22ºC, and (c) -28ºC. Results indicate that crossover modulus is related to microsurfacing mixture fracture energy, with a lower crossover modulus indicative of better performance. Recall R-value and crossover modulus are closely related, with a higher R-value generally indicating a lower crossover modulus and hence results of Figure D-43 and Figure D-42 are in good agreement. Microsurfacing crossover modulus trends also match the crossover modulus trends in chip seals shown in Figure D-38.

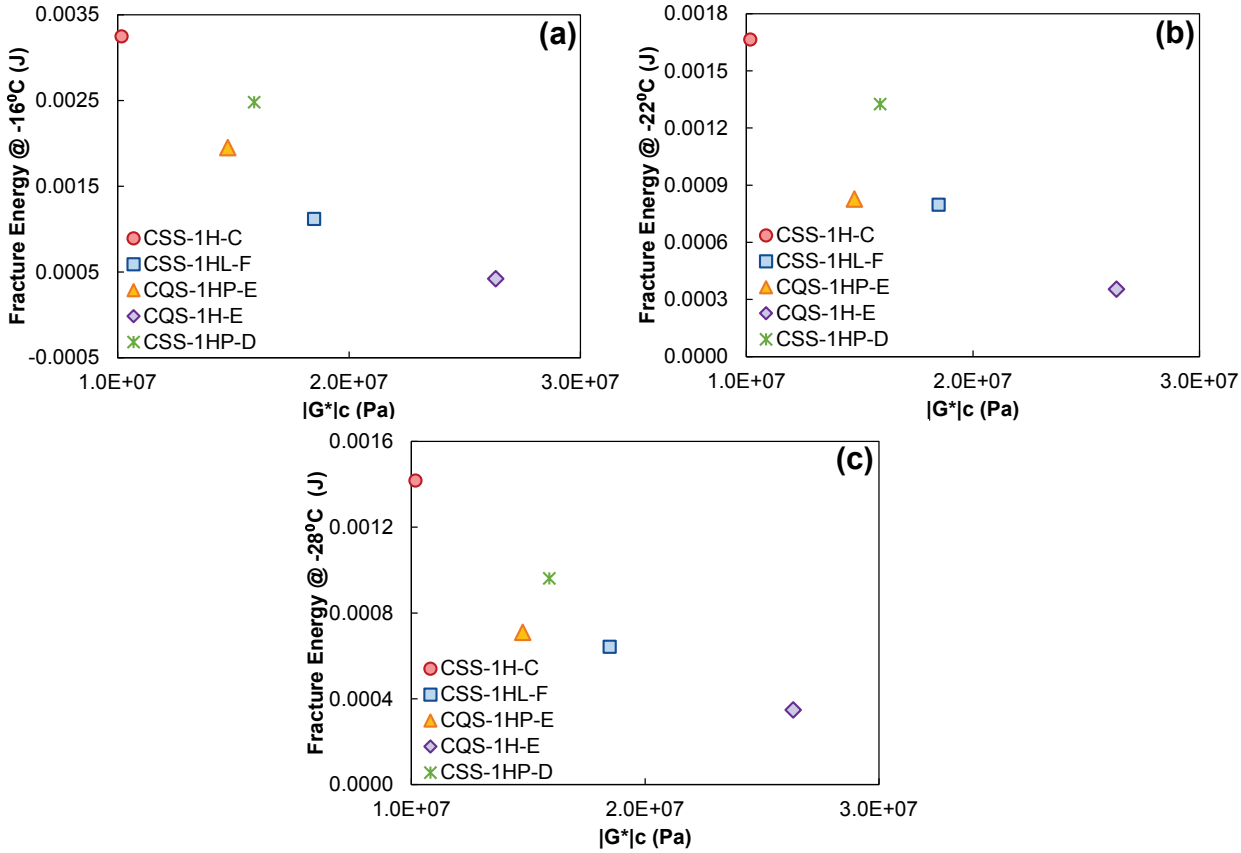

Figure D-43. Relationship between residual binder crossover modulus and microsurfacing mixture fracture energy at (a) -16ºC, (b) -22ºC, and (c) -28ºC.

Similar to chip seal results, the crossover point in microsurfacing residual binder results occurred within the range of measured data acquired from temperature-frequency sweep testing at temperatures ranging from 5ºC to 15ºC as shown in Figure D-32. However, at the reduced frequency where low temperature performance is deemed most critical, phase angle values can be significantly lower than 45º. Phase angle results at the low temperatures used in mixture testing and a frequency of 0.0008 Hz, were in in some instances closer to 20ºC (See Figure D-34 (b)). Therefore, to evaluate a similar property at conditions representing critical low temperature conditions, the G* values corresponding to a phase angle value of 20º were also analyzed.

The relationship between microsurfacing mixture fracture energy and residual binder crossover modulus is shown in Figure D-44 for three mixture test temperatures: (a) -16ºC, (b) -22ºC, and (c) -28ºC. Results match crossover modulus trends shown in Figure D-43. Thus, results indicate no advantage in relating binder and mixture results by using an iso-phase angle condition corresponding to low temperature which is consistent with findings of chip seal results.

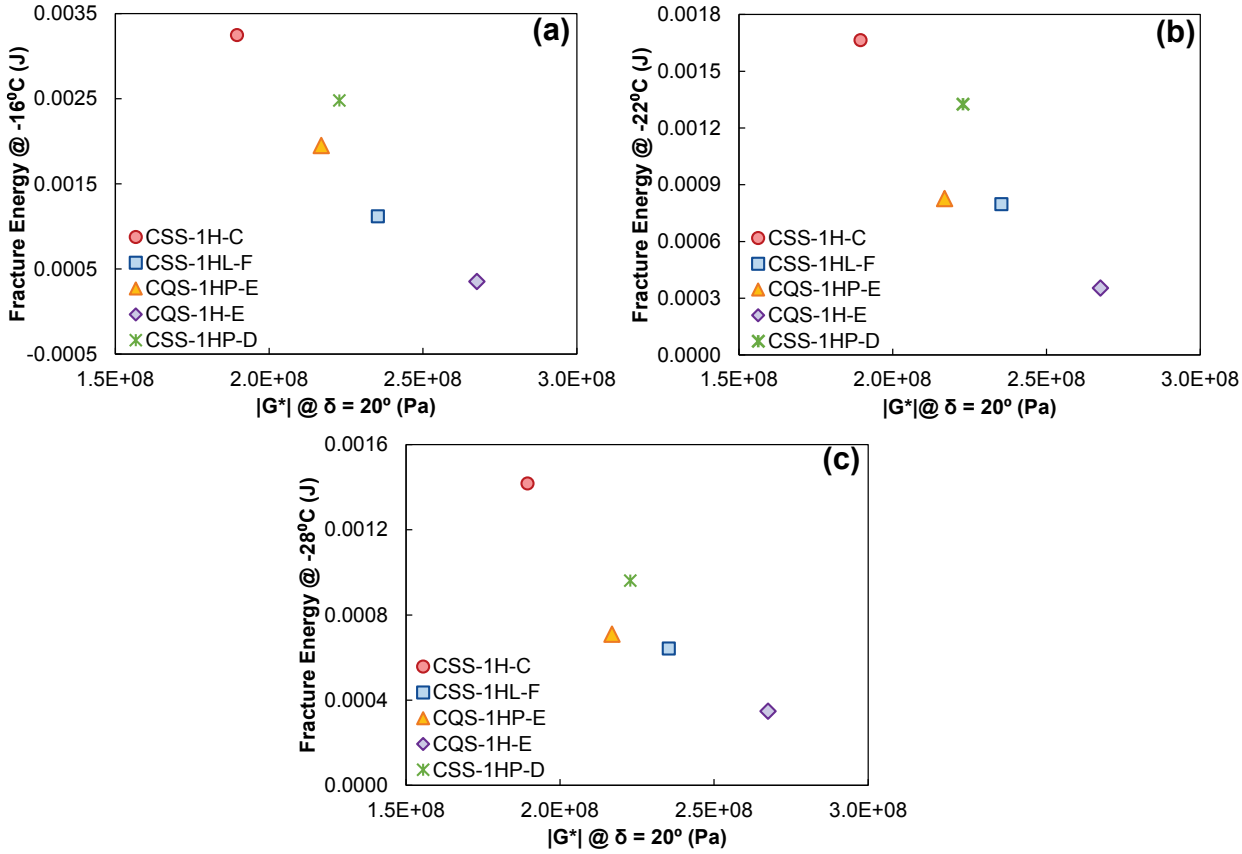

Figure D-44. Relationship between residual binder G* values corresponding to a phase angle of 5° and microsurfacing mixture fracture energy at (a) -16°C, (b) -22°C, and (c) -28°C.

Conclusions

The rheological residual binder property demonstrating the strongest relationship to both chip seal aggregate loss and microsurfacing fracture energy is the dynamic shear modulus (G*) at an iso-phase angle value. Results demonstrate the relationship between mixture performance and G* is strong irrespective of whether or not the iso-phase angle value was selected within the measured data range corresponding to intermediate temperature or extrapolated to critical low temperature conditions. Because DSR temperature-frequency sweep testing is only possible above 0°C in all rheometers, the final specification was developed based on crossover modulus (i.e., iso-phase angle condition of 45°), which can be readily measured at intermediate temperature. However, crossover modulus is a temperature-independent parameter. The underlying concept used to develop emulsion performance grading specifications herein is the existence of a temperature-independent relationship between binder properties and mixture performance which is violated by the use of crossover modulus. While mixture performance varies as a function of temperature, crossover modulus values do not. Therefore, to adapt the concept of crossover modulus to allow incorporation into the EPG specification framework, critical phase angle values were determined as a function of mixture test temperature to produce a temperature independent relationship between mixture low temperature performance and corresponding G* values. This analysis used to develop the final low temperature specification is presented in the main body of the report.

REFERENCES

Anderson, D. A., D. W. Christensen, H. U. Bahia, R. Dongre, M. G. Sharma, C. E. Angle, and J. Button. *Binder Characterization and Evaluation Volume 3: Physical Characterization*, SHRP A-369, Strategic Highway Research Program, National Research Council, Washington, D.C., 1994.

Anderson, D. A., and M. O. Marasteanu. Continuous Models for Characterizing Linear Viscoelastic Behavior of Asphalt Binders, *International Society for Asphalt Pavements Workshop on Asphalt Binders and Mastics*, Madison, WI, 2011.

Anderson, R. M., G. N. King, D. I. Hanson, and P. B. Blankenship. Evaluation of the Relationship between Asphalt Binder Properties and Non-load Related Cracking. *Journal of the Association of Asphalt Paving Technologists*, Vol. 80, pp. 615-663, 2011.

Brown, S. F. Determination of young's modulus for bituminous materials in pavement design, *Highway Research Record*, No. 431, pp. 38-49, 1973.

Ferry, J. D. *Viscoelastic Propertis of Polymers.* New York: John Wiley and Sons, 1980.

Hicks, R. G., F. N. Finn, C. L. Monishmith, and R. B. Leahy. Validation of the SHRP Binder Specification Through Mix Testing. Journal of the Association of Asphalt Paving Technologists, Vol. 62, pp. 565-614, 1993.

Im, J. K. Performance Evaluation of Chip Seals for High Volume Roads Using Polymer-Modified Emulsions and Optimized Construction Procedures, Ph. D. Dissertation. North Carolina State University, 2013.

Kim, Y. R. and J. Adams. *Development of a New Chip Seal Mix Design Method*. Publication HWY-2008-04, N.C. Department of Transportation, 2011.

Lee, J. and Y. R. Kim. *Performance-Based Analysis of Polymer Modified Emulsions in Asphalt Surface Treatments*. Publication FHWA-NC-07-06, FHWA, U.S. Department of Transportation, 2009.

Lee, J. and Y. R. Kim. Performance-Based Evaluation of Asphalt Surface Treatments Using the Third Scale Model Mobile Loading Simulator. North Carolina State University, Raleigh, NC. 2007.

Marasteanu, M. O. and D. A. Anderson. Improved Model for Bitumen Rheological Characterization. *Eurobitume Workshop on Performance Related Properties for Bituminous Binder*, Luxembourg, Paper No. 133, 1999.

Marasteanu, M. O., A. C. Falchetto, M. Turos, and J. Le. *Development of a Simple Test to Determine the Low Temperature Strength of Asphalt Mixtures and Binders*, Highway IDEA Project 151 Final Report, National Research Council, Washington, D.C., 2012.

McHattie, R. L. *Asphalt Surface Treatment Guide*. Publication FHWA-AK-RD-01-03, Alaska Department of Transportation and Public Facilities, 2001.

Moraes, R., R.Velasquez, and H. Bahia. Measuring Effect of Moisture on Asphalt-Aggregate Bond with the Bitumen Bond Strength Test. *Transportation Research Record: Journal of the Transportation Research Board*, Transportation Research Board of the National Academies,Washington D.C., No. 2209, pp. 70-81, 2011.

Rowe, G. Evaluation of the Relationship between Asphalt Binder Properties and Non-load Related cracking. *Journal of the Association of Asphalt Paving Technologists*, *Prepared Discussion*, Vol. 80, pp. 649-663, 2011.

Shuler, S. Chip Seals for High Traffic Pavements. *Transportation Research Record: Journal of the Transportation Research Board*, No. 1259, National Research Council, Washington, D.C., pp. 24-34, 1991.

Winter, H. H. Can the Gel Point of a Crosslinking Polymer be Detected by G' – G" Crossover? Polymer Engineering and Science, Vol. 27, No. 22, pp. 1698-1702, 1987.

Zeng, M., H. U. Bahia, R. M. Anderson, and P. Turner. Rheological Modeling of Modified Asphalt Binders and Mixtures, *Journal of the Association of Asphalt Paving Technologists*, Vol. 70, pp. 403-441, 2001.

Appendix E. Bibliography

Adams, J. and Y.R. Kim, "Mean Profile Depth Analysis of Field and Laboratory Traffic-Loaded Chip Seal Surface Treatments," International Journal of Pavement Engineering. Vol. 15, Nos. 7-8, 2013, pp. 645-656.

American Association of State Highway and Transportation Officials (AASHTO). Determining Rutting Susceptibility of HMA Using the Asphalt Pavement Analyzer. AASHTO TP 63-07: *Standard Specifications for Transportation Materials and Methods of Sampling and Testing*, Washington, DC, 2010.

Anderson, D. A., D. W. Christensen, H. U. Bahia, R. Dongre, M. G. Sharma, C. E. Antle, and J. Button. SHRP A-369: *Binder Characterization and Evaluation Volume 3: Physical Characterization*. Strategic Highway Research Program, National Research Council. Washington, D.C, 1994.

Asphalt Emulsion Manufacturers Association (AEMA). *Recommended Performance Guideline*. Third Edition, 2004.

Asphalt Institute. *A Basic Asphalt Emulsion*, Manual Series No. 19, Asphalt Institute, Lexington, Kentucky, 2008.

Austroads Incorporated. *Sprayed Sealing Guide.* Publication No. AP-676/104, Sydney, Australia, 2004, p. 104.

Bahia, H., D. I. Hanson, M. Zeng, H. Zhai, M. A. Khatri, and R. M. Anderson. *Characterization of Modified Asphalt Binders in Superpave Mix Design*. NCHRP Report, Issue 459, 2001, p. 176.

Bahia, H., A. Hanz, and J. Meng. *Low Temperature Performance Prediction Methods for Emulsion Residues*. Emulsion Task Force Technical Presentation, Boston, MA, Federal Highway Administration, 2010.

Bahia, H., A. Hanz, K. Kanitpong, and H. Wen. *Testing Methods to Determine Aggregate/Asphalt Adhesion Properties and Potential Moisture Damage*. WHRP 07-02. Wisconsin Highway Research Program, Madison, 2007.

Bahia, H., K. Jenkins, and A. Hanz. Performance Grading of Bitumen Emulsions for Sprayed Seals. *Proceedings of the 1st International Sprayed Sealing Conference*. Australian Road Research Board, Adelaide, Australia, 2008. pp. 1-13.

Bal, G., J. Patric, R. Stevenson, and P. Herringtong. *Assessment of Temperature-Sensitive Bitumen for Chipsealing on New Zealand Roads.* Research Report No. 154. Transfund New Zealand Roads, Wellington, New Zealand, 1999.

Barnes, A. H. *A Handbook of Elementary Rheology.* Aberystwyth, Wales: The University of Wales Institute of Non-Newtonian Fluid Mechanics, Department of Mathematics, University of Wales, Aberystwyth, 2000.

Benson, F. J. and B. M. Gallaway. *Retention of Cover Stone by Asphalt Surface Treatments*. Bulletin 133, Texas Engineering Experiment Station, Texas A&M University System, 1953, p. 58.

Button, J. W. Permeability of Asphalt Surface Seals and Their Effect on Aging of Underlying Asphalt Concrete. *Transportation Research Record: Journal of the Transportation Research Board*, No. 1535, Transportation Research Board of the National Academies, Washington, D.C., 1996, pp. 124-130.

California Department of Transportation (CALTRANS). Maintenance Technical Advisory Guide Volume I – Flexible Pavement Preservation Second Edition. 2009. pp. 9-10.

Colas Solutions, Inc. *Surface Defects*. http://www.colassolutions.com/solutions/defects.html. Accessed November 17, 2011.

Cooley Jr., L. A. *Permeability of Superpave Mixtures: Evaluation of Field Permeameters*. NCAT Report No. 99-1. 1999. http://ntl.bts.gov/lib/7000/7900/7935/rep99-1.pdf. Accessed February 15, 2012.

D'Angelo, J. A., M. Anderson, and D. Walker. *A Better Tool for Characterizing High Temperature Performance Properties. http://asphaltmagazine.com/mscr-a-better-tool-for-characterizing-high-temperature-performance-properties/.* Accessed June 2016.

D'Angelo, J. A., R. Dongre and G. Reinke. Creep and Recovery. *Public Roads,* Vol. 70, No.5, 2007, pp 24-30.

Daranga, C., C. Clopotel, and H. Bahia. Replacing the Elastic Recovery Test for Asphalt Binders with a DSR Test; Development of Protocol and Relationship to Binder Fatigue. *Proceedings of the 89th Annual Meeting of the Transportation Research Board*.

Determination of Binder Aggregate Adhesivity by the Vialit Plate Shock Test Method. EN12272-3: 2003.

Eley, R. Rheology and Viscometetry. *Paint and Coating Testing Manual, Gardner-Sward Handbook*, 14th ed. Philadelphia, PA: ASTM International, 1995, pp. 333-368.

Epps, A. L., C. J. Glover, and R. Barcena. *A Performance-Graded Binder Specification for Surface Treatments*. Publication FHWA/TX-02/1710-1, FHWA, U.S. Department of Transportation, Texas Transportation Institute, 2001.

Estakhri, C. K. and M. A. Gonzalez. *Design and Construction of Multiple Seal Coats*. Texas Transportation Institute, 1998.

Ferry, J. D. *Viscoelastic Propertis of Polymers.* New York: John Wiley and Sons, 1980.

Gransberg, D. D. and D. M. B. James. *Chip Seal Best Practices*. NCHRP Synthesis 342. Transportation Research Board, National Research Council, Washington, D.C., 2005.

Gransberg, D. D., S. Senadheera, and I. Karaca, *Analysis of Statewide Seal Coat Constructability Review.* Texas Department of Transportation, Publication TX-98/0-1787-1R, Texas Tech University, 1998.

Gueit, C., R. Durand, A. Kadrmas, and D. Hazlett. *Asphalt Emulsion Technology: Review of Asphalt Emulsion Residue Procedures.* Transportation Research Circular E-C122. Transportation Research Board of the National Academies, Washington, D.C, 2007.

Guylaine, B. and L. Claude. *Thermal Cracking of Asphalt Pavement*. 2nd Eurasphalt and Eurobitume Congress, Proceeding 0267, Barcelona, 2000. http://www.eecongress.org/2000/pdfbook3/session2/Proc0267uk.pdf. Accessed February 15, 2012.

F. M. Hanson. Bituminous Surface Treatments on Rural Highways. *Proceedings of the New Zealand Society of Civil Engineers*, Vol. 21, 1934-1935: 89.

Hanz, A., Z. Arega, and H. Bahia. *Rheological Properties of Emulsions Recovered Using Newly Proposed Evaporative Techniques*. Presented at the 88th Annual Meeting of the Transporation Research Board, Washington, D.C., 2009.

Hanz, A., Z. Arega, and H. Bahia. Rheological Behavior of Emulsion Residues Produced by Evaporative Recovery Method. *Transportation Research Record: The Journal of the Transportation Research Board*, No. 2179 Transportation Research Board of the National Academies, 2010, Washington D.C., pp. 102-108.

Hanz, A. and C. Franco. *Research Needs in Application of Emulsified Asphalts*. Emulsion Task Force (ETF) Update. Presentation by Modified Asphalt Research Center, Phoenix, Arizona, 2009.

Hanz, A., Johannes, P., and Bahia, H., "Development of Emulsion Residue Testing Framework for Improved Chip Seal Performance," In Transportation Research Record: Journal of the Transportation Research Board, Washington, D.C, Vol. 2293, 2012, pp. 106-113.

Hintz, C., R. Velasquez, Z. Li, and H. Bahia. Effect of Oxidative Aging on Binder Fatigue Performance. *Journal of the Association of Asphalt Pavement Technologists*, Association of Asphalt Pavement Technologists, 2011, Vol. 80.

Holmgreen, R. J., J. A. Epps, C. H. Hughes, and B. M. Gallaway. *Field Evaluation of the Texas Seal Coat Design Method.* Research Report 297-1F, Texas Transportation Institute, Texas A&M University System, 1985, p. 174.

Im, J. H. Performance Evaluation of Chip Seals for High Volume Roads Using Polymer-Modified Emulsions and Optimized Construction Procedures., Ph. D. Dissertation. North Carolina State University, 2013.

Isacsson, U. A Compilation of Laboratory Methods for Studying Stability of Bitumen Emulsions. *Materials and Structures,* Vol. 18, No. 3, 1995, pp. 228-236.

Jackson, D., N. Jackson, and J. Mahoney. Washington State Chip Seal Study. *Transportation Research Record*, No. 1259, Transportation Research Board, National Research Council, Washington, D.C., 1990, pp. 1-10.

James, A. *Overview of Asphalt Emulsions*. Transportation Research Circular Number E-C102, Asphalt Emulsion Technology. Transportation Research Board of the National Academies, Washington, D.C, 2006, pp. 16-25.

Jayawickrama, P.W., Prasanna, R., and S. P. Senadheera. Survey of State Practices to Control Skid Resistance on Hot-Mix Asphalt Concrete Pavements. Transportation Research Record 1536, Transportation Research Board, National Research Council, Washington, D.C., 1996, 52-58.

Johnson, C. *Estimating Asphalt Binder Fatigue Resistance Using an Accelerated Test Method.,* Ph. D. Thesis. Madison, University of Wisconsin – Madison, 2010.

Johnson, C. M. and H. U. Bahia. Evaluation of an Accelerated Procedure for Fatigue Characterization of Asphalt Binders. Submitted for publication in *Road Materials and Pavement Design*, 2010.

Johnston, J. B. and G. King. Using Polymer Modified Emulsions in Surface Treatments. Federal Lands Highway Interim Report. 2008.

Kadrmas, A. *Asphalt Emulsion Residue Recovery and Rheological Testing Update*. Technical Presentation Presented at the Asphalt Emulsion Manufacturers Association Annual Meeting, 2010.

Kadrmas, A. *Using the DSR-MSCR to Compare Emulsion Residue Recovery Methods*. Technical Presentation Presented at the 88th Annual Meeting of the Transportation Research Board, Washington D.C., 2009.

Kearby, J.P. Tests and Theories on Penetration Surfaces. *Transportation Research Record: Journal of the Transportation Research Board*, No 271, TRB, National Research Council, Washington, D.C. 1953: 232-237.

Kim, Y. R. and J. Adams. *Development of a New Chip Seal Mix Design Method*. Publication HWY-2008-04, N.C. Department of Transportation, 2011.

Kim, Y. R., S. Lee, Y. Seo, and O. El-Haggan. *Impact of Price Reductions on the Long-Term Pavement Performance of HMA Mixes in North Carolina*. Final Report to NCDOT, FHWA/NC/2005-09, 2005, pp. 53-54.

King, G. N. and H. W. King. *Spray Applied Polymer Surface Seals*, Foundation for Pavement Preservation, FHWA, Cooperative Agreement DTFH61-01-X-00004, August 2007.

King, G., H. King, L. Galehouse, M. Voth, L. Lewandowski, C. Lubbers, and P. Morris. Field Validation of Performance-Based Polymer Emulsion Residue Tests: The FLH Study.

Proceedings of the First International Conference on Pavement Preservation, New Port Beach, CA, FHWA, 2010, pp. 247-267.

Kucharek, A. *Measuring the Curing Characteristics of Chip Sealing Emulsions*. Presented at the Joint ARRA-ISSA-AEMA Meeting, Bonita Springs, CA. Asphalt Emulsion Manufacturers Association and McAsphalt, Scarborough, Ontario, 2007.

Lawson, W. D., M. Leaverton, and S. Senadheera. *Maintenance Solutions for Bleeding and Flushed Pavements Surfaced with a Seal Coat or Surface Treatment*. Texas Department of Transportation Research and Technology Implementation Office, Report 0-5230-1, 2007.

Lee, J. and Y. R. Kim. *Quantifying the Benefits of Improved Rolling of Chip Seals*. HWY-2006-06. FHWA, U.S. Department of Transportation, 2008.

Lee, J. and Y. R. Kim. *Performance-Based Analysis of Polymer Modified Emulsions in Asphalt Surface Treatments*. Publication FHWA-NC-07-06, FHWA, U.S. Department of Transportation, 2009.

Lee, J. and Y. R. Kim. Performance-Based Uniformity Coefficient of Chip Seal Aggregate. *Transportation Research Record: Journal of the Transportation Research Board*, No. 2108, TRB, National Research Council, Washington, D.C. 2009: 53-60.

Lee, J. and Y. R. Kim. Performance-Based Evaluation of Asphalt Surface Treatments Using the Third Scale Model Mobile Loading Simulator. North Carolina State University, Raleigh, NC. 2007.

Lee, S. and Y. R. Kim. Long-Term Performance Assessment of Asphalt Concrete Pavement Using the Third Scale Model Mobile Loading Simulator and Fiber Reinforced Asphalt Concrete. North Carolina State University, Raleigh, NC. 2003.

Lyttleton, D. and R. Traxler. Flow Properties of Asphalt Emulsions. *Industrial and Engineering Chemistry*, 1948, pp. 2115–2117.

McHattie, R. L. *Asphalt Surface Treatment Guide*. Publication FHWA-AK-RD-01-03, Alaska Department of Transportation and Public Facilities, 2001.

McLeod, N. W. A General Method of Design for Seal Coats and Surface Treatments. *Association of Asphalt Pavement Technology*, 1971, pp. 537-628.

Meng, J. *Affinity of Asphalt to Mineral Aggregate: Pull-off*. Master's Thesis. University of Wisconsin - Madison, 2010.

Miller, T., Z. Arega, and H. Bahia. Correlating Rheological Properties of Emulsion Residue to Early Chip Seal Performance. *Transportation Research Record: Journal of the Transportation Research Board*, No. 2179, Transportation Research Board of the National Academies Washington D.C., 2010, pp. 66-74.

Mohseni, A. *LTPP Seasonal Asphalt Concrete (AC) Pavement Temperature Models.* FHWA-RD-97-103, Pavement Systems (PavSys), Federal Highway Administration, Mc.Lean, VA, 1998.

Mohseni, A., S. H. Carpenter, and J. D'Angelo. Development of Superpave High-Temperature Performance Grade (PG) Based on Rutting Damage (With Discussion and Closure). *Journal of the Association of Asphalt Paving Technologists*, Vol. 74, No. 1, 2005, pp. 197-254.

Moraes, R., R.Velasquez, and H. Bahia. Measuring Effect of Moisture on Asphalt-Aggregate Bond with the Bitumen Bond Strength Test. *Transportation Research Record: Journal of the Transportation Research Board*, No. TBD, Transportation Research Board of the National Academies,Washington D.C., 2011.

North Carolina Department of Transportation. *Standard Specifications for Roads and Structures*. N.C. Department of Transportation Design Services Unit, 2002.

Parker, Jr., F. and E. R. Brown. *A Study of Rutting of Alabama Asphalt Pavements.* Final Report Project No. ST-2019-9, 1990.

Pavement Interactive. "Bending Beam Rheometer" April 21, 2011. http://www.pavementinteractive.org/article/bending-beam-rheometer/#sthash.RpiIis05.dpuf

Redelius P. and J. Walter. Bitumen Emulsions. *Emulsions and Emulsions Stability*, CRC Taylor and Francis, 2006, p. 383.

Robertson, R. E. SHRP-A/UWP-91-510: *Chemical Properties of Asphalts and Their Relationship to Pavement Performance*. National Research Council, Washington, D.C., 1991.

Roque, R., M. Thompson, and D. Anderson. Bituminous Seal Coats: Design, Performance Measurements and Performance Prediction. *Transportation Research Record 1300*, Transportation Research Board, National Research Council, Washington, D.C., 1991, pp. 90-97.

Rowe, G. M., M. J. Sharrock, and S. Raposo. (2016). Cracking and Linear Viscoelastic Binder Properties, *8th RILEM International Conference on Mechanisms of Cracking and Debonding in Pavements*, Vol. 13, pp. 3-8.

Salomon, D. *Characterization of Emulsified Asphalt: Present and Future*. Technical Presentation at the Pavement Performance Prediction Symposium, Laramie, Wyoming, 2010.

Salomon, D. and P. Michael. *Kinetic Properties of Emulsified Asphalts.* Research Report. Idaho Asphalt Supply, Inc., 2002. http://www.technopave.com/publications/Kinetic-Properties-of-Emulsifed-Asphalts-May-2002.pdf. Accessed Sept. 10, 2011.

Salomon, D., H. Zhai, C. Joe, and C. Frank. *New Tools for Measuring Emulsified Asphalt*, Research Report, 2004. http://www.integratedasphaltsolutions.com/images/publications/New%20tools%20to%20me

asure%20emulsified%20asphalt%20properties,%20ISAET,%20Nov,2004.pdf. Accessed Oct. 25th, 2011.

SANRAL (South African National Roads Agency Limited). *Surfacing Seals for Rural and Urban Road. Department of Transport*, Technical Recommendations for Highways, Pretoria, South Africa, 1998.

Senadheera, S. P. and J. R. Khan. *Standardized Seal Coat Terminology Pamphlet.* Texas Department of Transportation. Research Implementation Study Number 5-1787, Center For Multidisciplinary Research in Transportation, Texas Tech University, 2001, p. 4.

SFERB (Road Bitumen Emulsion Manufacturers Section). *Bitumen Emulsions.* Paris: Revue Générale des Routes et des Aérodromes (RGRA), 2008.

ShedWorks, Inc. *How Can I Test Single Lift Field Cores*. http://www.shedworks.com/pavementlabproducts/overlaytester.html. Accessed February 28th, 2012.

Shuler, S. Chip Seals for High Traffic Pavements. *Transportation Research Record 1259*, TRB, National Research Council, Washington, D.C., 1991, pp. 24-34.

Shuler, S. Design and Construction of Chip Seals for High Traffic Volume. *Flexible Pavement Rehabilitation and Maintenance.* ASTM Special Technical Publication (STP) Number 1348. ASTM, 1998.

Shuler, S., P. S. Khandal, and M. Stroup-Gardiner. *Flexible Pavement Rehabilitation and Maintenance: Design and Construction of Chip Seals for High Traffic Volumes*. 1998, p. 98.

Shuler, S., A. Lord, A. Epps-Martin, and D. Hoyt. *Manual for Emulsion-Based Chip Seals for Pavement Preservation.* NCHRP 14-17, National Cooperative Highway Research Program, Washington, D.C, 2010.

Sim, C. H., Gan, F. F., and T. C. Chang. *Outlier Labeling with Boxplot Procedures.* Journal of the American Statistical Association, Vol. 100, No. 470, 2005.

Tadros, T. Application of Rheology for Assessment and Prediction of the Long-Term Physical Stability of Emulsions. *Advances in Colloid and Interface Science,* 2004, pp. 227-258.

Takamura, K. *Comparison of Emulsion Residues Recovered by Forced Air Flow and RTFO Drying*. Presented at the Asphalt Emulsion Manufacturers Association Meeting, Amelia Island, Florida, 2000.

The Asphalt Institute. Mix Design Methods for Asphalt Concrete and Other Hot-Mix Types (MS-2), 6th Ed.,1997, pp. 141.

Transit New Zealand. *Notes for the Specification for Bituminous Reseals*. TNZ P17 Notes, 2002.

Transit New Zealand. *Chipsealing in New Zealand.* Transit New Zealand, Wellington, New Zealand, 2005.

Von Quintus, H. L., W. Jagannath, and S. Shen. *Techniques for Mitigation of Reflective Cracking.* AAPTP 05-04, 2009.

Vijaykumar, A., A. Epps-Martin, E. Arambula. Revision and Further Validation of Surface Performance-Graded (SPG) Specification for Chip Seal Binders. *Transportation Research Record. The Journal of the Transportation Research Board*, The Transportation Research Board of the National Academies, Washington, D.C., 2013.

Walubita, L., A. Epps-Martin, and C. J. Glover. *A Surface Performance Graded (SPG) Specification for Surface Treatment Binders: Development and Initial Validation*. Publication FHWA-TX-05/1710-2. FHWA, U.S. Department of Transportation, 2005, pp. 26-47.

Walubita, L., A. Epps-Martin, D. Hazlett, and R. Barcena, Initial Validation of a New Surface Performance-Graded Binder Specification. *Transportation Research Record. The Journal of the Transportation Research Board*, No. 1875, The Transportation Research Board of the National Academies, Washington, D.C., 2007, pp. 45-55.

Wang, Y. *Improving Pavements with Long-Term Pavement Performance (LTPP): Products for Today and Tomorrow*. Publication FHWA-RD-03-049. FHWA, U.S. Department of Transportation, 2005.

Winter, H. H. Can the Gel Point of a Crosslinking Polymer be Detected by G' – G" Crossover? *Polymer Engineering and Science*, Vol. 27, No. 22, 1987, pp. 1698-1702.

Wolshon, B., *NCHRP Synthesis 340: Convertible Roadways and Lanes.* A Synthesis of Highway Practice, Transportation Research Board, National Research Council, Washington, D.C., 2004, p. 105.

Wood, T. J., D. W. Janisch, and F. S. Gaillard. 2006. *Minnesota Seal Coat Handbook.* Minnesota Department of Transportation, Office of Minnesota Road Research, 2006.

Wyoming Department of Transportation. *Field Viscometer Test* (*WYDOT 538.0*)*,* WYDOT, 2010.

Zhai, H., D. Salomon, and E. Milliron. Using Rheological Properties to Evaluate Storage Stability and Setting Behaviors of Emulsified Asphalts*,* White Paper, 2004. http://www.technopave.com/publications/Using-Rheological-Properties-to-Evaluate-Emulsified-Asphalts-ISAET-Nov-2004.pdf. Accessed Oct. 1 , 2011.